Universidade de Aveiro Departamento de Biologia
2015

Cátia Liliana Marques da Silva

Estudo do papel da Profilina-1 na função de células da microglia: o impacto na produção de espécies reativas de oxigénio

Dissecting the role of Profilin-1 in microglial cell function: the impact on ROS production

Universidade de Aveiro
2015

Departamento de Biologia

Cátia Liliana Marques da Silva

Estudo do papel da Profilina-1 na função de células da microglia: o impacto na produção de espécies reativas de oxigénio

Dissecting the role of Profilin-1 in microglial cell function: the impact on ROS production

Dissertação apresentada à Universidade de Aveiro para cumprimento dos requisitos necessários à obtenção do grau de Mestre em Biologia Molecular e Celular realizada sob a orientação científica da Doutora Camila Cabral Portugal, Investigadora do Instituto de Biologia Molecular e Celular da Universidade de Porto, Professora Doutora Anabela Pinto Rolo, Professora Auxiliar do Departamento de Biologia da Universidade de Coimbra e Professora Doutora Maria de Lourdes Gomes Pereira, Professora Associada com Agregação do Departamento de Biologia da Universidade de Aveiro.

.

Apoio financeiro da FCT: PTDC|SAU-NMC|119937| 2010 FCOMP-01-0124-FEDER-021333; SFRH/BPD/91962/2012.

DECLARAÇÃO

Declaro que este relatório é integralmente da minha autoria, estando devidamente referenciadas as fontes e obras consultadas, bem como identificadas de modo claro as citações dessas obras. Não contém, por isso, qualquer tipo de plágio quer de textos publicados, qualquer que seja o meio dessa publicação, incluindo meios eletrónicos, quer de trabalhos académicos.

o júri

presidente	Doutora Maria Helena Abreu Silva, Professora Auxiliar do Departamento de Biologia da Universidade de Aveiro
orientadora	Doutora Camila Cabral Portugal Investigadora do Instituto de Biologia Molecular e Celular (IBMC) da Universidade de Porto
arguente	Doutor António Francisco Rosa Gomes Ambrósio Investigador Principal da Faculdade de Medicina da Universidade de Coimbra

agradecimentos

À minha orientadora, Camila Cabral, pela vontade de ensinar, pela paciência, pelo encorajamento e apoio constante ao longo de todo o trabalho, pela alegria contagiante e amizade. Obrigada por todas a soluções mágicas que arranjaste quando eu julgava que "tudo estava perdido". Sobretudo, obrigada por acreditares em mim!

Ao Doutor João Relvas pela oportunidade de estágio concedida, pela discussão de ideias e apoio prestados ao longo do trabalho desenvolvido. Por ser um exemplo enquanto investigador.

Ao Renato por todos os ensinamentos, paciência e disponibilidade. Obrigada por todas as horas em que me ajudaste a fazer quantificações, pelas ajudas no microscópio e discussão de ideias.

À Teresa por toda a ajuda, pela partilha de alegrias e angústias, pela amizade e companheirismo. (Desculpa por não teres a Camila só para ti… Ehehe)

Aos colegas do GCB pela ajuda que me prestaram ao longo do trabalho.

À família pelo apoio incondicional, pela motivação e por me ajudarem a crescer profissional e pessoalmente.

Às minhas meninas por todo o carinho e por serem uma alegria constante na minha vida.
Ps: A Catocha já acabou de escrever o "livro"! ☺

Ao Tiago, minha base e minha fonte de felicidade. Pela paciência, conselhos, motivação e inspiração. Obrigada!

A todos, **MUITO OBRIGADA!**

palavras-chave

Profilina 1, células da microglia, activação da microglia, neuroinflamação, espécies reativas de oxigénio.

resumo

As células da microglia são células imunes residentes no sistema nervoso central (SNC) e desempenham um papel importante em processos neuroinflamatórios. Estas células são responsáveis por monitorizar o parênquima neuronal, sendo capazes de responder rapidamente a danos no SNC. Após ativação, a microglia altera a sua morfologia e o seu perfil de expressão de proteínas. O processo de ativação induz a proliferação, migração para a foco da lesão, aumento da capacidade fagocítica, bem como produção e libertação de espécies reativas de oxigénio (EROs), espécies reativas de azoto e citocinas (pro- e anti-inflamatórias). A ativação da microglia é essencial para a reparação de tecidos e a manutenção da homeostasia do SNC. No entanto, a ativação crónica ou a sua desregulação podem contribuir para a patofisiologia de doenças neurodegenerativas. Assim sendo, o estudo dos mecanismos subjacentes à ativação das células da microglia é importante para ajudar a definir e desenvolver estratégias terapêuticas apropriadas para prevenir a sua ativação crónica. Um estudo anterior reportou o aumento dos níveis de RNAm da profilina (Pfn) em células da microglia no hipocampus de ratos após lesão unilateral no córtex entorrinal, sugerindo que a Pfn poderá estar envolvida no processo de ativação da microglia. A Pfn1 é uma proteína de ligação à actina que regula a polimerização do citoesqueleto de actina, sendo importante em diversos processos celulares, incluindo motilidade, proliferação e sobrevivência. Neste trabalho, nós estudamos o papel da Pfn1 na função da microglia. Para tal, utilizamos linhas celulares e células primárias de microglias corticais de rato nas quais reduzimos a expressão da Pfn1 e avaliamos o seu estado de ativação com base em marcadores clássicos de ativação, tais como: fagocitose, libertação de glutamato, produção e libertação de EROs e citocinas pro- e anti-inflamatórias. Nós demonstramos que a Pfn1 (i) se encontra mais ativa após estímulo da microglia por hipoxia, (ii) modula as assinaturas pro- e anti-inflamatória da microglia e (iii) desempenha um papel importante na produção de EROs pela microglia. Nesse estudo concluímos que a Pfn1 é uma proteína importante para o funcionamento da microglia, desempenhando um papel essencial na ativação da microglia, independentemente da polarização pró ou anti-inflamatória.

keywords

Profilin 1, microglia, microglial activation, neuroinflammation, reactive oxygen species.

abstract

Microglial cells are the resident immune cells of central nervous system (CNS) and the major players in neuroinflammation. These cells are also responsible for surveilling the neuronal microenvironment, and upon injury to the CNS they change their morphology and molecular profile and become activated. Activated status is associated with microglia proliferation, migration to injury foci, increased phagocytic capacity, production and release of reactive oxygen species (ROS), cytokines (pro- or anti-inflammatory) and reactive nitrogen species. Microglia activation is crucial for tissue repair in the healthy brain. However, their chronic activation or deregulation might contribute for the pathophysiology of neurodegenerative diseases. A better understanding of the mechanisms underlying microglial cell activation is important for defining targets and develop appropriate therapeutic strategies to control the chronic activation of microglia. It has been observed an increase in profilin (Pfn) mRNA in microglial cells in the rat hippocampus after unilateral ablation of its major extrinsic input, the entorhinal cortex. This observation suggested that Pfn might be involved in microglia activation. Pfn1 is an actin binding protein that controls assembly and disassembly of actin filaments and is important for several cellular processes, including, motility, cell proliferation and survival. Here, we studied the role of Pfn1 in microglial cell function. For that, we used primary cortical microglial cell cultures and microglial cell lines in which we knocked down Pfn1 expression and assessed the activation status of microglia, based on classical activation markers, such as: phagocytosis, glutamate release, reactive oxygen species (ROS), pro- and anti-inflammatory cytokines. We demonstrated that Pfn1 (i) is more active in hypoxia-challenged microglia, (ii) modulates microglia pro- and anti-inflammatory signatures and (iii) plays a critical role in ROS generation in microglia. Altogether, we conclude that Pfn1 is a key protein for microglia homeostasis, playing an essential role in their activation, regardless the polarization into a pro or anti-inflammatory signature.

Table of Contents

Abbreviations list

ALS	Amyotrophic lateral sclerosis
ARE	Antioxidant response element
ATP	Adenosine triphosphate
BSA	Bovine serum albumin
CD	Cluster of differentiation
CFP	Cyan fluorescent protein
CNS	Central nervous system
CX3CL1	CX3C-chemokine ligand 1
CX3CR1	CX3C-chemokine receptor 1
DAG	Diacylglycerol
DAMP	Damage-associated molecular pattern
DAPI	Diamidino-2-phenylindole
FBS	Fetal bovine serum
FRET	Förster resonance energy transfer
GAPDH	Glyceraldehyde 3-phosphate dehydrogenase
GCLC	Glutamate-cysteine ligase catalytic subunit
H3	Histone 3
HBSS	Hank's Balanced Salt Solution
HMGB1	High-mobility group box 1
HO-1	Heme oxygenase-1
Iba1	Ionized calcium-binding adapter molecule 1
IκB	Inhibitor of NF-κB
IKK	IκB kinase
IL	Interleukin
iNOS	Inducible nitric oxide synthase

IP3	Inositol 1,4,5-trisphosphate
Keap1	Cullin 3-specific adaptor protein
LB	Lysogeny broth
LPS	Lipopolysaccharide
MAPK	Mitogen-activated protein kinase
MP-PFA	Microtubule protection- paraformaldehyde
NADPH	Nicotinamide adenine dinucleotide phosphate
NF-κB	Nuclear factor kappa B
NO	Nitric oxide
NOS	Nitric oxide synthase
NOX	NADPH oxidase
NRF2	Nuclear factor erythroid 2–related factor 2
NTC	No temple control
PAMP	Pathogen-associated molecular pattern
PBS	Phosphate-buffered saline
PCR	Polymerase Chain Reaction
Pen/Strep	Penicillin Streptomycin
PFA	Paraformaldehyde
Pfn	Profilin
PIP2	phosphatidylinositide-4,5-bisphophate
PLC	Phospholipase-C
PLP	Proly-L-proline
PRR	Pattern-recognition receptor
RAGE	Receptor for advanced glycation end-products
RNS	Reactive nitrogen species
ROCK	Rho associated coil-coil kinase
ROS	Reactive oxygen species
RT	Room temperature

SEM	Standard error of the mean
shRNA	Small hairpin RNA
TGF-β	Transforming growth factor beta
TLR	Toll-like receptor
TNF	Tumor necrosis factor
Txnrd1	Thioredoxin reductase 1
YFP	Yellow fluorescent protein
Ywhaz	Tyrosine 3-monooxygenase/tryptophan 5-monooxygenase activation protein, zeta

List of figures

1. Introduction

1.1. Microglia

Microglial cells, the resident immune cells of central nervous system (CNS), are responsible for the surveillance of the neural microenvironment quickly responding to altered neuronal activity and injury. The concept of microglia as a defined cellular element of the CNS was introduced by Ramón y Cajal and Pío del Río Hortega during 1920s (Kettenmann, Hanisch et al. 2011). Microglial cells constitute up to 10% of the glial cells of the adult CNS, being heterogeneously distributed throughout different brain regions. The most microglia-enriched areas in the CNS are the hippocampus, olfactory bulb, telencephalon, basal ganglia and substantia *nigra* (Lawson, Perry et al. 1990).

1.1.1. Origin and development

Mice microglial cells derive from primitive myeloid progenitors that leave the yolk sac around E8.5–E9.0 and migrate to the neural tube via primitive bloodstream. The first precursors have low expression of cluster of differentiation 45 (CD45) and high expression of c-kit. After leaving the yolk sac, the progenitors begin to express lineage-specific genes and become differentiated into mature microglia. This population of microglia is maintained throughout life by self-renewal with little contribution from cells outside the CNS like bone-marrow macrophages (Salter and Beggs 2014).

After arriving at the brain parenchyma, microglia alters its morphology and become ramified. This phenotype may be induced by adenosine triphosphate (ATP) (Hanisch 2002) and transforming growth factor beta (TGF-β) released by astrocytes (Schilling, Nitsch et al. 2001). Furthermore, microglial cell development is regulated by colony stimulating factor 1 (CSF-1) receptor and its ligand interleukin-34 (IL-34), which is mainly produced by neurons (Kettenmann, Hanisch et al. 2011, Salter and Beggs 2014).

Although microglia and macrophage share immune functions and express diverse common proteins, such as CD11b, CD14 and EGF-like module-containing mucin-like hormone

receptor-like 1 (EMR1), they are highly distinguishable cell populations with different transcriptional patterns. There are growing evidences supporting the idea that microglial cells are not just classical immune effector cells, having critical functions in development, connectivity and plasticity of the CNS (Saijo and Glass 2011, Salter and Beggs 2014).

1.1.2. Surveilling microglia

In physiological conditions, microglial cells present a ramified morphology with thin and very motile processes that are continuously extending and retracting in order to sense the surrounding environment (fig. 1A). Microglial cells respond to neuronal activity and spread their processes toward active synapses, increasing the contact with highly active neurons. Microglial cells in homeostatic conditions are thus not in "resting" state, unlike what was previously thought. On the contrary, microglial cells are in a very active "surveilling" state (Salter and Beggs 2014). Such state is dependent on neuronal signals like CX3C-chemokine ligand 1 (CX3CL1), CD47, CD200 and CD22 (fig. 1B) (Kettenmann, Hanisch et al. 2011, Saijo and Glass 2011).

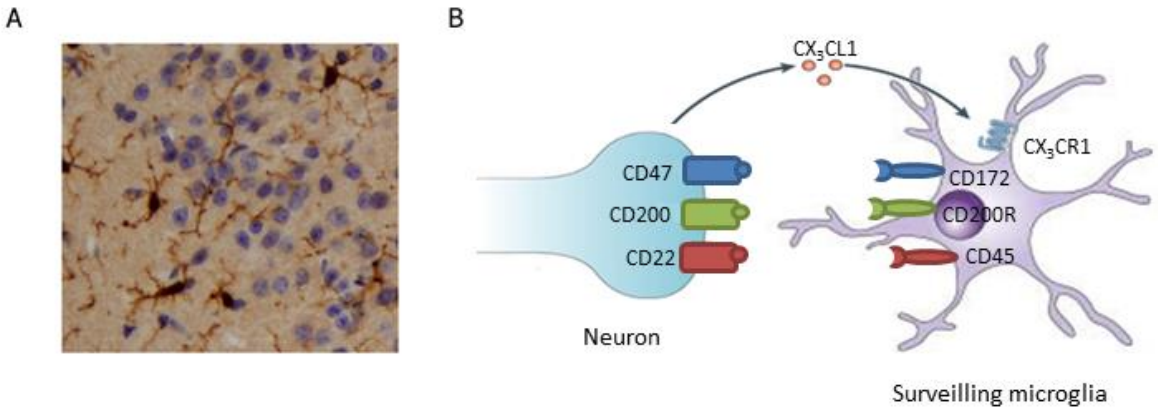

Figure 1 - Surveilling state of microglia. (A) Immunohistochemistry for ionized calcium-binding adapter molecule 1 (Iba1) in mouse cortex shows microglia and its classical ramified morphology in surveilling state. Adapted from Kettenmann, Hanisch et al. 2011. **(B)** Surveilling state of microglia is maintained through signals released by neurons - CX3CL1 -, that are recognize by microglia receptor CX3CR1 and interaction between neuronal cell-surface proteins CD47, CD200 and CD22 and respective microglia receptors CD172, CD200R and CD45. Adapted from Saijo and Glass 2011. CX3CL1: CX3C-chemokine ligand 1; CX3CR1: CX3C-chemokine receptor 1; CD: Cluster of differentiation.

Several *in vitro* studies indicate that microglia can secrete proteins that are important for the growth and development of neurons, as well as important substances for maintaining

neuronal maturation. Examples of these neurotrophic factors are insulin-like growth factor 1 (IGF1), brain-derived neurotrophic factor (BDNF) and TGF-β (Saijo and Glass 2011). Also, the phagocytic capacity of microglia is crucial for CNS development. During neurogenesis, a significant amount of neurons undergo programmed cell death and, in order to prevent damaging effects in the surrounding tissue, apoptotic neurons have to be quickly removed. Microglia can recognize, engulf and digest apoptotic neurons, contributing to the integrity of the nervous system (Peri and Nusslein-Volhard 2008). Moreover, these cells can sense neurons committed to die and can instruct neuronal apoptosis by secreting neurotoxic agents, for example tumor necrosis factor (TNF). Microglial cells are also critical for synaptic pruning, which consist in the elimination of excessive synapsis made by developing neurons (Saijo and Glass 2011, Salter and Beggs 2014).

1.1.3. Activated microglia

Microglia activation is a highly regulated process, in other to protect the brain parenchyma from damaging effects of an immune reaction. Microglia become activated upon diverse stimuli, ranging from altered neuronal activity, infections, trauma, ischemia to neurodegenerative diseases (Hausler, Prinz et al. 2002). During activation, microglia experience rapid and profound morphological changes, modifications in gene expression profile and functional behaviour. Activated microglia turn into an amoeboid-like phenotype with shorter and thicker processes and are able to proliferate and migrate to injury foci following chemotactic gradients released by neuronal or immune cells (Kettenmann, Hanisch et al. 2011).

1.1.3.1. Activation process

Microglial cells express a plethora of receptors that recognize multiple signs of homeostasis disturbance (fig.2), including receptors for pathogen-associated molecular patterns (PAMPs). These receptors, known as pattern-recognition receptors (PRRs), include toll-like receptors (TLRs) and NOD-like receptors (NLRs), among others. Besides pathogen recognition, TLRs also detect endogenous damage-associated molecular patterns (DAMPs), metabolic products or molecules released by dead cells (Saijo and Glass 2011).

Classically, microglia activation is studied upon stimulus with bacterial endotoxin lipopolysaccharide (LPS), a component of the cell wall of Gram-negative bacteria. LPS is recognized by TLR4 and CD14, which triggers downstream signalling cascades dependent on

adaptor molecules such as myeloid differentiation primary response protein 88 (MYD88) and TIR domain-containing adaptor protein inducing IFNβ (TRIF). These signalling cascades lead to activation of JNK and p38 signalling pathways and activation of transcription factor nuclear kappa B (NF-κB) resulting in the transcription of pro-inflammatory regulators (Kawai and Akira 2010).

Microglial cells also express diverse non-PRRs, important for recognition of DAMPs in CNS, such as purinergic receptors and receptors for advanced glycation end-products (RAGE). Purinergic receptors can detect nucleoside triphosphates released by damaged cells and activate downstream extracellular signal-regulated kinase (ERK) pathway, leading to signalling events that induce the transcription of pro-inflammatory mediators. On the other hand, RAGE receptors are able to detect glycation end-products and high-mobility group box 1 (HMGB1), a nuclear protein released by necrotic cells. HMGB1 detection also triggers the activation of pro-inflammatory genes (Saijo and Glass 2011).

Microglia activation can be amplified by activated astrocytes (fig. 2), increasing the production of neurotoxic factors. Astrocytes express TLR4 and react to LPS, although with less extent than microglia. Activated astrocytes increase the expression of pro-inflammatory genes and CSF1 which promotes further microglia activation and microgliosis. In turn, microglia activation is responsible for increasing astrocyte activation by releasing factors like IL-1β and TNF, creating a feedback loop (Saijo and Glass 2011).

1.1.3.2. Classical pro-inflammatory signature

As mentioned above, microglial cells have different receptors and signalling pathways involved in the activation process. Different stimuli may induce distinct gene expression profiles leading to different phenotypes (fig.2).

Microglia can be activated toward a classical pro-inflammatory phenotype in which cells release pro-inflammatory cytokines such as TNF, IL-1β and IL-6 and chemokines (Rojo, McBean et al. 2014). These molecules can further recruit other microglia in the vicinity and peripheral immune cells, affecting their activation state. Moreover, activated microglial cells phagocytose pathogens and present their antigens via major histocompatibility complex class II (MHCII) molecules. (Hanisch 2002, Saijo and Glass 2011).

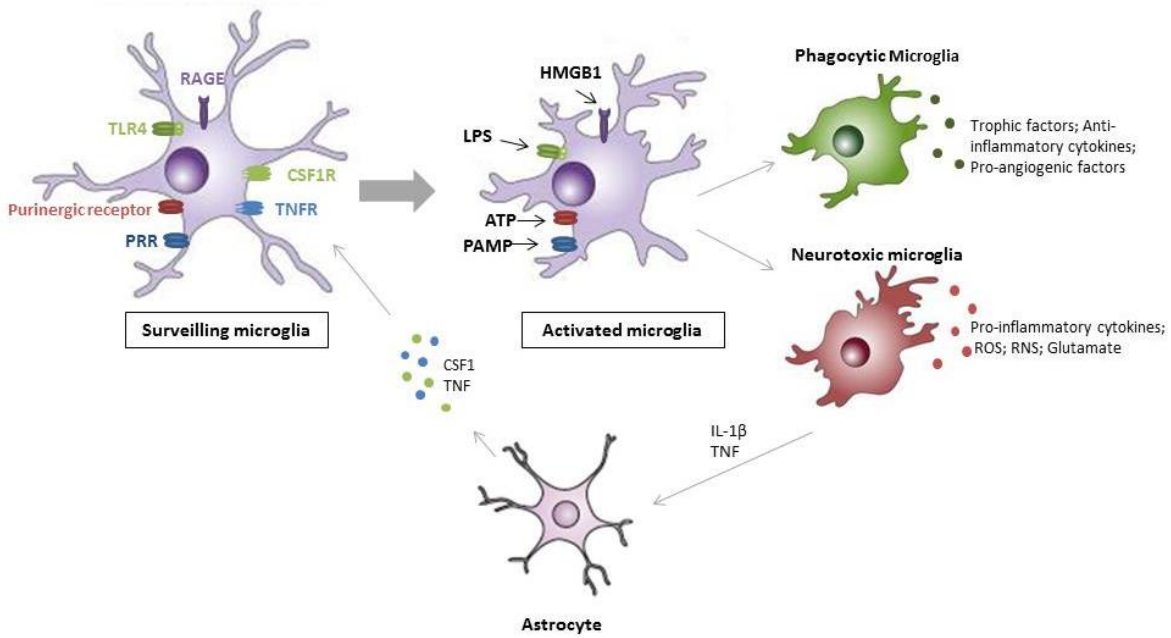

Figure 2 – Microglia activation process. In healthy central nervous system (CNS), microglial cells are continuously scanning their microenvironment. Surveilling microglia have multiple receptors that recognize signs of homeostasis disturbance, such as: pattern-recognition receptors (PRRs), that includes toll-like receptor 4 (TLR4); purinergic receptors and receptors for advanced glycation end-products (RAGE). PRRs recognize pathogen-associated molecular patterns (PAMPs) present in bacteria and virus. For example, lipopolysaccharide (LPS), a component of the cell walls of Gram-negative bacteria, is detected by TLR4. On the other hand, purinergic receptors and RAGE detect endogenous damage-associated molecular patterns (DAMPs) released by damaged cells, for example: adenosine triphosphate (ATP), histones and High-mobility group box 1 (HMGB1). After exposure to these chemical signals, microglia become activated and respond rapidly and migrate toward injury foci. Morphologically, microglia became less complex and appears with an amoeboid shape. Activated microglia can acquire two distinct phenotypes: neurotoxic microglia (red) and phagocytic microglia (green). The first phenotype corresponds to a classical pro-inflammatory phenotype, in which microglia produce and release high amounts of pro-inflammatory cytokines; reactive oxygen species (ROS); reactive nitrogen species (RNS) and glutamate. This phenotype is important to protect CNS against pathogens or damaged cells. Although, the factors released by this activated microglia are also neurotoxic. On other hand, the second phenotype corresponds to an alternative activation state in which microglia have increased phagocytic ability, express wound healing genes, produce and release anti-inflammatory cytokines and molecules that promote tissue repair, such as trophic factors and pro-angiogenic factors. Microglia activation leads to astrocytes activation trough release of interleukin-1 beta (IL-1β) and tumor necrosis factor (TNF). In turn, activated astrocytes produce and release TNF and colony-stimulating factor 1 (CSF1), which amplify microglia activation thus generating a feedback loop. Adapted from Saijo and Glass 2011, Garden and La Spada 2012.

Besides pro-inflammatory cytokines, activated microglia produce and release high amounts of reactive oxygen and nitrogen species (ROS and RNS), proteases, and glutamate. The elevation of ROS/RNS levels is mainly due to the activation of reduced nicotinamide adenine

dinucleotide phosphate (NADPH) oxidase (NOX) and nitric oxide synthase (NOS) enzymes, respectively. The production of ROS and RNS is part of a cytotoxic attack against invading pathogens (Saijo and Glass 2011, Rojo, McBean et al. 2014). Furthermore, ROS and RNS are important second messengers. The transcription factor NF-κB, key player in activation of inflammatory associated genes, can be regulated by ROS.

ROS and RNS production in microglia

ROS are a group of reactive oxygen-derived molecules, such as: oxygen radicals, hydrogen peroxide, peroxynitrite, and nitric oxide (NO). ROS can induce oxidative modification of nucleic acids, sugars, lipids and proteins. Also, they play a role in intracellular signalling through the inactivation of specific enzymes (e.g. the inactivation of protein tyrosine phosphatases leads to increased tyrosine kinase activity). Several enzymes can generate intracellular ROS, such as: Xanthine oxidase, cyclooxygenases, NOS, mitochondrial oxidases, and NOXes (Heyworth, Knaus et al. 1993). In microglia, as well as in others cells types, incomplete reduction of molecular oxygen in mitochondrial respiration generates ROS that are important for several cellular functions. However, one of the most important source of ROS in microglia is activation of NOX (Block and Hong 2005). NOX is a multi-subunit enzyme complex which activity results in the generation of superoxide anion as primary product by transferring electrons from NADPH to molecular oxygen. In normal conditions, some complex subunits are in the cytosol (p40phox, p47phox, and p67phox) and others are in the cell membrane (p22phox and gp91phox) (Heyworth, Knaus et al. 1993, Cheng, Diebold et al. 2006, McCann and Roulston 2013). Upon stimulation, the complex is assembled in the plasma membrane and becomes catalytically active. NOX can be activated in response to growth factors or inflammatory cytokines that signal through the Rho-like small GTPases Rac1 or Rac2 (fig.3) (Cheng, Diebold et al. 2006, McCann and Roulston 2013). ROS generated by NOX act on surrounding cells and constitute a cytotoxic attack. Further, ROS generated by NOX play an important role in modulating microglia function, including the release of neurotransmitters and production of pro-inflammatory cytokines (Giudice, Arra et al. 2010).

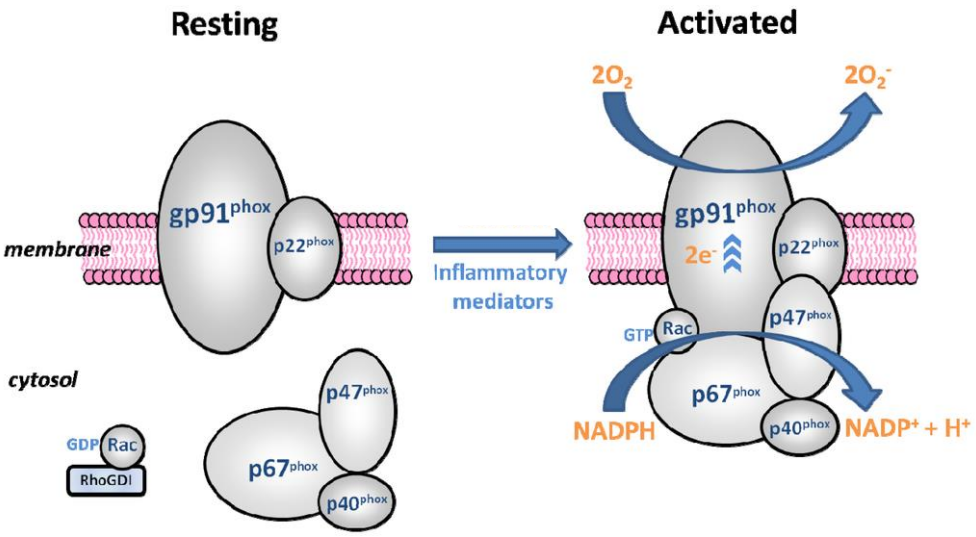

Figure 3 – Schematic representation of NADPH oxidase in resting and activated conditions. In resting conditions, NADPH oxidase is inactive and some complex subunits are in the cytosol (p40phox, p47phox, and p67phox) while others are in the cell membrane ($p22^{phox}$ and $gp91^{phox}$). Rac is stabilized in cytosol by Rho GDP-dissociation inhibitor (RhoGDI) which prevents nucleotide exchange and membrane association. Upon stimulation by inflammatory mediators, the complex is assembled in the plasma membrane, becoming activated. After activation, p47phox becomes phosphorylated triggering conformational changes that result in its translocation to the membrane and assembly to p22phox and gp91phox complex (known as flavocytochrome). Furthermore, cell activation leads to activation of guanine nucleotide exchange factors (GEFs, not represented), causing exchange of GDP for GTP in Rac and its consequent activation and translocation to the membrane. Activated Rac binds to the flavocytochrome. When assembled, NOX generate superoxide (O^{2-}) by transferring electrons ($2e^-$) from NADPH to molecular oxygen ($2O^2$). Adapted from McCann and Roulston 2013.

As mentioned before, one of the outcomes of activated microglia is the production of NO. In general, NO can be synthetized by tree isoforms of NOS: NOS1 (or neuronal NOS); NOS2 (inducible NOS – iNOS) and NOS3 (endothelial NOS). NOS 1 and NOS3 are constitutively expressed and become activated upon increase of intracellular Ca^{2+} (Brown 2010). On the other hand, iNOS is transcriptionally induced by inflammatory mediators (e.g. LPS, TNF, IL-1β) and its activation is independent of the increase in intracellular Ca^{2+} (Murphy 2000). In microglia, the main source of NO is iNOS, which is synthetized from L-Arginine. Nitric oxide and L-citrulline are generated from L-arginine, in the presence of oxygen, NADPH, as well as the following co-factors: flavin mononucleotide (FMN), flavin adenine dinucleotide (FAD), haem and tetrahydrobiopterin (BH4) (Rojo, McBean et al. 2014). At low concentrations, NO is important in CNS physiology and participates in neurotransmission and cognition (Calabrese, Mancuso et al. 2007), while high

concentrations of NO are cytotoxic and may cause neuronal death by energy depletion mediated-necrosis, or by nitrosative stress mediated-apoptosis (Brown and Cooper 1994, Brown 2010).

Nuclear factor-kappa B

NF-κB consists of a family of transcription factors that play critical roles in inflammatory responses and environmental and cellular damage (Rojo, McBean et al. 2014). In mammals, the NF-κB family consists of five proteins: NF-κB1 (p50), NF-κB2 (p52), RelA (p65), RelB, and c-Rel. These proteins have 300 amino acid long amino-terminal Rel homology domain (RHD) (Oeckinghaus and Ghosh 2009). This conserved sequence is required for dimerization, binding to DNA, interaction with inhibitors of NF-κB proteins (IκBs) and nuclear translocation. The association of different dimers leads to different signals mediated through NF-κB. The p65/p50 dimer is the most well characterized in microglia and it is able to activate pro-inflammatory genes (Rojo, McBean et al. 2014).

In normal conditions, NF-κB dimers remain inactive in the cytosol through interaction with IκBs. Degradation of IκBs is induced by IκB kinase (IKK) phosphorylation. This phosphorylation targets IκB for ubiquitin/proteasome degradation, and consequent NF-κB stabilization and translocation to the nucleus (fig. 4). NF-κB translocation to the nucleus induces the transcription of many target genes, for instance, cytokines (e.g. TNF; IL-1β, IL-6), chemokines (C-X-C motif) ligand 1, 2 and 10 (CXCL1, CXCL2 and CXCL10), adhesion molecules (e.g vascular cell adhesion molecule 1 (VCAM1), intercellular adhesion molecule 1 (ICAM1) and enzymes (e.g. iNOS) (Oeckinghaus and Ghosh 2009, Rojo, McBean et al. 2014). Although NF-κB activity is inducible in most cells, it can be constitutively active in some cell types, such as macrophages and neurons (Oeckinghaus and Ghosh 2009).

ROS can regulate NF-κB activity by different mechanisms, for example, ROS can activate IKK (e.g. IKKβ) leading to phosphorylation of specific serines in IκB. This phosphorylation targets IκB for ubiquitin/proteasome degradation, and consequent NF-κB stabilization and translocation to the nucleus (Rojo, McBean et al. 2014).

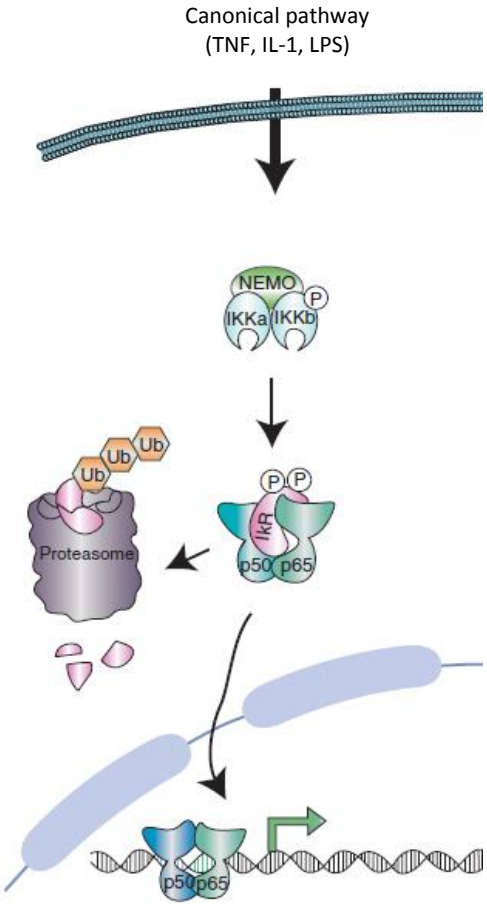

Figure 4 – Canonical activation pathway of NF-κB. In normal conditions, NF-κB dimers remain inactive in cytosol trough interaction with IκBs (e.g IκR). However, when stimulated (e.g through TNF; IL-1; LPS) there is activation of IκB kinase (constituted by two catalytically active kinases, IKKa and IKKb, and the regulatory subunit -NEMO) which phosphorylates IκB and leads to its ubiquitination and proteasomal degradation. As a consequence, free p50/p65 is translocated to nucleus where it can activate the transcription of target genes. Adapted from Oeckinghaus and Ghosh 2009. IκBs: Inhibitor of NF-κB; TNF: Tumor necrosis factor; IL-1:Interleukine 1; LPS: lipopolysaccharide; NEMO:NF-kappa-B essential modulator.

Glutamate release

Glutamate is an excitatory neurotransmitter released by microglia that induces excitotoxicity and may contribute to neuronal damage in neurodegenerative diseases. Glutamate can be released from microglia by different mechanisms, one of which is the increased expression and/or activity of the cystine/glutamate antiporter xc- (Kettenmann, Hanisch et al. 2011). This transporter exchanges glutamate for cystine according to the respective concentration gradients. In activated microglial cells increased activation of this exchanger is associated to high demand for

cystine/cysteine. Cystine is required for the synthesis of glutathione, the major antioxidant molecule in microglia, which is rapidly consumed in activated microglia due to increased oxidizing conditions (Kettenmann, Hanisch et al. 2011, Rojo, McBean et al. 2014). As a consequence, the release of glutamate can induce neuronal loss and toxicity to other CNS cells by either overstimulation of glutamate receptors or by reversing xc- (Kumar, Singh et al. 2010). Another mechanism for glutamate release is mediated by TNF. This cytokine induces extensive glutamate release from microglia in an autocrine fashion by up-regulating glutaminase, an enzyme that generates glutamate from glutamine. Such TNF-induced glutamate release occurs mainly through the connexin-32 hemichannel (Takeuchi, Jin et al. 2006).

1.1.3.3. Alternative anti-inflammatory signature

The pro-inflammatory activation of microglia is often followed by the acquisition of an alternative activation phenotype in which microglia assume a neuroprotective profile with increased phagocytic capacity and production and release of high amounts of anti-inflammatory cytokines such as TGF-β and IL-10 (Ransohoff and Perry 2009, Kettenmann, Hanisch et al. 2011, Rojo, McBean et al. 2014). After a pro-inflammatory response, both ROS and RNS amounts must be lowered. In order to achieve that, microglia activate the transcription factor nuclear factor erythroid 2–related factor 2 (NRF2), which is considered the master modulator of redox homeostasis (fig.5) (Rojo, McBean et al. 2014). Moreover, anti-inflammatory phenotype is characterized by expression of wound healing genes, such as genes coding for arginase-1, scavenger receptors, neurotrophins and growth factors. This response is crucial for recovering homeostasis and to turn off the pro-inflammatory phenotype in microglia (Rojo, McBean et al. 2014)

Arginase-1 expression and activity

Microglia anti-inflammatory phenotype is associated to the expression and activity of arginase-1. Arginase-1 is an enzyme that uses L-arginine, the same substrate used by iNOS, to generate ornithine. Since both enzymes compete by the same subtract, arginase-1 is considered an important regulator of NO production. In the anti-inflammatory phenotype, iNOS expression is decreased and arginase-1 expression can be induced by IL-4 and IL-13, for example. On the

contrary, in pro-inflammatory conditions, both iNOS expression and activity are up-regulated. (Rojo, McBean et al. 2014).

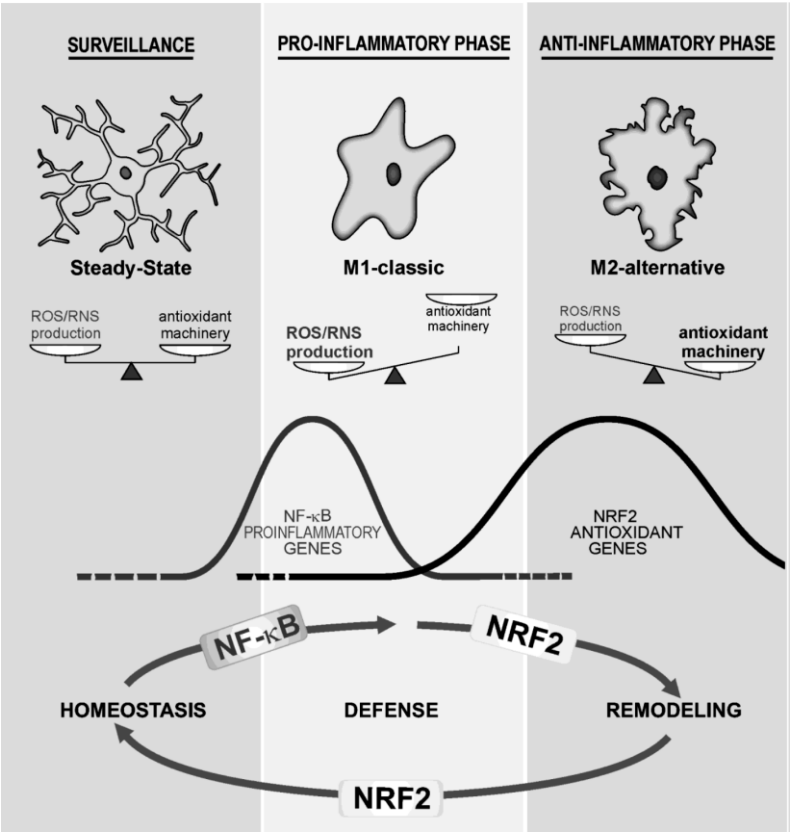

Figure 5 – Microglial cell phenotype is regulated by ROS through activation of NF-κB and NRF2. In homeostatic conditions, microglia present low levels of ROS/RNS, in a balance that is maintained by the antioxidant machinery of the cell. Upon pro-inflammatory stimulation, microglia increase ROS/RNS production, which function as a cytotoxic attack against pathogens or damaged cells. Also, ROS/RNS are involved in intracellular signalling cascades. NF-κB activity is induced by increased levels of ROS and leads to expression of pro-inflammatory mediators, resulting in more ROS/RNS production. After the pro-inflammatory response, NRF2 activity is increased in response to ROS/RNS in order to restore redox homeostasis, thus favouring an anti-inflammatory phenotype. Adapted from Rojo, McBean et al. 2014. NF-κB: Factor nuclear kappa B; NRF2: Nuclear factor erythroid 2–related factor 2; ROS: reactive oxygen species; RNS: reactive nitrogen species.

NRF2 signalling pathway

The transcription factor NRF2 plays an important role in antioxidant protection of microglial cells by enhancing the expression of cytoprotective genes (Rojo, McBean et al. 2014). For example, it has been demonstrated that the administration of LPS or MPTP (1-Methyl-4-

phenyl-1,2,3,6-tetrahydropyridine) results in enhanced microglial pro-inflammatory response in NRF2-null mice when compared to control animals. Moreover, the anti-inflammatory response is decreased in NFR2 deficient mice (Rojo, Innamorato et al. 2010).

NRF2 controls the expression of genes encoding enzymes involved in ROS clearance (e.g. superoxide dismutase-3 - SOD3), synthesis of reducing factors (e.g. glutamate-cysteine ligase - GCLC, which is involved in the generation of glutathione), production of antioxidant molecules (e.g. heme oxygenase, HO-1), and production of reduced cofactors and proteins (e.g. thioredoxin reductase 1 - TXNRD1) (Jung and Kwak 2010).

In homeostatic conditions, NRF2 has a short half-life due to binding to a Cullin 3-specific adaptor protein (Keap1). Keap1 anchors NRF2 in the cytoplasm targeting it for ubiquitination and proteasomal degradation (Kensler, Wakabayashi et al. 2007, Giudice, Arra et al. 2010). Upon exposure to oxidative conditions, critical cysteine residues in Keap1 are oxidized and its ligase activity is inhibited. As a consequence, NFR2 escapes degradation and is translocated to the nucleus where it heterodimerizes with other transcription factors (e.g., sMaf, ATF4, JunD, PMF-1). Heterodimers are able to bind to cis-acting antioxidant response elements (ARE) located in the promoter region of target genes and induce their expression (fig.6). Moreover, NRF2 may be controlled by other mechanisms such as: signalling kinases regulated by ROS, or epigenetic mechanisms like acetylation, CpG island methylation of its promoter region and micro ribonucleic acid (miRNA) generation (Bryan, Olayanju et al. 2013, Rojo, McBean et al. 2014).

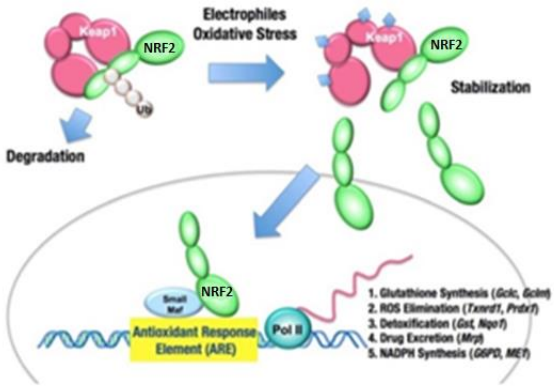

Figure 6 - The Keap1-NRF2 system. Under homeostatic normal, Keap1 reduces the levels of NRF2 in cytosol by directing it to ubiquitination and proteasomal degradation. Upon oxidative or electrophilic stress, Keap1 becomes oxidized in critical cysteine residues and is inactivated. Free NRF2 is stabilized and translocated to nucleus, where it binds to antioxidant response elements (AREs) through heteromerizing with the small Maf protein and activates the expression of cytoprotective genes. Adapted from Mitsuishi, Motohashi et al. 2012. Keap1: Cullin 3-specific adaptor protein; NRF2: Nuclear factor erythroid 2–related factor 2.

Microglia phagocytosis

Microglial cells are able to migrate toward the site of injury and phagocytose pathogens or damaged cells. In general terms, the process of phagocytosis implies the vesicular ingestion of extracellular particles. After antigen recognition, the cell extends protusions (pseudopodia) that surround the material. The pseudopods fusion encloses the material in a phagosome, entering the endocytic processing pathway. Inside the cell, phagosomes fuse with lysosomes, forming phagolysosomes where several enzymes hydrolyse the material. Digested contents are eliminated by exocytosis. The phagocytic process is highly dependent on rearrangements of the actin cytoskeleton triggered by environmental signals (Neumann, Kotter et al. 2009).

Phagocytes have two different types of phagocytic receptors for antigen recognition: (i) receptors that recognize pathogens and trigger a pro-inflammatory response, such as TLRs that recognize PAMPs or Fc receptors that interact with opsonized antigens (Neumann, Kotter et al. 2009); and (ii) receptors recognizing exposure of apoptotic material, including those that recognize phosphatidylserine (Neumann, Kotter et al. 2009). The latter are associated with an anti-inflammatory response.

1.1.4. Microglia in neuroprotection versus neurodegeneration

While microglia-mediated inflammation is crucial for tissue repair for the maintenance of healthy brain, their chronic activation or deregulation contributes to the pathophysiology of several neurodegenerative diseases. For instance, microglia activation has been reported in the brain and spinal cord of patients with Amyotrophic Lateral Sclerosis (ALS), a progressive neurodegenerative disease of motor neurons. Microglia activation in the asymptomatic phase of ALS might be beneficial by playing a protective role in the CNS. However, during disease progression, microglia activation becomes deleterious contributing to neuronal injury and loss (Boillee, Vande Velde et al. 2006).

In chronic neuroinflammatory diseases (e.g. multiple sclerosis), microglial cells are constantly exposed to disease-related molecules or damaged cells that lead to chronic activation of microglia. As mentioned in previous sections, activated microglia release toxic compounds, increase phagocytic activity and activate an inflammatory response. Microglia activation induces pro-inflammatory phenotypes in other microglial cells, which might generate a net effect in

microglia population. A large pool of activated microglia releasing toxic factors (such as glutamate, ROS, RNS, TNF and proteases) leads to bystander damage to neurons and other CNS cells.

Considering both pathologic and beneficial roles of microglia in the CNS, the simple inhibition of microglial cell-mediated inflammation would not contribute to a beneficial outcome. In order to define targets and develop appropriate therapeutic strategies to fight excessive inflammation mediated by microglia, it is essential to understand the mechanisms underlying the process of microglial cell activation.

1.2. Microglia and profilin

Dong and colleagues suggested that profilin (Pfn), an actin-binding protein that regulates actin cytoskeleton polymerization and participates in other cellular process, might be involved in microglial activation (Dong, Ying et al. 2004). The authors used unilateral destruction of principal extrinsic input from the entorhinal cortex to the hippocampus to study microglia reactivity in rats. In this model, microglia activation is the first detectable response in the hippocampus of these rats. Microglia activation results in induction of a pro-inflammatory response and clearance of axonal debris by phagocytosis. In order to find genes associated with lesion-induced plasticity, the authors performed a cDNA microarray analysis and they found that Pfn was up-regulated upon lesion, which was further confirmed by Northern blot and in situ hybridization analysis. They also showed that Pfn expression was increased in microglial cells using the combination of in situ hybridization for Pfn messenger RNA with *in vivo* labelling for microglia using the Griffonia simplicifolia IB4 staining. The authors proposed that Pfn might modulate microglia activation via the regulation of the actin cytoskeleton. Asides from the study of Dong and colleagues, the role of Pfn in microglia function is elusive.

1.3. Profilin-1

Profilins (Pfns) are a class of evolutionarily conserved small actin-binding proteins (12-15 kD) that regulate the dynamics of actin polymerization (Carlsson, Nystrom et al. 1977). Pfn1 is the founding member of the family and Carlsson and colleagues in 1976 were the first to describe its

expression in the calf spleen. Since then, Pfn expression was observed in many organisms, such as insects, plants and mammals (Jockusch, Murk et al. 2007). In mammals, there are four distinct genes encoding for Pnfs: Pfn1 codes for the ubiquitously expressed Pfn1; Pfn2 codes for two splicing variants, one of which is expressed only in developing nervous system and differentiated neurons (Pfn2a), and the other one being mainly found in kidney (Pfn2b); Pfn3 and Pfn4 code for Pfn3 and Pfn4, respectively, which are both restricted to testis (Witke 2004, Jockusch, Murk et al. 2007).

Although Pfns are highly conserved in evolution, its sequence homology is low. Secondary and tertiary structures, on the other hand, are very similar throughout species and family members, suggesting that conformation is more important to function than amino acid sequence. Mammalian Pfns have a compact center consisting of seven beta sheets, surrounded by four alpha helices. The N- and C-terminal domains are adjacent to each other (Schutt, Myslik et al. 1993, Fedorov, Magnus et al. 1994, Domke, Federau et al. 1997). The structure of Pfn1 is represented schematically in fig.7.

In general, Pfns bind to three main classes of ligands: actin, proteins containing poly-L-proline (PLP) motifs and phosphoinositides, with preference for phosphatidylinositide-4,5-bisphophate (PIP2) (fig.7). The actin-binding site of Pfn1 do not enclose the N- and C- terminal in the folded molecule (Schutt, Myslik et al. 1993) (fig.7). Besides the potential to interact with actin, this Pfn1 domain also interacts with actin-related proteins (ARPs), such as ARP2 and ARP3.

Pfn1 interacts with proteins containing PLP motifs: 3-5 prolines residues flanked by a glycine or a alanine residue (Ding, Bae et al. 2012). The PLP interaction domain involves both the N- and C-terminal domains of Pfn1 (fig.7), not interfering with actin binding site. The vasodilator stimulated phosphoprotein (VASP) was the first ligand identified for Pfn1's PLP binding site (Reinhard, Giehl et al. 1995). Since then, several ligands have been identified, with variable function, structural organization and cellular location. Pfn1 can interact with important proteins for actin dynamics and organization, signal perception, motility, storage, transport and transcription (Jockusch, Murk et al. 2007, Ding, Bae et al. 2012).

Pfn1 also interacts with phosphatidylinositides with preference for PIP2 (Lassing and Lindberg 1985). PIP2 binding site overlaps with both actin and PLP binding sites (fig. 7). Hence, there is a competition between PIP2 and actin binding for Pfn, as well as between PIP2 and PLP (Ding, Bae et al. 2012). PIP2 binds not only to Pfn, but also to Pfn1-actin complexes, which leads to

complex dissociation. Furthermore, PIP2-Pfn interaction has the potential to interfere with several intracellular signalling cascades, since this interaction inhibits the hydrolysis of PIP2 by phospholipase C (PLC), and consequently the formation of the second messengers: Diacylglycerol (DAG) and inositol 1,4,5-trisphosphate (IP3). DAG activates protein kinase C, which activates other cytosolic proteins by phosphorylation, while IP3 activates IP3 receptors in the endoplasmic reticulum, inducing calcium release to the cytosol, which, in turn, participates in other signalling pathways. PIP2 bounded to Pfn1 can only be hydrolysed into second messengers by phosphorylated PLCγ1 (Goldschmidt-Clermont, Kim et al. 1991) (fig.8).

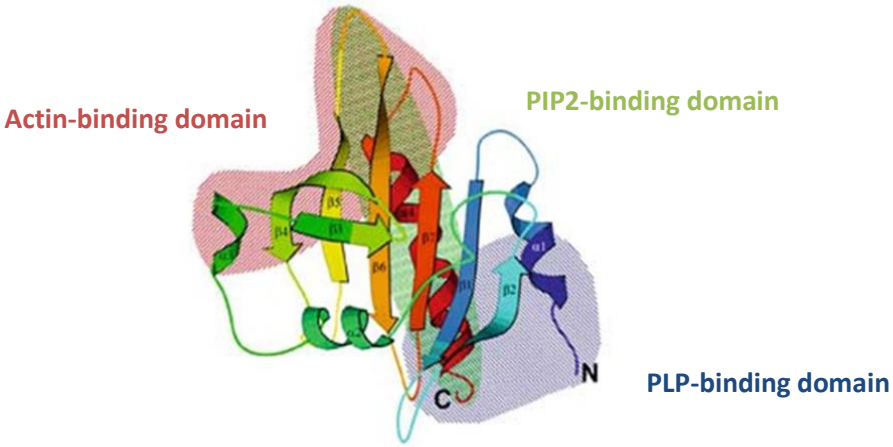

Figure 7 - Schematic representation of a profilin tertiary structure. Actin-binding domain is represented in red; PLP-binding domain in blue and PIP2-binding domain in green. Adapted from Jockusch, Murk et al. 2007. PIP2: phosphatidylinositide-4,5-bisphophate. PLP: Poly-L-proline.

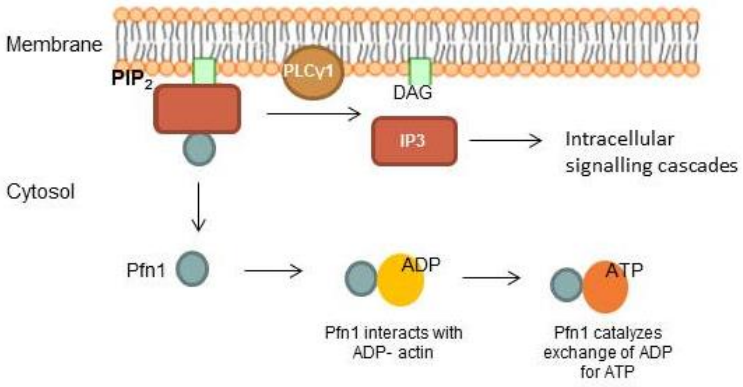

Figure 8 - Schematic representation of Pfn1 and PIP2 interaction. Pfn1 binds to phosphatidylinositides with preference for PIP2. PIP2 bounded to Pfn1 can only be hydrolysed by PLCγ1. PIP2 hydrolysis in DAG (diacylglycerol) and IP3 (inositol 1,4,5-trisphosphate) leads to Pfn1 release. In cytosol Pfn1 binds to ADP-actin and catalyses the exchange of ADP for ATP. IP3 is a second messenger and participates in intracellular signalling cascades.

1.3.1. Profilin and actin dynamics

1.3.1.1. Actin cytoskeleton

The actin cytoskeleton is a highly dynamic network composed of microfilaments (polymers of actin) and a large number of actin-binding proteins (Schmidt and Hall 1998). Classical functions of the actin cytoskeleton are to mediate cell shape changes, surface remodelling and motility. Moreover, the actin cytoskeleton is involved in cell-cell and cell-substrate interactions, in transmembrane signalling, endocytosis and secretion (Schmidt and Hall 1998, Le Clainche and Carlier 2008).

Actin exists in both as monomeric (G-actin) and polymeric (F-actin) form. The dynamic of the actin cytoskeleton is regulated by the balance between these two forms, in response to external stimuli (Schmidt and Hall 1998, Le Clainche and Carlier 2008, Lee and Dominguez 2010). Actin polymerization takes place at the barbed end of the filaments, while at the point end depolymerisation occurs (fig. 9). Actin cytoskeleton assembly is regulated at several levels, including the organization of monomers in polymers and the organization of filaments into a network. This regulation is dependent on multiple actin binding proteins that assume a wide range of functions, including: actin filament nucleation (formation of the initial 3 actin monomers complex), elongation (polymerization), severing (depolymerizing), capping (prevents adding or loss of actin subunits) and crosslinking (superorganization of actin polymers into a filamentous network) (Jockusch, Murk et al. 2007).

Moreover, the assembly and disassembly of the actin cytoskeleton are tightly regulated, thus divergent signalling pathways target diverse actin-associated proteins. The Rho family of small GTPases are key players in the actin cytoskeleton dynamics. They regulate signalling pathways linking the assembly and organization of either actin or microtubule cytoskeleton with external and internal signals. Among other Rho GTPases, RhoA, Rac1 and Cdc42 have been extensively characterized. Concerning the regulation of the actin cytoskeleton, RhoA is well known for mediating the formation of stress fibers (bundles of actin filaments that traverse the cell and reaches out focal adhesions), Rac1 induces lamellipodia (extensions of flat protusions) formation and Cdc42 promotes arrangement of filopodia (fingerlike protusions) (Schmidt and Hall 1998, Stankiewicz and Linseman 2014).

1.3.1.2. Profilin 1

Among other proteins, Pfn1 assumes an important role in regulating actin polymerization. Pfn1 forms 1:1 complexes with monomeric actin (Carlsson, Nystrom et al. 1977) and, by catalysing the exchange of ADP for ATP in actin, provides a pool of ATP-bounded monomers, which can be incorporated in free barbed ends of actin filaments (fig.9).

Furthermore, Pfn1 is important for *de novo* actin nucleation and elongation of new or pre-existing filaments, processes that are involved in membrane protrusion that is required for cell motility (fig. 10). Pfn1 is able to interact directly with N-WASP/WAVE, Ena/VASP and formins through the PLP binding domain. Members of Ena/VASP, formin and WASP/WAVE families are the majors catalysers of actin nucleation and elongation. Those are large multidomain proteins that are able to bind Pfn, G- and F-actin. The PLP stretches exposed in Ena/VASP, formin and WASP/WAVE members are able to interact with several Pfn-actin complexes simultaneously, promoting their polymerization (Jockusch, Murk et al. 2007).

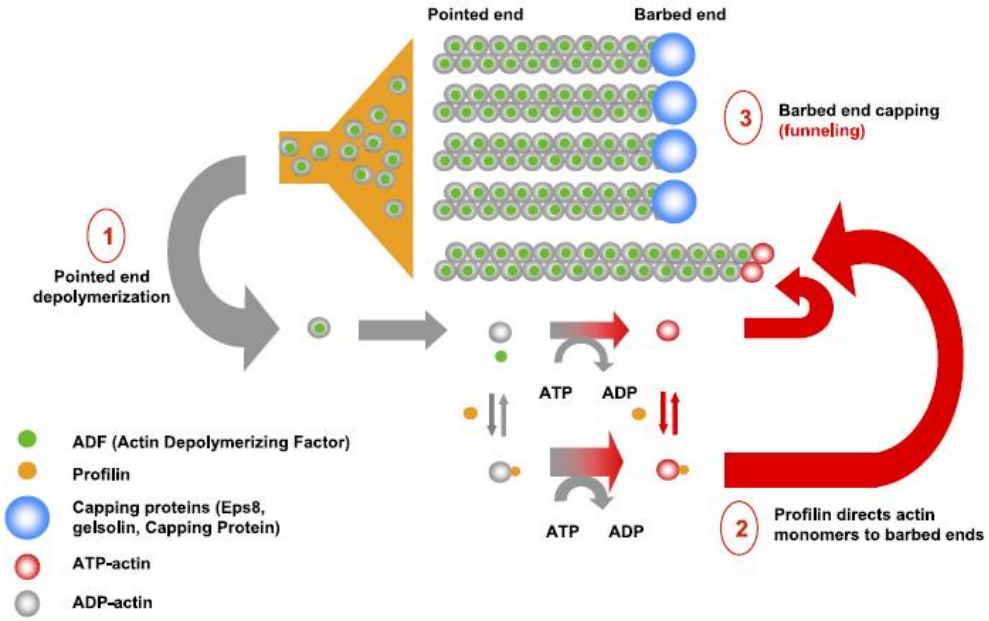

Figure 9 – Actin polymerization process. (1) Actin depolymerizing factor (ADF) induces actin depolymerisation at pointed end. **(2)** Profilin interacts with actin and catalyses the exchange of ADP for ATP, providing a pool of ATP-actin that can be rapidly incorporated at actin filament free barbed end**. (3)** Capping proteins block the majority of barbed ends. Adapted from Le Clainche and Carlier 2008. ATP Adenosine triphosphate; ADP: adenosine diphosphate.

1.3.2. Profilin and membrane trafficking

Pfns are involved in endocytosis and membrane trafficking, as suggested by the presence of Pfn1 at budding Golgi vesicles and the existence of a Pfn1-dependent recruitment of dynamin 2 to the Golgi (Dong, Radau et al. 2000). Furthermore, the interaction between Pfn2 and dynamin 1 is better characterized in the mouse brain (Gareus, Di Nardo et al. 2006). Overexpression of Pfn2 inhibits endocytosis by sequestering dynamin 1, the central regulator of endocytosis in neurons, thus preventing dynamin interaction with other effector molecules.

1.3.3. Nuclear profilin

Due to their globular structure and small size Pfn (15 kDa) and Pfn-actin (57 kDa) are able to enter in the nucleus by diffusion. However, there is a specific export system to remove profilin-actin from the nucleus, the exportin 6 (Stuven, Hartmann et al. 2003).

Despite the fact the functions of Pfn and its ligands in the nucleus are less understood, studies suggest that Pfn might have a role in mRNA splicing and maturation, since (i) anti-Pfn1 antibodies interfere with mRNA splicing in vitro; (ii) Pfn interacts with proteins involved in those processes (Survival motor neuron –SMN; and p80 coilin) and (iii) immunolocalization studies show the presence of Pfn1 in splicing speckels and Cajal bodies (Skare, Kreivi et al. 2003). Besides, some studies suggest a role for Pfn in regulating gene expression in neuronal cells (Lederer, Jockusch et al. 2005). In this study, the authors showed that Pfn1 interacts and regulates p42POP that is a transcriptional modulator, suggesting that Pfn1 might participate in transcriptional regulation.

1.3.4. Profilin 1 regulation

As mentioned before, Pfn1 interaction with PIP2 functions as a link through which the signalling pathways communicate with the dynamics of the actin cytoskeleton. Previously, it has been reported *in vitro* that Pfn1-PIP2 binding can inhibit hydrolysis mediated by phospholipase-Cγ (PLCγ) (Goldschmidt-Clermont, Machesky et al. 1990). However, the phosphorylation of phospholipase C-gamma 1(PLCγ1) can overcome the inhibitory effect of Pfn1 binding (Goldschmidt-Clermont, Kim et al. 1991). PLCγ becomes phosphorylated in response to external stimuli, for instance by the epidermal growth factor receptor tyrosine kinase. Upon hydrolysis, Pfn1 is released in the cytoplasm where it can execute its function. Pfn1 binding to PIP2, or PIP to

a lesser extent to PIP, compromise PIP2 availability in the membrane, interfering with intracellular signalling cascades. For instances, there are studies in cancer cells reporting that PI3K/AKT pathway is sensitive to perturbations in Pfn1 expression (Das, Bae et al. 2009, Jin, Song et al. 2012).

Post-transcriptional modifications of Pfn1 can alter its proprieties and function. In HEK293 cells and primary neurons, the Rho associated coil-coil kinase (ROCK) phosphorylates Pfn1 at serine residue 137, leading to Pfn1 inactivation and concomitant impairment of actin binding activity (Shao, Welch et al. 2008). On the other hand, phosphorylation of Pfn-1 at tyrosine 129 by chemotactic activation of VEGF receptor kinase-2 (VEGFR2) and Src promotes Pfn-1 binding to actin and actin polymerization in endothelial cells (Sathish, Padma et al. 2004).

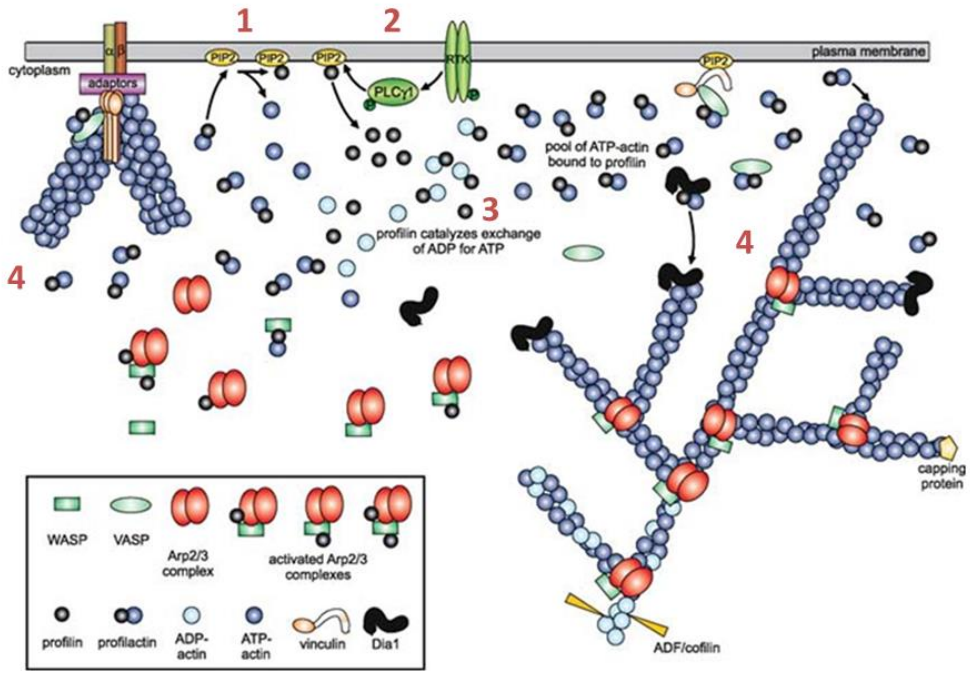

Figure 10 - Schematic representation of Pfn1 actin-associated functions. (1) Pfn1 interacts with PIP2 regulating Pfn1 availability in cytosol. **(2)** Phosphorylated PLCγ1 is able to hydrolyse PIP2. In consequence, Pfn1 is released for cytoplasm where it can execute its function. **(3)** Free Pfn1 binds to G-actin and catalyses the exchange of ADP for ATP, providing a pool of monomers that can be rapidly polymerized**. (4)** The profilin-ATP-G-actin complex can be added to nascent actin filaments. Pfn1 is important for *de novo* actin nucleation and elongation of new or pre-existing filaments through interaction with several mediators with PLP stretches. Adapted from Jockusch, Murk et al. 2007. PIP2: phosphatidylinositide-4,5-bisphophate; PLCγ1: Phospholipase Cγ1; ATP Adenosine triphosphate; ADP: adenosine diphosphate.

1.3.5. Profilin 1 *in vivo*

Several studies have demonstrated that deletion of Pfn1 is incompatible with life. Pfn1 deletion in mice leads to embryonic lethality before implantation probably due to defects in cytokinesis, indicating a critical role for Pfn1 in initial stages of mouse development (Witke, Sutherland et al. 2001). Heterozygous mice for Pfn1 are viable, but present alteration in brain morphology and have reduced survival and Pfn2 presence in brain does not compensate for Pfn1 loss. In contrast, Pfn2 deficient mice are viable and the overall brain morphology is apparently normal, although these mice show behavioural abnormalities (Pilo Boyl, Di Nardo et al. 2007).

Pfns have been implicated in many pathological conditions, such as allergies, cardiovascular diseases, muscular atrophy, diabetes, dementia and cancer. Regarding cancer, Pfn1 has been considered a tumor-suppressor since its protein expression is constitutively downregulated in breast and other cancer cell lines (Janke, Schluter et al. 2000). In addition to promoting actin polymerization, membrane protrusion and motility, Pfn1 reduction has been shown to enhance motility and invasion in several tumor cells (Zou, Jaramillo et al. 2007). On the other hand, Pfn1 overexpression leads to the formation stress-fibers, increases focal adhesion, promotes cell spreading and impairs motility and invasion (Janke, Schluter et al. 2000).

Pfn1 has also been implicated in many neurodegenerative diseases. For example, Pfn1 interacts with huntingtin, the protein mutated in Huntington disease. Mutant huntingtin leads to downregulation of Pfn protein in Drosophila eye. Disease phenotype can be restored by increasing Pfn1 expression (Shao, Welch et al. 2008). A recent study also showed that missense mutations in the human PFN1 gene are linked to familial amyotrophic lateral sclerosis (ALS) (Wu, Fallini et al. 2012).

1.4. Aims

The main goal of this work was to dissect the role of Pfn1 in microglia cell function. In particular, we were interested in determining: (i) Pfn1 expression and phosphorylation in activated microglia, (ii) the impact of Pfn1 reduction in anti- and pro-inflammatory mediators, and (iii) the role of Pfn1 in microglia ROS production.

2. Experimental procedures

2.1. Reagents

Hank's Balanced Salt Solution 1x (HBSS), Penicillin Streptomycin (Pen/Strep), DMEM (1x) + Glutamax TM-I, trypsin-EDTA (Trypsin-Ethylenediamine tetra-acetic acid), DMEM/F12 and CellROX® Deep Red Reagent were acquired from Life Technologies. FBS (Fetal bovine serum), poly-D-lysine, latex beads, protease, phosphatase and TRI reagent were acquired from Sigma-Aldrich. Lysogeny broth-agar (LB-agar) and bovine serum albumin (BSA) acquired from NZYtech. Super Optimal Broth media and NucBuster™ Protein Extraction Kit were acquired from Novagen. NucleoBond® Xtra plasmid purification was acquired from MACHEREY-NAGEL. iQ™ SYBR® Green Supermix and transference buffer Trans Blot Turbo were acquired from BioRad. jetPrime®was acquired from Polyplus transfectionTM; Puromycin from Calbiochem; Triton X-100 from VWR; Direct-zol™ RNA MiniPrep from Zymo Research; SuperScript™ III First-Strand Synthesis SuperMix for qRT-PCR from Invitrogen; GoTaq® Green Master Mix from Promega and Pierce™ BCA Protein Assay Kit fromThermo Scientific).

2.2. Animals

All animal experiments were performed according to European Union and National guidelines and approved by Animal Ethics Committee of the Institute for Molecular and Cell Biology (IBMC) and Portuguese Veterinarian Board. Animals were housed at IBMC facility under controlled temperature and light conditions (12 hours light/12 hours dark cycles) with water and standard rodent food *ad libitum*. To perform mixed glial cultures, Wistar rats were sacrificed by decapitation at P1-P2. P60 mouse expressing an IRES-EYFP (internal ribosome entry site-enhanced yellow fluorescent protein) under the control of *CX_3CR1* promoter was used to show the expression of Pfn1 in microglia *in vivo* (Parkhurst, Yang et al. 2013).

After being anesthetized with pentobarbital, CX3CR1-EYFP mouse was perfused with phosphate-buffered saline (PBS) followed by 4% paraformaldehyde (PFA). Brains were collected and post fixed at 4°C overnight. Tissues were subjected to sucrose gradient (15% and 30%

sucrose) for cryopreservation and sectioned at 20 µm in a cryostat (Leica). Sagittal sections were collected in Superfrost glass-slides (Thermo Scientific) for immunohistochemistry.

2.3. Cell culture

2.3.1. Mixed glial cell cultures

Wistar rat litters (6-15) were sacrificed by decapitation at P1-P2, cerebral cortices and hippocampus were dissected and placed in cold HBSS with 1% Pen/Strep. After removing the meninges, tissues were incubated with 0.0025% Trypsin-EDTA and 50µg/mL DNase for 10 minutes at 37°C. The trypsinization was terminated with 12mL of DMEM (1x) + GlutamaxTM-I supplemented with 10% FBS + 1% Pen/Strep. Samples were centrifuged at 200g for 7 minutes. The supernatant was discarded and the pellet was resuspended and homogenized in 20mL medium. Cell suspension was filtered through a 100µm cell strainer and distributed by 75cm^2 culture flasks previously coated with poly-D-lysine (10 µg/mL) (at approximately 2 pups/flask). The mixed glial cell cultures were maintained at 37°C in a humidified atmosphere with 5% CO_2 for 10 days and the medium was changed twice a week. Each mixed glia cell culture was subjected to tree shakes (with seven days interval) to obtain purified microglia cell cultures.

2.3.2. Purified microglia cell cultures

After 10 days in culture, microglial cells were visually identifiable in mixed glial cell cultures as the smallest and brightest cells in culture. Mixed glial cell cultures were subjected to orbital shaking (200 rotations per minute (rpm)) for 2 hours at 37°C. The medium enriched in microglia was collected and the cells were pelleted by centrifugation (200g for 10 minutes). After discarding the supernatant, the pellet was resuspended in DMEM/F12-Glutamax^{TM}-I supplemented with 10% FBS + 1% Pen/Strep and the cells were counted using a hemocytometer. Cells were seeded at 1 x 10^5 cells per mL on 12-well tissue culture plates with glass coverslips or 35 mm^2 dishes, or at 2 × 10^5 cells per mL in 100mm dishes (all surfaces were previously coated with poly-D-lysine). On the following day, culture medium was replaced. Cells were maintained at 37°C in a humidified atmosphere with 5% CO_2. Previous tests in our laboratory demonstrated that this method provides cultures that reach 99% purity (Socodato, Portugal et al. 2015).

2.3.3. Microglial cell lines

BV-2 microglial cells were kindly supplied by Dr. Francisco Ambrósio (University of Coimbra, Coimbra, Portugal). This cell line was derived from murine newborn animals (C57BL/6 strain) and immortalized by transformation with the v-raf and v-myc oncogenes of the J2 retrovirus (Blasi, Barluzzi et al. 1990). This cell line is often used as a substitute for primary microglia, as several studies demonstrated that BV-2 is similar to primary microglia function (Bocchini, Mazzolla et al. 1992, Guzy, Hoyos et al. 2005, Lund, Christensen et al. 2006, Henn, Lund et al. 2009).

The human microglial cell line CHME3 was kindly supplied by Dr. Dora Brites, (University of Lisbon, Lisbon, Portugal). This cell line was derived from human fetal microglia immortalized with SV-40 large T-antigen (Janabi, Peudenier et al. 1995). CHME3 line is often used as a substitute for primary microglia (Green, Elkington et al. 2010, Hjorth, Frenkel et al. 2010).

BV-2 and CHME3 were cultivated with DMEM (1x) + Glutamax^{TM}-I supplemented with 10% FBS + 1% Pen/Strep. Cells were maintained at 37°C in a humidified atmosphere with 5% CO_2. Both cell lines were used to generate microglia Pfn1 knocked down stable cell sub-clones, as described in a subsequent section. BV-2 cells were employed for western blotting experiments due to their fast proliferation rate, while CHME3 cells were used for Förster resonance energy transfer (FRET) experiments, since those cells express the FRET biosensor with very high signal-to-noise ratio.

2.4. Bacteria transformation and plasmid DNA purification

Competent bacteria were incubated with 3,3 µg of plasmid on ice for 5 minutes and heat-shocked at 42°C for 30 seconds. Then, cultures were cooled on ice for 5 minutes and 300µL of Super Optimal Broth media was added. Transformed bacteria were incubated at 37°C with shaking for 1 hour. Positively transformed colonies were selected by plating on LB-agar with 100µg/mL ampicillin (since the plasmid of interest had an antibiotic resistance cassette). Bacteria were allowed to grow overnight at 37°C.

A starter culture was firstly prepared based on single positive colony picked from agar plate. Bacteria were inoculated in 5mL of LB medium under selection with 100µg/mL ampicillin in order to guarantee plasmid propagation. Bacteria were allowed to grow for 8 hours at 37°C with orbital shake (approximately 300 rpm). Then, a larger culture was prepared by diluting the starter culture in 150 mL of LB with 100µg/mL ampicillin. Bacteria were allowed to grow for 12-16 hours at 37°C with orbital shake. Afterwards, bacteria were harvest by centrifugation at 9000g for 10 minutes at 4°C. Plasmid DNA was isolated and purified using NucleoBond® Xtra plasmid purification according to manufacturer's instructions. Briefly, the bacterial pellet was resuspended with resuspension Buffer + RNase A and lysed with Lysis Buffer based on the NaOH / SDS lysis method. The whole lysate was loaded onto NucleoBond® Xtra Column together with NucleoBond® Xtra Column Filter where nucleic acids bind to the filter. The plasmid DNA was purified with wash buffer, eluted in elution buffer, precipitated with isopropanol, and resuspended in 400µL of nuclease-free water. Concentration of plasmid DNA was measured with NanoDrop spectrophotometer (Thermo Scientific) by optical density (OD) at 260nm wavelength and sample purity was determined using OD_{260}/OD_{280} ratio. Plasmid DNA was stored at -20°C until use.

2.5. Profilin 1 knockdown

2.5.1. Lentivirus production

The human HEK293T cell line (Human Embryonic Kidney 293 cells express SV40 large T antigen) was used for production of lentiviruses particles containing the plasmid encoding Pfn1 small hairpin RNA (shRNA) (TRCN0000011972, Sigma) or the empty vector, pLKO. Low passage HEK293T cells were seeded in a 100mm^2 plate with DMEM (1x) + Glutamax ^{TM}-I supplemented with 10% FBS and 1% Pen/Strep and maintained at 37°C in a humidified atmosphere with 5% CO_2. When 80% of confluence was reached, cells were co-transfected using jetPrime® with the plasmid of interest together with packaging (psPAX2) and enveloping (PLP-VSVG) plasmids for the production of viral particles coding for the Pfn1 shRNA. Viral plasmids and the interested plasmid (Pfn1 shRNA or pLKO) were diluted in 500 µL of jetPRIME® buffer (4,2 µg psPAX2; 2,7 of PLP-VSVG and 3,1 µg plasmid Pfn1 shRNA) and thoroughly mixed. 20 µL of jetPRIME® was added to diluted DNA and, after vortexing for 10 seconds, the transfection mix was incubated for 10 minutes at

room temperature. Afterwards, the mix was added drop wise to the cells and the plate was gently rocked to ensure distribution of transfection mix. The transfection medium was replaced by fresh medium 4 hours after transfection. At 48 hours post-transfection, the medium containing viral particles was recovered by centrifugation at 1811g for 15 minutes at 4°C. Lentiviruses were stored at -80°C until use.

2.5.2. Profilin 1 knockdown

Primary microglial cells were infected 24 hours after plating with lentiviruses carrying Pfn1 shRNA or empty vector (pLKO). For infection, the culture medium was removed and the virus was added drop wise to the cells. Then, microglia growth medium was added and the plates were gently rocked to ensure distribution of viral supernatant. In all experiments, a proportion of 1:4 (lentivirus: culture medium) was used. Cells remained in culture for 72 hours following infection. Pfn1 knockdown was confirmed by immunofluorescence and qRT-PCR analyses (in primary microglia) and western blotting (in BV-2 microglia).

2.5.3. Microglia stable cell sub-clones

In order to generate BV-2 and CHME3 stable lines, cells were infected with lentiviruses carrying Pfn1 shRNA or empty plasmid (1:1 lentivirus and medium) and allowed to grow for 48 hours. Then, infected cells were selected with puromycin (6µg/mL) for 48 hours. The selection process was finished when non-infected control cultures were completely eliminated by puromycin. When necessary, a second round of puromycin treatment was performed. Stable cell sub-clones were maintained in culture with 2 µg/mL of puromycin prior to experiments.

2.6. Phagocytosis efficiency assay

Phagocytic efficiency assay was performed using fluorescent 0.5µm latex beads (L5530). Primary microglia were incubated with beads, previously resuspended in culture medium (1:1000 (v/v)), for 45 minutes at 37°C. Then, cells were washed twice in PBS and fixed in 4% PFA in microtubule protection buffer (MP buffer; 65mM PIPES, 25mM HEPES, 10mM EGTA, 3mM $MgCl_2$; pH 6.9) for 12 minutes. Microglia cells were immunostained with ionized calcium-binding adapter

molecule 1 (Iba-1) as described in section 3.8. Image acquisition was performed in a Leica DMI6000B inverted microscope. The protocol for calculating phagocytic efficiency was adapted from Koenigsknecht and colleagues (Koenigsknecht and Landreth 2004). In brief, the number of beads inside each cell was counted in Fiji software using an automated algorithm. For each cell, a score was assigned depending on the number of phagocytosed particles. Attributed scores and the corresponding range of phagocytosed beads are represented in table 1. Phagocytosis efficiency was calculated based on weighted arithmetic mean of phagocytosed beads per cell, using the following equation:

$$\bar{X} = \frac{(nº\ cells\ in\ score\ 1 \times 1) + (nº\ cells\ in\ score\ 2 \times 2) + \cdots + (nº\ cells\ in\ score\ 6 \times 6)}{Total\ number\ of\ cells}$$

Table 1 – List of scores attributed to cells considering the number of particles phagocytosed.

Phagocytosed Beads	Score
1 - 7	1
8 - 14	2
15 - 21	3
22 - 28	4
28 - 35	5
+ 36 beads	6

2.7. ROS production assay

In order to evaluate ROS production, primary microglial cells were incubated with the fluorogenic probe CellROX® Deep Red Reagent. CellROX® is a cell-permeant dye that emits fluorescence upon oxidation by ROS. Cells were incubated with CellROX® at a final concentration of 5µM for 30 minutes at 37°C. Afterwards, cells were washed twice in PBS and fixed in 4% MP-PFA for 12 minutes. Coverslips were mounted on glass-slides with Shandon ImmuMount (ThermoScientific). Image acquisition was performed in a Leica DMI6000B inverted microscope.

2.8. Anoxic and hypoxic challenge

For western blot, BV-2 cells were plated in 100 mm^2 dishes. Anoxia experiment was performed when cells reached 70% confluence. Before treatment, culture medium was replaced with fresh medium. Cells were exposed to anoxia by placing them in a chamber filled with a gas mixture of 95% N_2 + 5% CO_2 for 4 hours at 37°C. Control cells remained in the cell incubator under normoxia. After anoxia, cells were washed twice with PBS and protein extracts were performed.

For FRET experiments, hypoxia was performed in the IBIDI micro-chamber coupled to Leica DMI6000B inverted microscope. Hypoxia conditions were reached by decreasing O_2 levels to 2%. During the time-lapse humidity (85%) and temperature (37°C) were controlled. With this approach, we studied the same cell both in normoxic and hypoxic conditions.

2.9. Overexpression of Profilin 1 mutants in microglia cell line

Plasmids encoding Pfn1 mutants were kindly supplied by Dr. Mónica Sousa (Institute for Molecular and Cell Biology - IBMC, Oporto, Portugal). Mutant Pfn1 plasmids were generated by site-directed mutagenesis: $Pfn1^{R74E}$ - actin binding domain defective Pfn1; $Pfn1^{H133S}$ - PLP binding domain defective Pfn1; $Pfn1^{S137D}$ – phospho-mimetic Pfn1. Overexpression of Pfn1 mutants was performed in CHME3 microglia cell line. CHME3 cells were co-transfected with plasmids for Pfn1 mutants (500ng) and ROS FRET probes (500ng) as described in section 3.13.1. The co-transfection with Pfn1 wild type (Addgene, clone IRATp970C034D) and ROS FRET probe was used as control. FRET experiment was performed 24 hours after transfection. Western blot for total Pfn1 was done to confirm the overexpression of Pfn1 24 hours after transfection.

2.10. Immunofluorescence

Coverslips containing purified microglia cell cultures were washed twice with PBS and fixed with 4% MP-PFA for 12 minutes. After washing, microglial cells were permeabilized with 0.25% Triton X-100 in PBS for 10 minutes. Unspecific epitopes were blocked with 3% BSA in PBS

for 1 hour. Afterwards, cells were incubated with primary antibody for 1 hour at room temperature (RT), washed and incubated with secondary antibody conjugated to a fluorochrome for 1 hour at RT. All antibodies were diluted in blocking solution. The dilution was specific for each antibody used (see Table 2). Finally, the coverslips were washed and the cells nuclei were counterstained with diamidino-2-phenylindole (DAPI). All washing steps consisted of 3 washes with PBS for 10 minutes; all incubations were performed in a humidified chamber.

Immunofluorescence in tissue sections was performed as described above, with the exception that primary antibodies were incubated overnight at 4°C, and blocking solution was: 5% BSA + 5% FBS + 0,1% Triton x-100.

Table 2 – List of antibodies used in immunofluorescence experiments.

Antibody	Reference
Rabbit anti-IBA1 (1:500 ICC and IHC)	016-20001 (Wako)
Rabbit anti-iNOS (1:200 ICC)	Sc-650 (Santa Cruz Biotechnology)
Rabbit anti-Profilin 1 (1:50 ICC and IHC)	ab50667 (Abcam)

2.11. Image acquisition and fluorescence intensity quantification

Image acquisition was performed using a Leica DMI6000B inverted microscope coupled with a digital CMOS camera (ORCA-Flash4.0 V2, Hamamatsu Photonics). A PlanApo 63X 1.3NA glycerol immersion objective was used. Images obtained in 4X4 binning were exported as TIF using Leica LAS AF. Fluorescence intensity was quantified in Fiji software. Firstly, the background was subtracted using 50%-off pixels radius using rollerball algorithm. Cells were then segmented using different algorithms with standard thresholds according to the fluorescence pattern obtained: Otsu algorithm was used for Pfn1 and CellRox staining, while Huang algorithm was used for iNOS and IBA-1 staining. Individual segmented cells were transposed to ROI manager in FIJI. Only particles larger than 50 pixels were considered. Finally, a mean grey value for the intensity of

each cell was retrieved using the multi measure function and the mean fluorescence intensity for each group was obtained.

2.12. Gene expression analysis

2.12.1. RNA isolation

The mRNA was isolated using Direct-zol™ RNA MiniPrep according to the manufacturer's instructions. Briefly, adherent cells (approximately 2×10^6 cells per 100 mm^2 dish) were lysed directly in culture dish with 1mL of TRI reagent. The TRI reagent was mixed by pipetting and it was added 1 mL of absolute ethanol. The samples were loaded into spin columns where the RNA was purified with several washing steps after being bound to the column. The RNA was eluted in 30µL DNase/RNase free water. RNA concentration was measured by NanoDrop at 260nm OD and the purity was determined using OD_{260}/OD_{280} ratio. All samples used had OD_{260}/OD_{280} ratios between 1.8 and 2.1. The samples were stored at -80°C until use.

2.12.2. cDNA synthesis

Reverse transcription was performed using SuperScript™ III First-Strand Synthesis SuperMix for qRT-PCR according to manufacturer's instructions. Briefly, cDNA was synthetized from 500ng of total RNA. For each reaction 10µL of 2×RT Reaction MIX, 2µL of RT Enzyme Mix, 500µg of RNA and DEPC-treated water were mixed in a final volume of 20µL. The reaction was prepared on ice and incubated for 10 minutes at 25°C. Afterwards, the samples were incubated at 50°C for 30 minutes and the reaction was terminated at 85°C for 5 minutes. The remaining RNA was digested by adding 1µL of 2U *E. Coli* RNase H to each reaction and incubating for 20 minutes at 37°C. The samples were stored at -20°C until use.

2.12.3. Quantitative RT-PCR

qRT-PCR was performed using iQ^{TM5} multicolour real time PCR system (Bio Rad). The reaction was prepared with iQ™ SYBR® Green Supermix according to the manufacturer protocol. Briefly, a master mix was prepared containing 10µl of iQ™ SYBR® Green Supermix, reverse and

forward primers (primers sequences and concentrations are listed in table 3) and nuclease-free water to reach a final volume of 20µl per reaction. The mix was distributed into a 96-well qPCR plate. Each sample was run in duplicate. The general cycling protocol was: initial denaturation at 94°C for 3 minutes, followed by 40 cycles of denaturation, annealing and extension (see optimized details in appendix I). Subsequently to the PCR reaction, the temperature was raised from 55°C to 95°C to generate a melting curve.

Table 3 - List of primers used in PCR with respective sequences and concentrations used.

Primers	Sequences (5'- 3')		
	Forward	Reverse	[ ]
IL-10	ATCCGGGGTGACAATAACTG	TGTCCAGCTGGTCCTTCTTT	200nM
IL-1β	TAAGCCAACAAGTGGTATTC	AGGTATAGATTCTTCCCCTTG	250nM
IL-6	ACTCATCTTGAAAGCACTTG	GTCCACAAACTGATATGCTTAG	300nM
Profilin 1	CGTAGGCTACAAGGACTCGC	GGTCTTTGCCTACCAGGACA	200nM
TNF	CTCACACTCAGATCATCTTC	GAGAACCTGGGAGTAGATAAG	200nM
Ywhaz	GATGAAGCCATTGCTGAACTTG	GTCTCCTTGGGTATCCGATGTC	250nM
HO-1*	GAAGGGTCAGGTGTCCAGAGAAGG	CGCTCTATCTCCTCTTCCAGGGC	200nM
TXNRD1*	CAGGGTGACTGCTCAATCCACAAAC	CTCTTCCTACCGCCAGCAACACTG	200nM
GCLC*	AGGTTGACGAGAACATGAAAGTGGC	CCGCCTTTGCAGATGTCTTTCCTGA	200nM

Results were analysed using iQ^{TM}5 Optical System software version 2.1 (Bio Rad). No temple controls (NTC) were always performed to exclude contamination during preparation of PCR. Melting point analyses were performed to ensure single amplified products. Gene expression was extrapolated based on standard curves generated with cDNA dilution series for each gene. Gene expression was normalized for the housekeeping gene Ywhaz (tyrosine 3-

* kindly supplied by Dr. Tiago Duarte (Institute for Molecular and Cell Biology - IBMC, Oporto, Portugal)

monooxygenase/tryptophan 5-monooxygenase activation protein, zeta (Bonefeld, Elfving et al. 2008). Relative gene expression analyses were performed using the Livak method (Livak and Schmittgen 2001).

2.12.4. End-point PCR

End-point PCR was performed with GoTaq® Green Master Mix. To each reaction, cDNA, 6,25 µl of master mix, 1 µl of forward and reverse primer at 5µM, and 3,25 µl of nuclease free water were added. The reaction consisted in 3 minutes of initial denaturation, followed by 30 cycles of 20 seconds denaturation at 95°C, 30 seconds annealing at 59°C and 30 seconds extension at 72°C. The reaction ends with additional 10 minutes of elongation at 72°C and the samples were cooled at 4°C. PCR was run on control gene Ywhaz. PCR products were run at 100V in 1% (w/v) agarose gel in Tris/acetate/EDTA buffer, containing ethidium bromide. Images were captured in Gel Doc XR+ system (Bio Rad).

2.13. Protein expression analysis

2.13.1. Total protein extracts

After washing twice with PBS, cells were homogenized in RIPA-DTT lysis buffer (50mM Tris base, pH 8.0; 150mM NaCl; 1% NP-40; 0,5% Sodium deoxylcholate; 0,1% SDS; 1mM EDTA; 100mM DTT) supplemented with protease (1:100) and phosphatase (1:100) inhibitor cocktail. Adherent cells were scraped off from the dish with a plastic cell scraper, transferred to a 1,5mL tube and sonicated.

2.13.2. Nuclear and cytosolic extracts

Nuclear and cytosolic extracts were prepared using NucBuster™ Protein Extraction Kit according to the manufacturer's instructions. Briefly, adherent cells were trypsinized to obtain a single cell suspension. Cells were centrifuged (200g for 10 minutes), the supernatant was discarded and the pellet was resuspended in NucBuster Extraction Reagent 1. The mix was homogenized and incubated on ice for 5 minutes. Afterwards, the mix was vortexed and

centrifuged at 16000g for 5 minutes at 4°C. The supernatant corresponding to the cytosolic fraction was collected and immediately stored at -80°C. The pellet was washed in PBS and resuspended in NucBuster Extraction Reagent 2 with protease inhibitor (1:50) and 100mM DTT. The mix was vortexed, incubated on ice for 5 minutes, vortexed again and the nuclear fraction was collected and immediately stored at -80°C until use.

2.13.3. Protein quantification

The protein content was quantified by the bicinchoninic acid (BCA) method (Pierce™ BCA Protein Assay Kit), which is based on the reduction of Cu^{2+} to Cu^{1+} by protein in an alkaline medium with colorimetric detection of the Cu^{1+} by BCA. The protein amount was determined by comparing total protein concentration with a protein standard (BSA). A standard solution of 2 mg/mL BSA was diluted to concentrations ranging between 12.5 to 800 µg/µL and applied in duplicates to 96 multiwell plate in other to construct a standard curve. The samples were diluted (1:9) and were applied in duplicates to the same plate. The BCA reagent was added and the samples were incubated at 37°C for 30 minutes. The optical density was recorded at 562 nm in the Synergy 2 plate reader (BioTeK). Protein concentration was calculated using the following equation:

$$\text{protein concentration } (\mu g/\mu L) = \frac{(\text{samples absorbance mean} - \text{blank absorbance}) \times \text{standard curve slope}}{\text{sample dilution after denaturation}}$$

2.13.4. Western blot

For sodium dodecyl sulphate-polyacrylamide gel electrophoresis (SDS-Page), proteins were diluted (5/6) in 6X denaturation buffer (0.5M Tris-HCl/0,4% SDS, pH 6.8; 30% glycerol; 10% SDS; 0.6M DTT; 0,01% bromophenol blue) and denatured by heating at 95°C for 10 minutes. After denaturation, samples were loaded in 15% acrylamide/bisacrilamide gels and were separated by SDS-PAGE using protein running buffer (250 mM Tris, 1.92 M glycine, 1% SDS). Proteins were then electrophoretically transferred (1.3A, 2.5V, 15 minutes) to a polyvinylidene difluoride (PVDF) membrane (Immobilon-P, Millipore) using the Trans-Blot® Turbo™ Transfer System (Bio Rad). The membranes were then blocked in 5% low-fat milk in TBS-T buffer (20mM Tris; 0.137M NaCl; 0.1% Tween 20) for 1 hour at room temperature. The primary antibodies were incubated overnight at

4°C in 3% BSA (table 4). After washing tree times (3 X 10 minutes) with TBS-T, membranes were incubated with secondary antibody conjugated with horseradish peroxidase (HRP) for 1-2 hours at room temperature. For the loading control, membranes were incubated with the primary antibodies mouse anti-Glyceraldehyde 3-phosphate dehydrogenase (GAPDH) (total extracts) and rabbit anti-Histone 3 (H3) (nuclear extracts). Protein immunoreactive bands were developed using an enhanced chemiluminescence kit (Life Technologies). Images were acquired in ChemiDoc XRS System (BioRad) and quantified using the Image Lab™ Software version 4.1.

Table 4 - List of antibodies used in western blotting.

Antibody	Reference
Rabbit anti-IBA1 (1:100)	016-20001 (Wako)
Rabbit anti-iNOS (1:200)	Sc-650 (Santa Cruz Biotechnology)
Rabbit anti-Profilin 1 (1:1000)	ab50667 (Abcam)
Mouse anti-GAPDH (1:5000)	MAb 6C5 (HY tests)
Rabbit anti-H3 (1:5000)	ab1791 (Abcam)
Rabbit anti-NF-κB (1:200)	sc-372 (Santa Cruz Biotechnology)
Phosphoprofilin-1 (1:1000)	pS137-PFN1 (Shao and Diamond 2012)

2.14. FRET

2.14.1. Cell preparation

Primary cortical microglial cells were plated on plastic-bottom culture dishes (µ-Dish 35 mm^2, iBidi), approximately 1×10^5 cells per mL. Cultures were infected (300µL virus: 1200 µL medium) 24 hours after plating (as described above) and transfected with plasmids encoding FRET probes 48 hours before image acquisition. Transfection was performed with jetPRIME® reagent with similar protocol previously described for HEK293T cells. For each plate, 20µL jetPRIME® buffer, 3 µg of plasmid and 2 µL of jetPRIME® were used. Plasmids used: pFRET HSP33 cys (Guzy,

Hoyos et al. 2005), pDisplay FLIPE-600n (Okumoto, Looger et al. 2005) and Raichu-Rac1 probe (Itoh, Kurokawa et al. 2002). Transfection medium was replaced by fresh medium 4 hours after transfection.

Stable cell lines used in FRET experiments were plated at the same density as primary cells and were transfected with plasmids for FRET probes 24 hours after plating. Transfection conditions used were similar to those described above, except that 1µg of plasmids was used and cell imaging was performed 24 hours after transfection. Prior to image acquisition, cell medium was replaced with 2 mL of HBSS.

2.14.2. Image acquisition and FRET quantification

Image acquisition was performed with a Leica DMI6000B inverted microscope equipped with a high-speed low vibration external excitation/emission filter wheels (Fast Filter Wheels, Leica Microsystems), a digital CMOS camera (ORCA-Flash4.0 V2, Hamamatsu Photonics) and a chamber that allows regulation of temperature and O_2 levels. Individual cells were monitored over time and at each time point CFP (CFP excitation and CFP emission) and FRET (CFP excitation and YFP emission) images were captured, using different filter combinations.

Images acquired were exported to Fiji software where they were filtered using a Kalman stack macro. The background was subtracted and, if necessary, photo bleaching was corrected using an exponential fitting function. Then ratiometric images were generated: CFP/FRET for ROS probe and glutamate release probe; FRET/CFP for RAC-1 activation probe. Mean grey intensity values were calculated in Fiji software exported to GraphPad Prism software for statistical analyses.

2.15. Statistical analyses

All data shown in this work represent, at least, 3 independent experiments. The results were analysed using Microsoft Excel and GraphPad Prism 6 and statistical analysis was performed with GraphPad Prism. Data were presented as mean and standard error of the mean (SEM), unless otherwise indicated. S*tudent's* t-test was used in cases where the variances of only two groups were compared. One-sample t-test was used when results of a test group were normalized

against those of a control group. Paired t-test was used to compare the means of two related groups. A one-way analysis of variance (ANOVA) was used to compare 3 or more data sets. Results were considered statistically significant when *p* value was smaller than 0.05.

3. Results

3.1. Dissecting the role of Pfn1 in microglial cell function

Pfn1 is an actin binding protein ubiquitously expressed, except in muscle cells (Carlsson, Nystrom et al. 1977, Witke 2004, Jockusch, Murk et al. 2007). Differences in Pfn1 expression play significant roles in both the dynamics of actin cytoskeleton and signal transduction cascades of several biological processes (Jockusch, Murk et al. 2007, Birbach 2008). Previously, Dong and colleagues (2004) observed the expression of Pfn1 mRNA in microglial cells from the hippocampus by *in situ* hybridization (Dong, Ying et al. 2004). In order to better characterize the expression of Pfn1 in microglial cells we performed an RT-PCR to detect the mRNA for Pfn1 in primary purified microglial cell cultures and in N9 microglial cell line. The brain cortex and the spinal cord were used as positive controls (Murk, Wittenmayer et al. 2012) (fig. 11A). Besides, western blotting was used to observe the protein expression of Pfn1 in cultured microglia. The cortex was, again, used as positive control (fig. 11B). In order to show microglial Pfn1 expression *in vivo,* we used sections from the brain cortex of the CX3CR1-EYFP mouse (with an EYFP knocked in the Cx3cr1 allele and displays fluorescent microglia in the brain). We used imunostaining for Iba-1 as a microglial cell marker to confirm the specificity of EYFP fluorescence and we observed that Iba-1 and EYFP fluorescence were coincident, indicating that EYFP fluorescence was specific for microglia (fig.11C). Then, we performed an immunohistochemistry for Pfn1 and a co-localization analysis. We observed that Pfn1 fluorescence was co-localize with EYFP fluorescence (co-localization is represented in white), demonstrating microglial Pfn1 expression *in vivo* (fig. 11D).

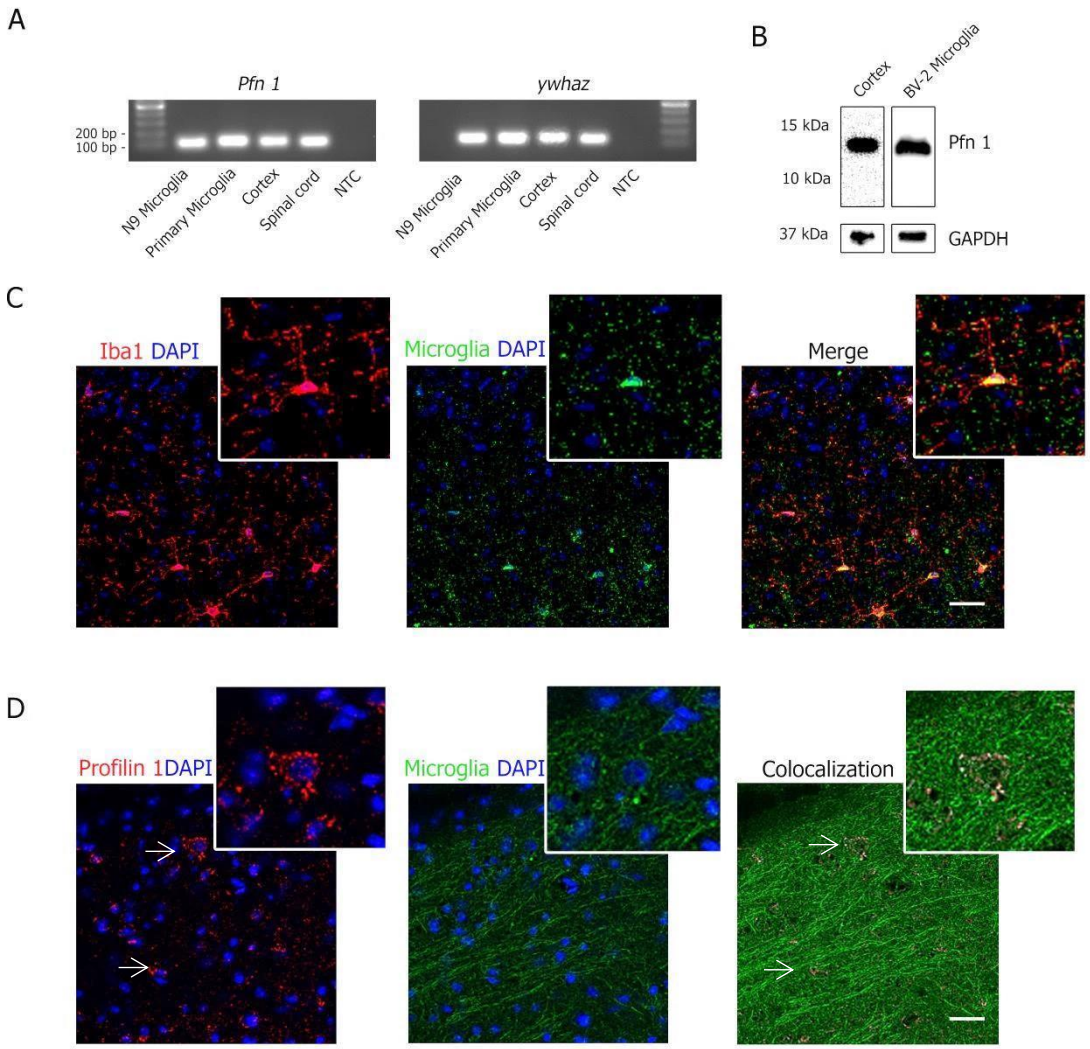

Figure 11 - Pfn1 expression in microglial cells. (A) The mRNA detection of Pfn1 was assessed by RT-PCR. Cortex and spinal cord were used as positive control. ywhaz was used as reference gene. **(B)** Pfn1 protein detection was assessed by western blot in BV-2 microglial cell line. Cortex was used as positive control. GAPDH was used as loading control. **(C, D)** Representative images of CX3CR1-CreERT2 mouse cortex. Imunolabelling for Iba 1 (red) co-localizes with YFP microglia (green), demonstrating YFP specific signal (C). Immunohistochemistry for Pfn1 (Red) shows that this actin-binding protein is expressed in microglial cells (D). Co-localization signal is represented in white. Nuclei were stained with DAPI. Images were acquired in confocal microscope. Scale bar: 15 µm (C) 25 µm (D).

3.1.1. Pfn1 is less phosphorylated in activated microglia

Considering that Pfn1 might have a role in microglia activation, we analysed Pfn1 expression and phosphorylation changes upon a pro-inflammatory stimulation of microglial cells. For that, we challenged BV-2 microglial cells with anoxia (95% N_2 + 5% CO_2 during 4 hours), a strategy to activate microglia (Park, Lee et al. 2002, Yao, Kan et al. 2013). Comparing Pfn1 expression levels between normoxia and anoxia, by western blot, we did not observe significant differences in Pfn1 expression, as depicted in fig. 12A and B. We also analysed Pfn1 phosphorylation at Serine 137 (hereafter termed p-Pfn1). As previously reported, an increase in Serine 137 phosphorylation indicates reduced capacity of Pfn1 to modulate actin polymerization (Shao, Welch et al. 2008). We observed a significant decrease in Pfn1 phosphorylation induced by anoxia (fig. 12A,C), indicating an increased capacity of Pfn1 for polymerizing the actin cytoskeleton in activated microglia. Altogether, these data suggested that Pfn1 might have a role in microglia activation.

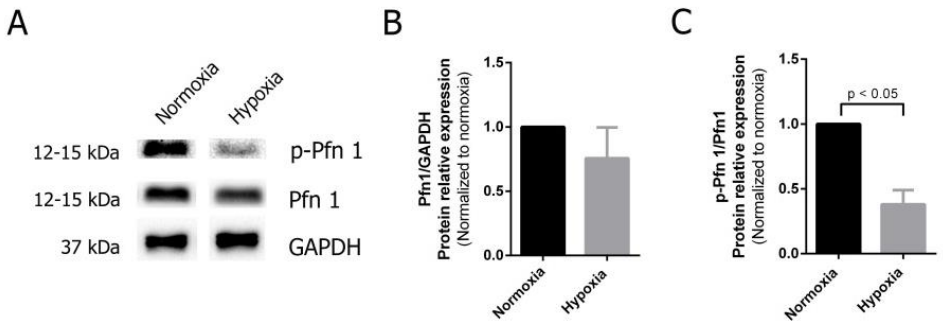

Figure 12 - Pfn1 was less phosphorylated in activated microglia. (A) Western blot and quantification of **(B)** Pfn1 and **(C)** p-Pfn1 protein relative expression in BV-2 microglia in normoxic and anoxic conditions. GAPDH expression was used as loading control. All data are expressed as mean ± SEM normalized to control. N=3, $p < 0.05$ using one sample t test.

3.1.2. The effect of Pfn1 knockdown in microglial function

As we previously demonstrated, the actin polymerization capacity of Pfn1 was increased in anoxia-challenged microglia. In order to investigate the role of this protein in microglia activation, we performed Pfn1 knockdown in primary cortical microglial cell cultures and in BV-2 microglial cell line via lentivirus-mediated shRNA delivery. We confirmed Pfn1 knockdown in primary

microglia, by qRT-PCR (fig. 13A) and immunofluorescence (fig. 13B). Pfn1 knockdown in BV-2 sub-clones stably expressing Pfn1 shRNAs was confirmed by western blotting (fig. 13C) relative to cell carrying an empty control plasmid (pLKO).

After confirming the efficiency of Pfn1 knockdown, we used this approach to analyse the activation status of microglia based on classical activation markers, such as: phagocytosis; glutamate release; ROS production; NF-κB activation; iNOS, Iba-1; arginase-1 expression and differences in mRNA levels of both pro- and anti-inflammatory cytokines.

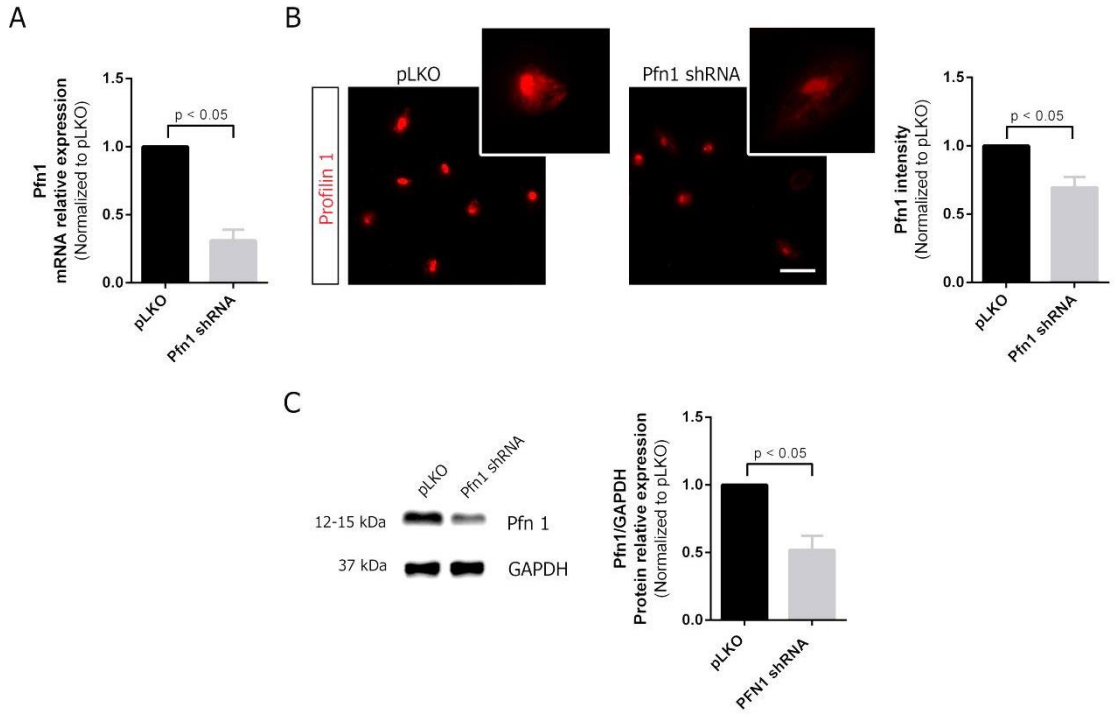

Figure 13 - Infection with lentivirus carrying Pfn1 shRNA lead to Pfn1 knockdown. Microglial cells were infected with lentivirus carrying Pfn1 shRNA or an empty plasmid (pLKO) as control. Pfn1 levels were quantified 72 hours post-infection. **(A)** Relative mRNA levels determined by qRT-PCR in primary microglial cells using ywhaz as a reference gene **(B)** Representative images of Pfn1 (red) immunocytochemistry and fluorescence intensity quantification in primary microglial cells. Scale bar: 50µm. **(C)** Western blot and quantification of Pfn1 protein relative expression in BV-2 microglia puromycin selected clones. GAPDH expression was used as loading control. All data are expressed as mean ± SEM and normalized to control. N=4 (A), N=3(B,C), $p < 0.05$ using one sample t test (A,C); paired t test (B).

3.1.2.1. Pfn1 knockdown decreases the phagocytic efficiency of microglia

We evaluated the phagocytic efficiency of primary cortical microglia. After Pfn1 knockdown, cells were incubated with inert fluorescent beads for 45 min, fixed and observed in a fluorescence microscope. As represented in fig. 14A, Pfn1 knockdown decreased the phagocytic efficiency of microglia. We also analysed the expression of Iba-1, a calcium binding protein whose expression is associated to membrane ruffling and phagocytosis in microglia (Ohsawa, Imai et al. 2000) - Iba-1 participates in Rac1 signalling, that is important to coordinate actin remodelling in phagocytic process (Imai and Kohsaka 2002). We observed that shPfn1 sable BV-2 cell sub-clones express less Iba-1 in comparison to control (fig.14B). Here we concluded that Pfn1 knockdown decreased phagocytic efficiency of microglial cells.

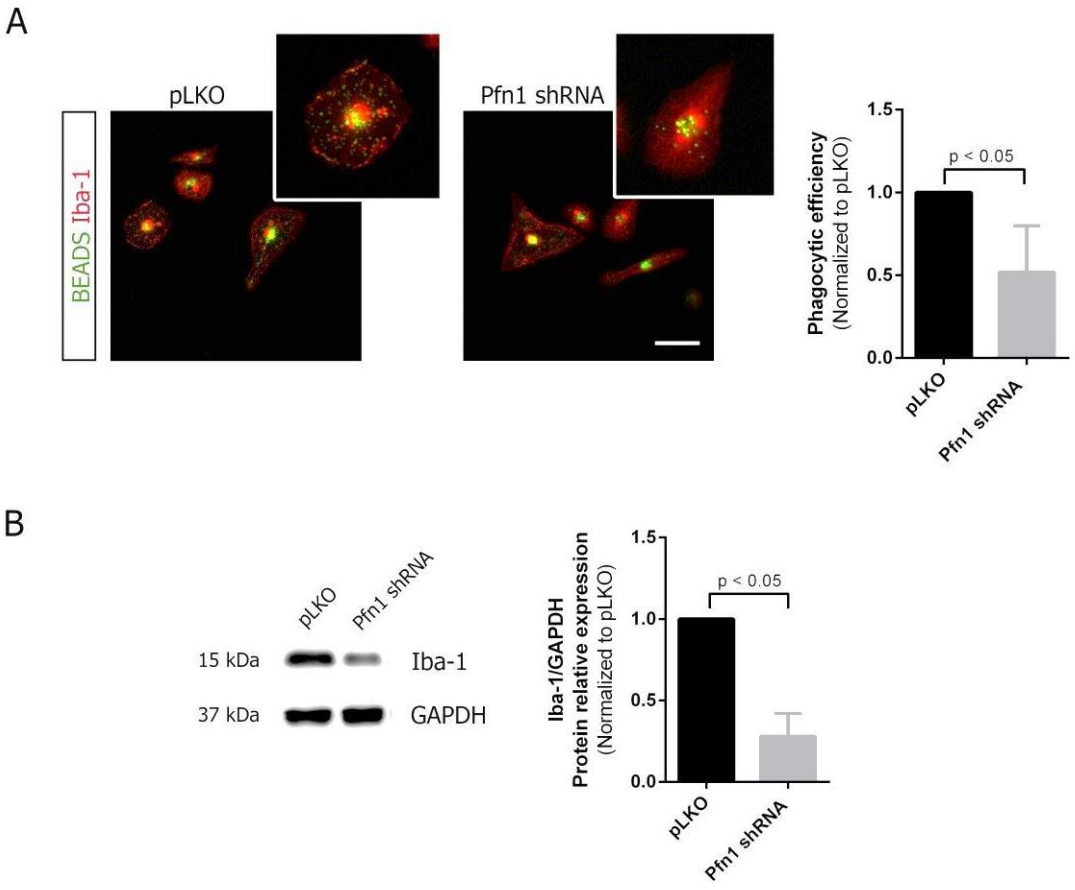

Figure 14 - Pfn1 knockdown decreased the phagocytic efficiency of microglia. (A) Representative images of phagocytosis efficiency assay in primary microglial cells. After 71 hours of lentivirus mediated delivery of pLKO and Pfn1 shRNA, microglial cells were incubated with fluorescence latex beads (green) for 45 minutes and stained with Iba-1 (red). Scale bar: 50 µm. The graph represents the quantification of phagocytic efficiency. **(B)** Western blotting and quantification of Iba-1 protein relative expression in total extracts of BV-2 microglia puromycin selected clones. GAPDH expression was used as loading control. All data are expressed as mean ± SEM and normalized to control. N=4 (A), N=3 (B), $p < 0.05$ using unpaired t test (A) and one sample t test (B).

3.1.2.2. Pfn1 knockdown regulates microglia anti-inflammatory signature

In order to investigate anti-inflammatory markers in microglial cell cultures, we first analysed NRF2 target genes. This transcription factor regulates the expression of cytoprotective genes carrying ARE sequences within their promoters (Rojo, Innamorato et al. 2010, Bryan, Olayanju et al. 2013). As previously observed, NRF2 modulates anti-inflammatory activation signatures of microglia (Cuadrado, Martin-Moldes et al. 2014, Rojo, McBean et al. 2014). We studied NRF2 activation by analysing the mRNA levels of tree NRF2 target genes: glutamate-cysteine ligase catalytic subunit (Gclc), thioredoxin reductase 1 (Txnrd1) and heme oxygenase-1 (HO-1) (fig. 15A). We could not observe any differences in Gclc or Txnrd1 mRNA levels, although we found a significant decrease in the mRNA for HO-1 in Pfn1 knocked down microglia, suggesting a reduced transcriptional activity of NRF2. We also analysed the expression of IL-10 and arginase 1 as other anti-inflammatory markers. We did not detect any difference between IL-10 mRNA levels of control and Pfn1 knocked down cells (fig. 15B). On the other hand, arginase 1 expression was significantly decreased in Pfn1 knocked down microglia when compared to the control (fig. 15C). These results indicated that Pfn1 knockdown decreases the levels of anti-inflammatory mediators in microglial cells.

3.1.2.3. Pfn1 knockdown reduces the pro-inflammatory activation markers in microglia

NF-κB activation is a key step for microglia activation (Oeckinghaus and Ghosh 2009). Translocation of NF-κB to the nucleus induces the expression of several pro-inflammatory signals, for instance, iNOS and pro-inflammatory cytokines (Rojo, McBean et al. 2014). We observed that Pfn1 knockdown decreased NF-κB in the nucleus of BV-2 microglial cells in comparison to control microglia (fig. 16A). We also analysed mRNA levels of pro-inflammatory cytokines in primary microglia and observed a significant reduction in IL-6 and IL-1β relative expression in Pfn1 knockdown cells (fig. 16B). Regarding TNF, there was no significant difference between control and Pfn1 knocked down cells. Moreover, we evaluated the expression of iNOS in primary microglia (fig. 16C) and BV-2 microglia (fig. 16D) by immunofluorescence and western blotting, respectively. In both cases, knocking down Pfn1 led to a significant decrease in iNOS expression. These results suggested that Pfn1 knockdown decreases the pro-inflammatory activation of microglia.

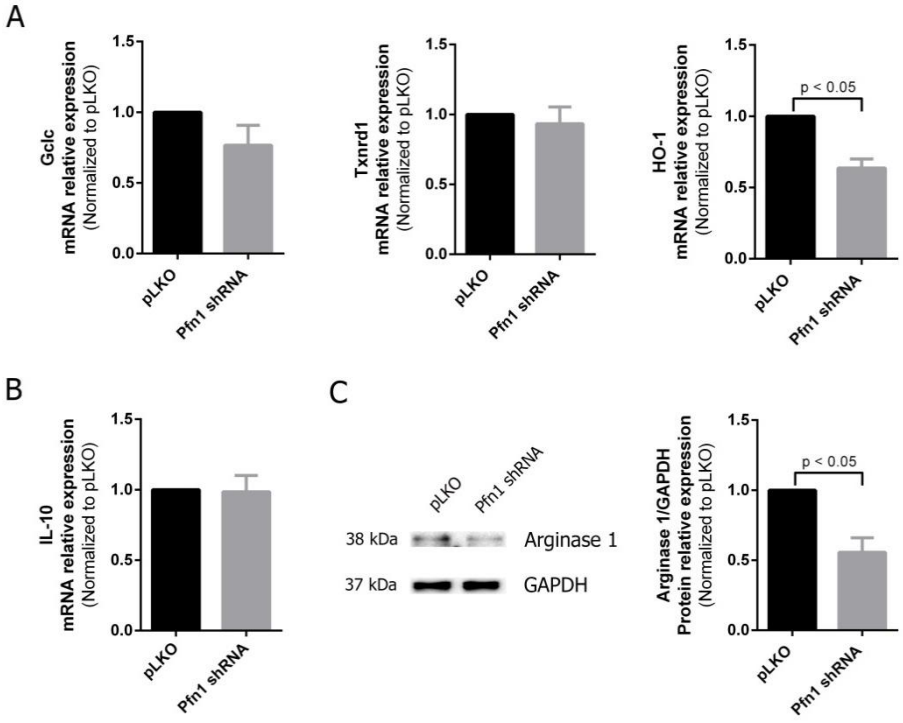

Figure 15 - Pfn1 knockdown regulated microglia anti-inflammatory signature. (A) Relative mRNA levels of NRF2 target genes (Glutamate-cysteine ligase catalytic subunit -Gclc; thioredoxin reductase 1-Txnrd1; *heme oxygenase-1* -HO-1) determined by qRT-PCR in control (plKO) and Pfn1 knockdown (Pfn1 shRNA) primary microglial cells. **(B)** Relative mRNA levels of anti-inflammatory cytokine IL-10 in control (plKO) and Pfn1 knockdown (Pfn1 shRNA) primary microglial cells. Ywhaz was used as reference gene. **(C)** Western blotting for Arginase 1 and quantification of its relative expression in total extracts of BV-2 microglia puromycin selected clones. GAPDH expression was used as loading control. All data are expressed as mean ± SEM and as percentage of control. N=3, $p < 0.05$ using one sample t test.

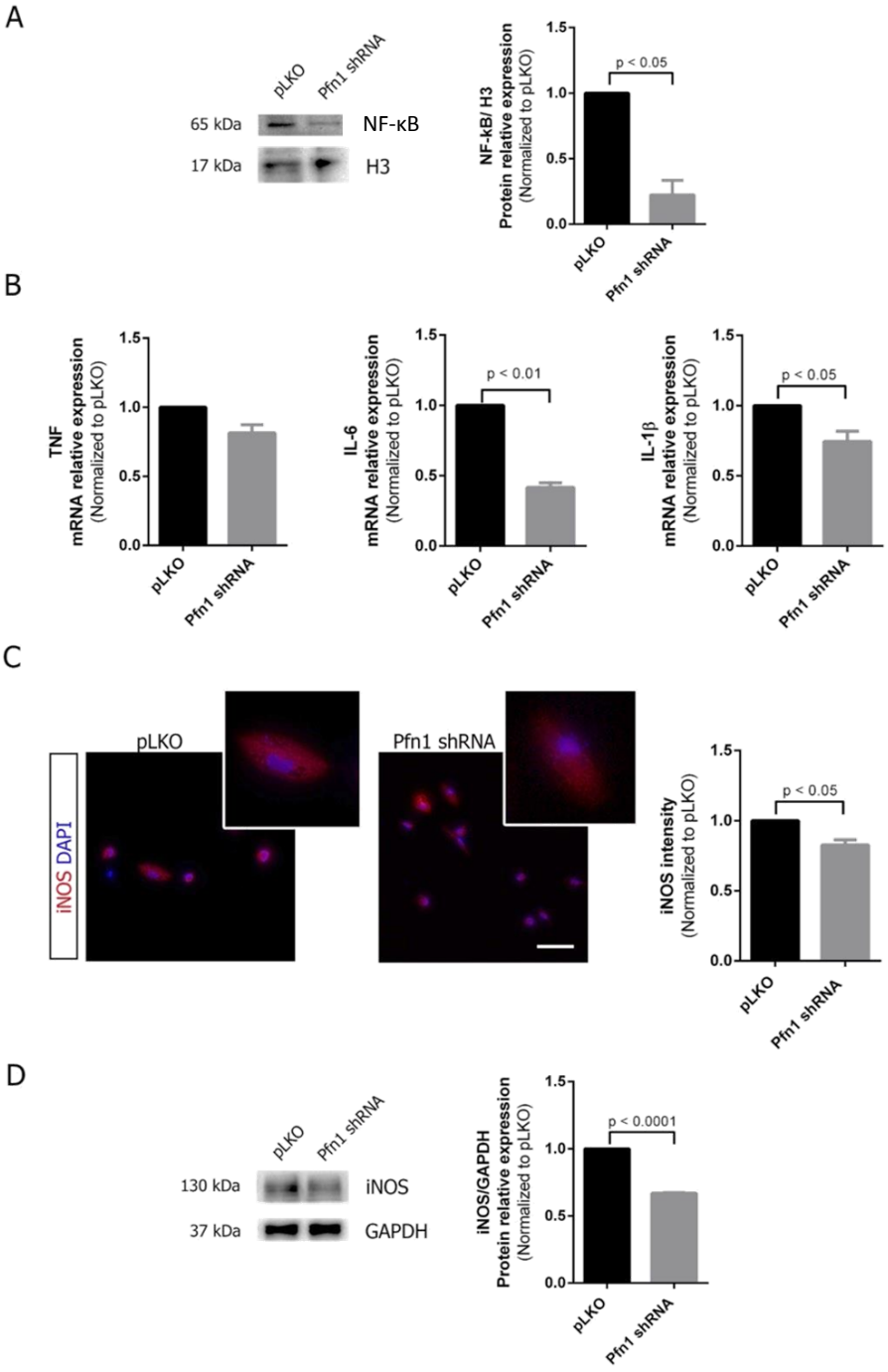

Figure 16 - Pfn1 knockdown reduced the pro-inflammatory activation markers in microglia. (A) Western blot for NF-κB and quantification of its relative expression in nuclear extracts of BV-2 microglia (puromycin selected clones for pLKO and Pfn1 shRNA). Histone 3 (H3) expression was used as nuclear loading control. **(B)** Relative mRNA levels of pro-inflammatory cytokines (TNF, IL-6 and IL-1β) were determined by qRT-PCR in control (plKO) and Pfn1 knockdown (Pfn1 shRNA) primary microglial cells. ywhaz was used as reference gene. **(C)** Representative images of iNOS (red) immunocytochemistry and fluorescence intensity quantification in primary microglial cells. Nuclei were stained with DAPI (blue). Scale bar: 50 µm. **(D)** Western blot for iNOS and quantification of its relative expression in total extracts of BV-2 microglia puromycin selected clones. GAPDH was used as loading control. All data are expressed as mean ± SEM and as normalized to control. N=3, $p < 0.05$ (A-C), $p < 0.01$ (B) and $p < 0.0001$ using one sample t test.

3.1.2.4. Pfn1 knockdown has no effect on glutamate release

Increased glutamate release is also an activation parameter for microglia activation (Piani, Spranger et al. 1992, Barger and Basile 2001). In order to test whether Pfn1 reduction impacts on glutamate release we used FRET-based live cell imaging with a high sensitive biosensor for detecting glutamate release (FLIPE 600n^{Surface}). The functioning of this biosensor is represented in fig. 17A.

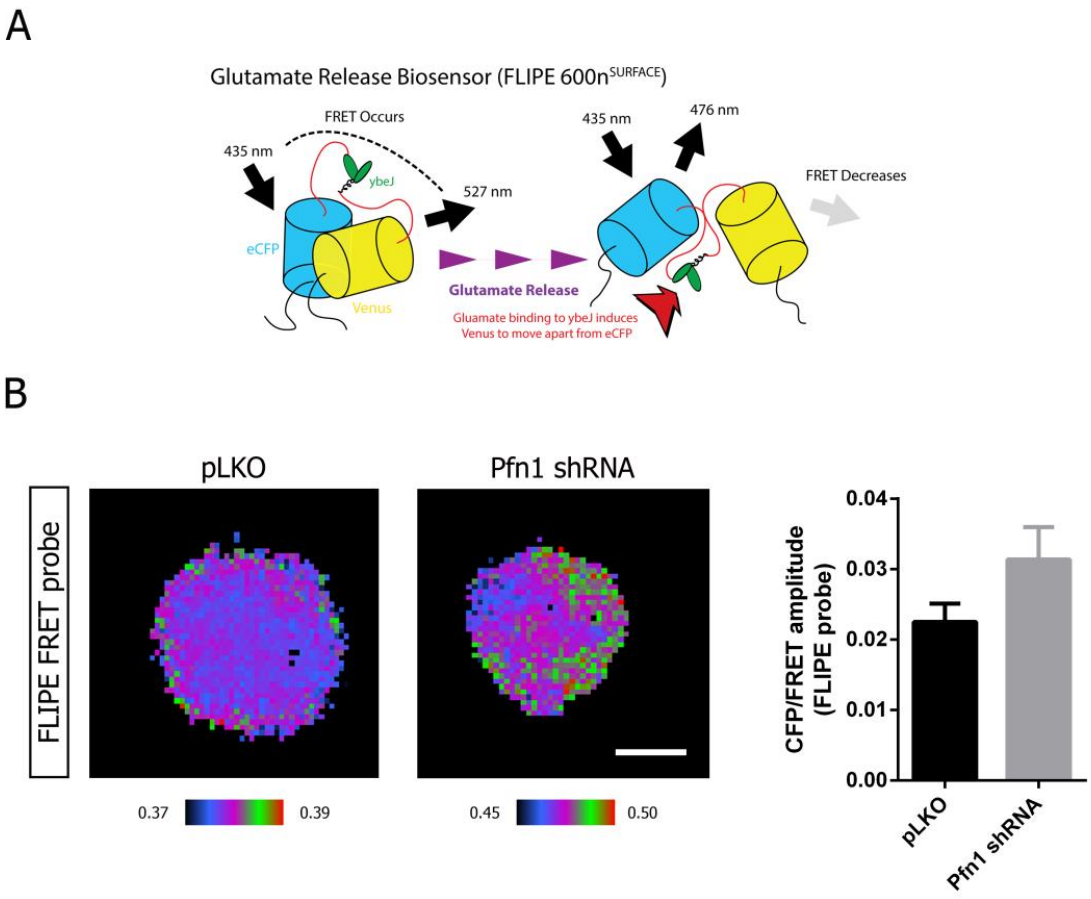

Figure 17 - Pfn1 knockdown had no effect on glutamate release. After Pfn1 knockdown, primary microglial cells were transfected with the glutamate release FRET probe (FLIPE probe). Imaging was performed 42 hours post-transfection. **(A)** Schematic illustration of glutamate release FRET probe (Socodato, et al. 2014). **(B)** Representative images of FLIPE probe in control and Pfn1 knockdown in primary cortical microglia. CFP/FRET images were colour-coded using the colour ramp showed. Scale bar: 10 µm. Graph demonstrating CFP/FRET amplitudes from 6 cells in pLKO and 9 cells in Pfn1 shRNA during 8 minutes imaging. Data are expressed as mean ± SEM, no significant changes were found using unpaired t test.

FLIPE 600n^{Surface} was composed of two fluorescent molecules: enhanced cyan fluorescent protein (eCFP) and the YFP variant Venus. These fluorescent molecules were linked by a glutamate/aspartate binding protein (ybeJ). Without glutamate, these fluorescent molecules were close enough to FRET. When glutamate bound to aspartate binding protein, there are conformational changes that separate the fluorescent molecules, reducing FRET. Once FLIPE 600n^{Surface} was tagged to the cell surface, it allowed detecting the release of glutamate specifically, without interference of glutamate metabolism (Itoh, Kurokawa et al. 2002). As represented in fig. 17B, there were no significant changes in the amplitude of CFP/FRET ratio between control and microglia knocked down for Pfn1, suggesting that Pfn1 did not affect glutamate release in microglia.

3.1.2.5. Pfn1 knockdown decreases ROS production

Increased ROS production and release by microglia is a hallmark of activation (reviewed in (Rojo, McBean et al. 2014). To study ROS accumulation in microglia, we used the CellROX® deep red reagent, a fluorogenic ROS probe. We observed that Pfn1 knockdown resulted in robust decrease (up to 80%) of CellROX® fluorescence (fig. 18A), indicating a dramatic reduction in ROS production, compared to control microglia. To corroborate this intense reduction in ROS production, we, again, used a FRET-based live cell imaging, with a high sensitive ROS biosensor, the HSP FRET probe. This FRET probe was composed by two fluorescent proteins (eCFP and eYFP) linked by a ROS sensitive domain (Hsp33; fig. 18B). Without ROS generation, these fluorescent molecules were close enough to produce FRET. When Hsp33 protein was oxidized by ROS, the oxidation promoted conformational changes in the probe, resulting in the separation of the fluorescent molecules, reducing FRET (Guzy, Hoyos et al. 2005). We observed that the amplitude of CFP/FRET ratio was decreased in Pfn1 knocked down microglia when compared to control cells, indicating less ROS generation (fig. 18C). Here we concluded that Pfn1 was crucial to the ROS production in microglial cells.

In line with this, we asked if Pfn1 would also be important for ROS production upon microglia activation. For that we challenged primary microglial cells with hypoxia, a well-known pro-inflammatory stimulus that increases ROS production in microglia (Wong and Crack 2008). We clearly observed an increased in ROS production in control cells submitted to hypoxia (2% O_2). However, microglial cells knocked down for Pfn1 did not increase the ROS production in response to hypoxia (fig. 19). We concluded that Pfn1 was not only important for basal ROS production, but

also for hypoxia-induced ROS generation. This finding supported the importance of Pfn1 for the generation of ROS in microglia.

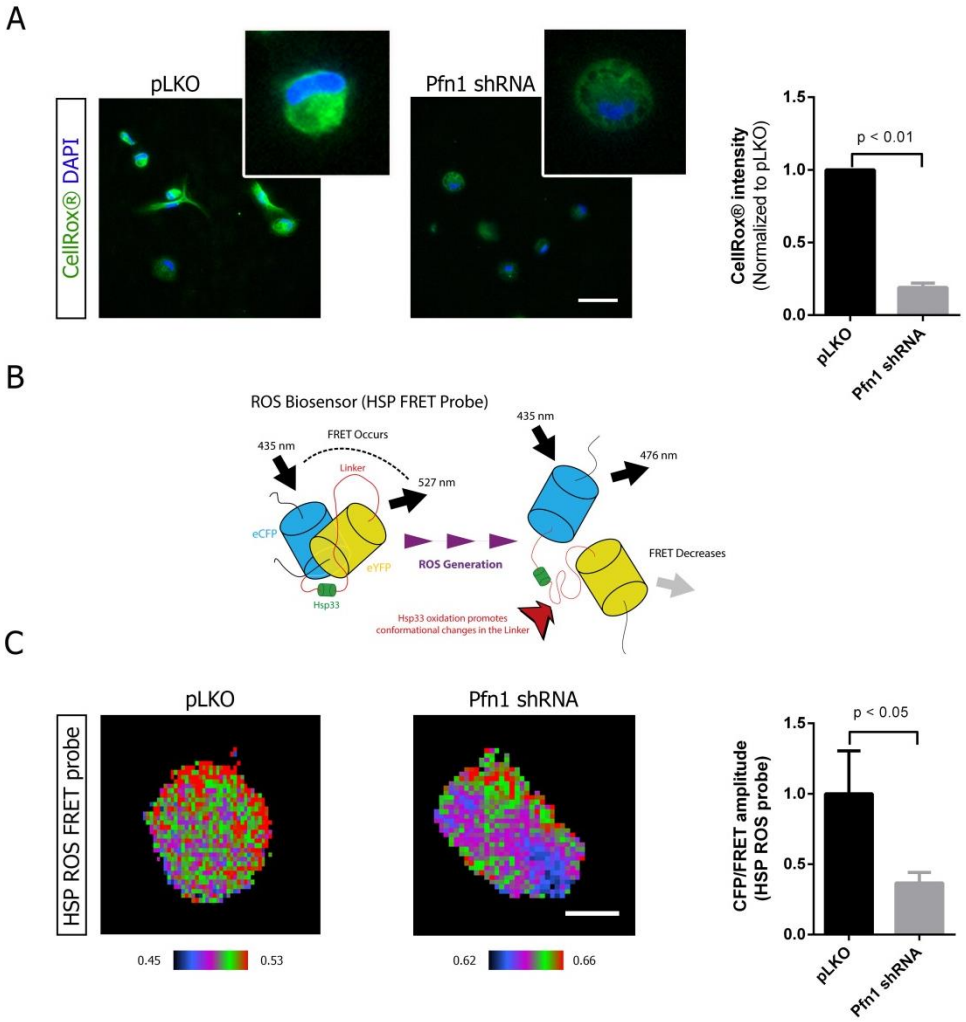

Figure 18 - Pfn1 knockdown lead to dramatic decrease in ROS production in microglial cells. (A) Representative images of CellROX® fluorescence (green) in microglial control cells (pLKO) and in cells with decreased Pfn1 expression (Pfn1 shRNA). Nuclei were stained with DAPI (blue). 71 hours post-infection with lentivirus, cells were incubated with CellROX® probe for 30 minutes. Scale bar: 50 µm. The graph shows CellROX® fluorescence intensity quantification. **(B)** Schematic illustration of the ROS FRET probe (HSP) (Socodato, et al. 2014). **(C)** Representative images of HSP ROS probe in control and Pfn1 knockdown in primary cortical microglia. After Pfn1 knockdown, primary microglial cells were transfected with a HSP ROS FRET probe. Imaging was performed 42 hours post-transfection. CFP/FRET images were colour-coded using the colour ramp showed. Scale bar: 10 µm. Graph demonstrating CFP/FRET amplitudes from 9 cells in pLKO and 9 cells in Pfn1 shRNA during 8 minutes imaging. Data are expressed as mean ± SEM and normalized to control (A). $p < 0.01$ (A) and $p < 0.05$ (B) using paired t test and unpaired t test, respectively.

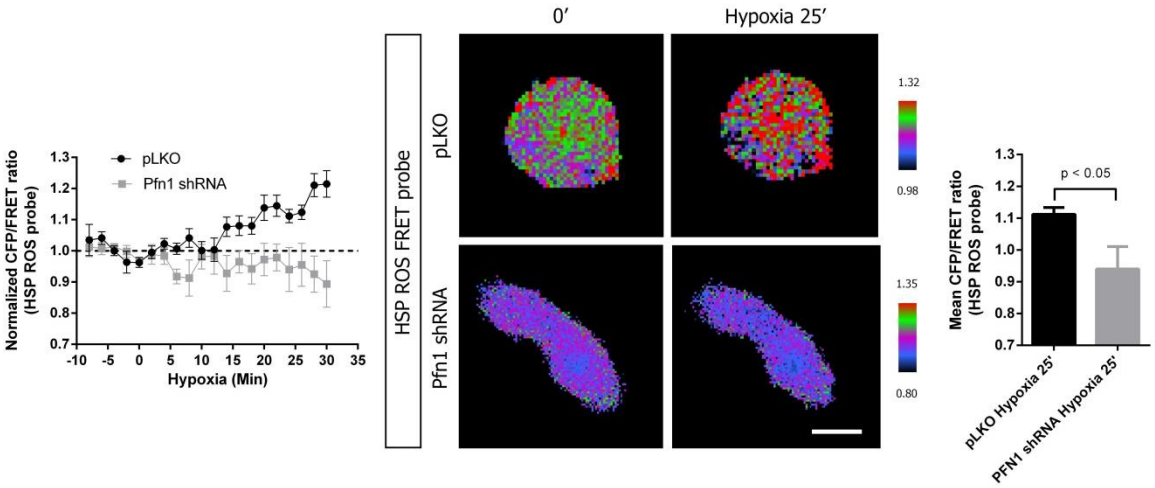

Figure 19 - Pfn1 knockdown prevented ROS increase upon hypoxia. After Pfn1 knockdown, primary microglial cells were transfected with the HSP ROS FRET probe. Imaging was performed 42 hours post-transfection. Each cell was studied for 10 minutes in normoxia conditions, followed by 30 minutes in hypoxia (2% O_2). At the left, graph showing normalized CFP/FRET ratio in time-lapse. CFP/FRET emission ratios were normalized at last frame before hypoxia. In the middle, CFP/FRET representative images of HSP ROS probe in control and Pfn1 knockdown in primary cortical microglia both in normoxia conditions and at 25 minutes of hypoxia stimulation. Scale bar: 10 µm. CFP/FRET images were colour-coded using the colour ramp showed. At the right, graph demonstrating CFP/FRET mean from 5 cells in pLKO and 4 cells in Pfn1 shRNA at 25 minutes of hypoxia. Data are expressed as mean ± SEM. $p < 0.05$ using unpaired t test.

3.2. Dissecting the molecular mechanism for Pfn1-regulated ROS production in microglia

Given that the knockdown Pfn1 had a dramatic effect in ROS production and the importance of redox signalling for the modulation of microglia responses, we decided to better investigate the mechanism by which Pfn1 affects ROS generation.

3.2.1. Does Pfn1 affect ROS generation in a NOX dependent manner?

Considering that NOX is the main source of ROS generation in microglia, it would be plausible that Pfn1 might affect ROS generation in a NOX-dependent manner. To test this hypothesis we compared the status of Rac1 activation (which is important for NOX complex assemble) in Pfn1 knockdown and control microglia. For that we used the Raichu-Rac1 FRET probe to detect differences in Rac1 activation. This probe was composed of a Rac1 interactive binding motif of PAK and two fluorescence proteins: YFP and CFP (fig. 20A). Inactive Rac1 (GDP-Rac1) did

not bind to PAK, so fluorescent molecules were distant and do not produce FRET. On the other hand, activated Rac1 (GTP-Rac1) bound to PAK, producing FRET upon CFP excitation. In our experiment we observed that the amplitude of FRET/CFP ration of Raichu-Rac1 was decreased in Pfn1 knockdown microglia, indicating that Rac1 was less activated in this context (fig. 20B). This result was consistent with our hypothesis that Pfn1 might influence ROS generation in a NOX-dependent manner.

We also analysed Rac1 activity upon hypoxic challenge (fig. 20C). Considering our hypothesis, we were expecting that Rac1 activation would follow the levels of ROS production in hypoxia. In fact, there was a decrease in Raichu-Rac1 activation in Pfn1 knockdown hypoxia. However, we didn't observe an increase in Rac1 activation upon hypoxia in control microglia. All together, these results suggested that the hypoxia-mediated ROS generation was independent of NOX.

3.2.2. How different Pfn1 mutants affect ROS generation?

In order to better understand the importance of Pfn1 in ROS production in microglia, we studied how the disruption of different ligand sites in Pfn1 would impact ROS production in microglia. We transfected CHME3 human microglial cell line with different Pfn1 plasmids: Pfn1 WT - Pfn1 wild-type; $Pfn1^{R74E}$ - actin binding domain defective; $Pfn1^{H133S}$- PLP binding domain defective and $Pfn1^{S137D}$ - phospho-mimetic. Firstly, we confirmed the overexpression of Pfn1 constructs in microglia by western blotting (fig. 21A) and then, we compared, by FRET, the levels of ROS production among the different Pfn1 constructs. We observed a significant decrease in ROS production in microglia overexpressing Pfn1 with mutations in the actin ($Pfn1^{R74E}$) and PLP ($Pfn1^{H133S}$) binding domains (fig. 21B) in comparison to microglia overexpressing the Pfn1 WT. Regarding the phospho-mimetic Pfn1 ($Pfn1^{S137D}$) construct, there was no significant differences in basal ROS production when compared to the control (Pfn1 WT).

We also analysed the effect of Pfn1 mutants in ROS generation during hypoxia. We observed a significant decrease in ROS generation in microglia overexpressing all the Pfn1 mutants relative to Pfn1 WT (fig. 21C). However, the phospho-mimetic Pfn1 construct was much less effective in preventing the increase in ROS production during hypoxia. These results showed that defects, in the actin and in the PLP binding domain might directly impact the Pfn1-mediated ROS production in microglia.

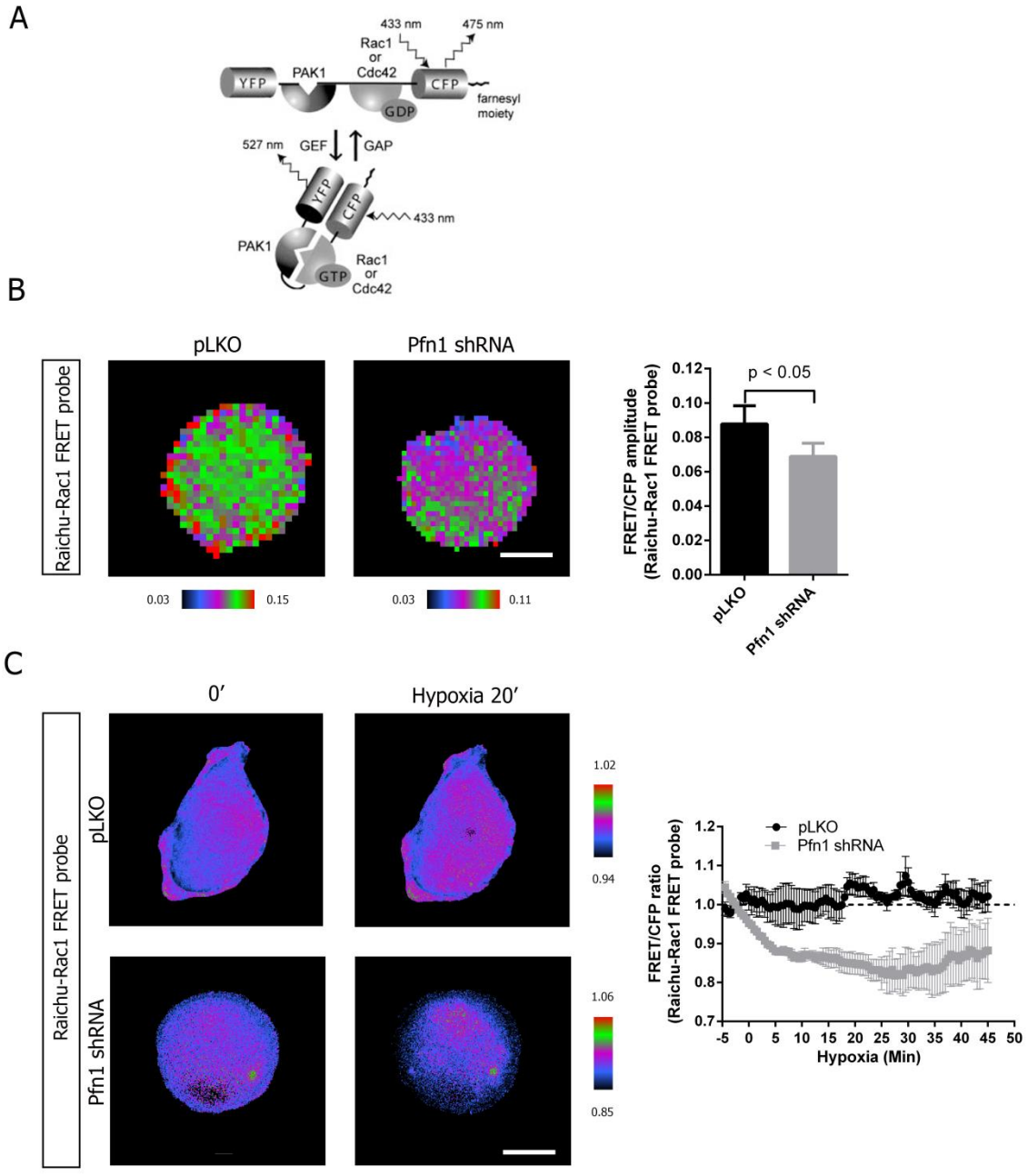

Figure 20 - How Pfn1 knockdown affected Rac1 activity in microglial cells. (A) Schematic illustration of Raichu-Rac1 FRET (Matsuda et al., 2002). **(B)** Representative images of Raichu-Rac1 FRET probe in control and Pfn1 knockdown in primary cortical microglia. After Pfn1 knockdown, primary microglial cells were transfected with plasmid for FRET probe. Imaging was performed 42 hours post-transfection. FRET/CFP images were colour-coded using the colour ramp showed. Scale bar: 10 µm. Graph demonstrating FRET amplitudes from 11 cells in pLKO and 11 cells in Pfn1 shRNA during 10 minutes imaging. **(C)** FRET/CFP representative images of Raichu-Rac1 FRET in control and Pfn1 knockdown BV-2 microglia both in normoxia conditions and at 20 minutes of hypoxia. Images were colour-coded using the colour ramp showed. Scale bar: 10 µm. Each cell was studied for 10 minutes in normoxia conditions, followed by 45 minutes in hypoxia (2% O2). The graph shows normalized FRET/CFP ratio in time-lapse. CFP/FRET emission ratios were normalized at last frame before hypoxia. Data are expressed as mean ± SEM. N=3-4, $p < 0.05$ using unpaired t test.

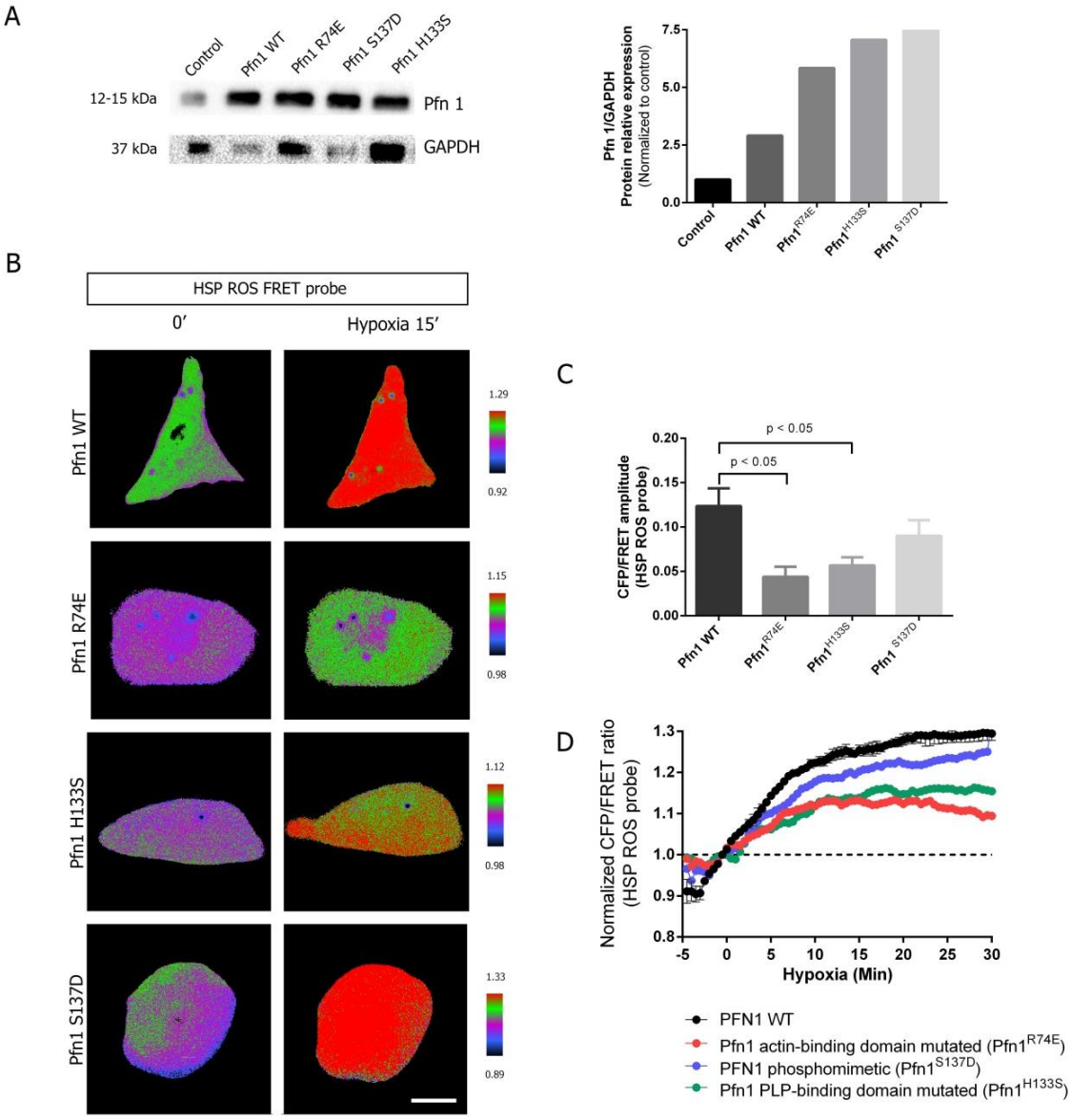

Figure 21 - How different Pfn1 mutants affected ROS generation. (A) Western blot and graphic representation of total Pfn1 protein relative expression in BV-2 microglia 24 hours post-transfection with Pfn1 wild type (Pfn1 WT) and different mutants for Pfn1: Pfn1^{R74E} - actin binding domain defective Pfn1; Pfn1^{H133S}- PLP binding domain defective Pfn1; Pfn1 ^{S137D} – phospho-mimetic Pfn1. Non transfected BV-2 microglia was used as control. GAPDH expression was used as loading control. **(B)** CFP/FRET representative images of HSP ROS probe in BV-2 microglia transfected with Pfn1 WT and Pfn1 mutants both in normoxia conditions and at 15 minutes of hypoxia. Scale bar: 10 µm. CFP/FRET images were colour-coded using the colour ramp showed. **(C)** Graph demonstrating CFP/FRET amplitudes in Pfn1 wild type (Pfn1 WT) and different mutants during 5 minutes imaging in normoxic conditions. **(D)** Graph demonstrating normalized CFP/FRET ratio in time-lapse during normoxia and hypoxia. CFP/FRET emission ratios were normalized at last frame before hypoxia. Imaging was performed during 30 minutes in hypoxia. All data are expressed as mean ± SEM and normalized to control (A,C). $p < 0.05$ using one-way ANOVA.

4. Discussion

Chronic activation of microglia induces neuronal cell death and is implicated in many neurodegenerative diseases, especially though the production and release of ROS, NO and glutamate (Ransohoff and Perry 2009, Kettenmann, Hanisch et al. 2011, Rojo, McBean et al. 2014). Understanding the mechanisms underlying microglial cell activation is important to define targets and develop strategies to counteract the noxious effects of microglia activation. A work by Dong and colleagues (2004) showed that Pfn1, an actin-binding protein, was upregulated in activated microglia, which suggested that it may play a role in the process of microglia activation. However, this putative role of Pfn1 remains elusive.

The aim of the present work was to investigate the role of Pfn1 in microglial cell function. We demonstrate that (i) Pfn1 is more active in hypoxia-challenged microglia, (ii) Pfn1 modulates microglia pro- and anti-inflammatory signatures, and (iii) Pfn1 plays a critical role in ROS production by microglia. We also provide insights on the impact of Pfn1 on ROS production in microglia.

Pfn1 expression has been detected in almost every mammalian cell type studied to date, including monocyte-derived macrophages (Kadiu, Ricardo-Dukelow et al. 2007) and microglial cells (Dong, Ying et al. 2004). Here, we detected Pfn1 mRNA and protein expression in primary microglial cell cultures, in microglial cell lines and in microglia from the brain cortex *in viv*o. As expected, we observed that microglial cells express high levels of Pfn1 (fig. 11).

Considering that (i) Pfn1 plays an essential role in promoting actin dynamics and (ii) the microglial cell activation process is associated with morphological changes, migration into damaged areas and increased phagocytic ability, which are strictly dependent on rearrangements of the actin cytoskeleton, it is conceivable that Pfn1 may play a critical role in microglia activation. Moreover, there is evidence relating macrophage activation to an increase in Pfn1 expression. An increase in Pfn1 expression has been described in macrophages within the atherosclerotic lesions of apoE null mice (Romeo, Frangioni et al. 2004). Macrophages within atherosclerotic lesions are activated and drive inflammatory processes (Dickhout, Basseri et al. 2008).

In order to test the hypothesis that Pfn1 plays a role in microglial activation, we analysed Pfn1 expression and phosphorylation in BV-2 microglia upon anoxia, which triggers a pro-

inflammatory response (fig.12). Several studies support that, both *in vivo* or *in vitro,* challenging microglial cells with reduced levels of oxygen leads to their activation with concomitant production of pro-inflammatory mediators, such as ROS, NO, and TNF, IL-1β and iNOS expression (Park, Lee et al. 2002, Wong and Crack 2008, Yao, Kan et al. 2013). In our model, Pfn1 protein content did not change upon anoxia. This result was apparently not in agreement with the increased Pfn1 mRNA levels reported by Dong and colleagues in activated microglial cells. However, these authors reported differences in the mRNA level, which do not necessarily translate into differences in protein expression. Also, the authors used a different model in which microglial cells were activated in the mouse hippocampus after unilateral destruction of the entorhinal cortex, while we used BV-2 microglia activated by hypoxia. Regarding the phosphorylation at Ser-137, we observed a decrease after hypoxia. Since Pfn1 phosphorylation at Ser-137 inhibits actin polymerization (Sathish, Padma et al. 2004, Shao, Welch et al. 2008), these results indicated that Pfn1 was more active upon hypoxia. Altogether, our data suggested a role for Pfn1 in microglia activation.

To dissect the role of Pfn1 in microglial cell function we knocked down Pfn1 expression in microglia cultures. We observed decreased phagocytic efficiency in Pfn1 knocked down microglial cells (fig. 14A). Taking into consideration the importance of the actin cytoskeleton to the phagocytic process and to actin dynamics, these results were expected and agree with our hypothesis that Pfn1 is important for microglia activation. Furthermore, the idea that Pfn1 is important for phagocytosis is supported in the literature. Coppolino and colleagues showed that Pfn1 is recruited to nascent phagosomes (Coppolino, Krause et al. 2001) and also, Pfn1 siRNA decreases phagocytosis of serum (C3bi)-opsonized zymosan in macrophages (Kim, Moon et al. 2012).

Besides phagocytic efficiency, we also compared Iba-1 expression in Pfn1 knocked down and control microglia. Iba-1 expression is upregulated in situations that cause microglia activation, including ischemia (Ito, Tanaka et al. 2001) and brain diseases (Mori, Imai et al. 2000). Iba-1 also co-operates with both F-actin and signalling molecules to promote membrane ruffling and phagocytosis in monocytic cells (Ohsawa, Imai et al. 2000). There is evidence that (i) Iba-1 is recruited from the cytosol to phagocytic cups during phagocytosis of zymogen particles induced by M-CSF and (ii) Iba-1 mutations inhibit zymogen phagocytosis (Ohsawa, Imai et al. 2000). In our context, we observed decreased Iba-1 expression in Pfn1 knocked down cells, which was in

accordance with the decreased phagocytic efficiency that we had found, suggesting that microglia became less activated upon Pfn1 knockdown (fig.14B).

Moreover, there is evidence that Iba-1 participates in Rac1 signalling (Ohsawa, Imai et al. 2000). Rac1 is a member of the Rho family of small GTPases, which are key players in the dynamics of the actin cytoskeleton. These proteins regulate signalling pathways that link the assembly and organization of the actin cytoskeleton to external and internal signals. In particular, the Rho GTPase Rac1 induces lamellipodia formation and plays an important role in regulation of other cellular processes, including Fcγ receptor-mediated phagocytosis in macrophages and NADPH oxidase-dependent ROS production (Castellano, Montcourrier et al. 2000), Cheng, Diebold et al. 2006, McCann and Roulston 2013). In agreement with previous results, we observed that Rac1 activity was decreased in Pfn1 knocked down microglia, both in basal and hypoxia-challenged cells (fig.20).

Since our results support the hypothesis that Pfn1 is important for microglia activation, we studied the impact of Pfn1 knockdown on the levels of anti- and pro-inflammatory mediators. Regarding the former, we analysed NRF2 activity, IL-10 mRNA expression, and arginase-1 protein expression. NRF2 is a master regulator of the cellular redox state and is implicated in inflammation control (Cho, Reddy et al. 2004, Rojo, Innamorato et al. 2010, Bryan, Olayanju et al. 2013). In microglia, this function was demonstrated in NRF2-deficient mice challenged with systemic administration of LPS. Authors observed increased neuroinflammation in NRF2-deficient mice comparing to wild type animals (Innamorato, Rojo et al. 2008). Also, NRF2 induction with sulforaphane decreased the production of microglial pro-inflammatory mediators (iNOS, IL-6 and TNF) in response to LPS (Innamorato, Rojo et al. 2008). To study the impact of Pfn1 knockdown in NRF2 activity, we analysed the relative expression of Txnrd1, Gclc, and HO-1 (NRF2 target genes). Our results showed that HO-1 was reduced in microglial cells with decreased Pfn1 levels (fig. 15A). HO-1 is the inducible isoform of heme-oxygenase that is responsible for catalysing heme degradation, generating carbon monoxide, biliverdin and free iron as end products. These molecules exert protective effects, for instance, by scavenging free radicals (reviewed in (Rojo, McBean et al. 2014). Also, different studies described that HO-1 end products decreases monocyte activation, with inhibition of NOX activity and TLR-4 signalling (Lanone, Bloc et al. 2005, Taille, El-Benna et al. 2005, Nakahira, Kim et al. 2006). Moreover, it has been reported that anti-inflammatory compounds used to counteract over-activation of microglial cells are responsible for increasing HO-1 expression (Lee, Ko et al. 2014, Gan, Zhang et al. 2015).

Concerning arginase 1, we observed a decrease in its protein expression upon Pfn1 knockdown (fig.15C). As mention in previous sections, arginase 1 competes with iNOS for the same substrate – L-arginine – and produce ornithine as end product. This molecule can be used as substrate for others enzymes giving raise to polyamines, which can be used as antioxidants for redox regulation (reviewed in (C.C. Portugal 2014). Arginase 1 activity leads to decrease in NO production (Chang, Liao et al. 1998) and is associated with an anti-inflammatory signature in microglial cells (Rojo, McBean et al. 2014).

IL-10 is an immunosuppressive cytokine that modulates microglial cell activation by inhibiting the production of pro-inflammatory mediators, such as IL-1β, TNF and iNOS (Hanisch 2002, Park, Lee et al. 2007). The Pfn1 knockdown did not induce significant differences in IL-10 mRNA expression when compared to control (fig.15B). Altogether, these results indicated that Pfn1 reduction lead to a decrease in anti-inflammatory mediators, suggesting that Pfn1 could be important for the acquisition of an anti-inflammatory signature by microglial cells.

Regarding pro-inflammatory mediators, we analysed the activation of transcription factor NF-κB and its target genes, glutamate release and ROS production. NF-κB is a multifunctional transcription factor that is important for transcription of several pro-inflammatory mediators, such as pro-inflammatory cytokines (TNF, IL-6 and IL-1β) and iNOS (Oeckinghaus and Ghosh 2009). Firstly, we observed decreased levels of NF-κB in the nucleus of Pfn1 knocked down microglia (fig. 16A). Consistently, we detected decreased mRNA of pro-inflammatory cytokines (IL-6 and IL-1β) and iNOS (fig. 16B-D). Although the differences in pro-inflammatory cytokines should be confirmed by enzyme-linked immunosorbent assay (ELISA), these results indicated that Pfn1 reduction also impacted on the production of pro-inflammatory cytokines and iNOS in microglial cells. In fact, there are numerous studies in the vascular disease that support this idea. There are studies linking Pfn1 to vascular inflammation, by increasing iNOS activity and peroxynitrite production (Romeo, Moulton et al. 2007, Jin, Song et al. 2012) and also by activating signalling pathways involved in inflammation, such as p38 mitogen-activated protein kinases (p38 MAPK). Romeo and colleagues (2007) showed that both p38 MAPK and iNOS, usually activated upon inflammation, were reduced in macrophages from Pfn1 heterozygous mice exposed to oxidized low-density lipoproteins. Moreover, spontaneous hypertensive rats with overexpression of Pfn1 show increase p38 phosphorylation, which was reversed by Pfn1 knockdown, reinforcing that Pfn1 impacts the p38 pathway (Wang, Zhang et al. 2014). Although this relationship has to be further evaluated, other studies demonstrated that actin remodelling can alter the localization of

inflammatory members of the MAPK signalling, including p38 (Yang, Patel et al. 2007). Considering that (i) Pfn1 may be involved in p38 MAPK signalling, (ii) p38 MAPK signalling can activate NF-κB in microglial cells (Wilms, Rosenstiel et al. 2003) and (iii) NF-κB modulates the expression of pro-inflammatory cytokines and iNOS, it is conceivable that Pfn1 would impact on pro-inflammatory mediators via p38 signalling.

As mention above, activated microglia can increase glutamate release (Piani, Spranger et al. 1992, Barger and Basile 2001). In microglia, glutamate release can be mediated by the increased expression and/or activity of the cystine/glutamate antiporter xc- (Kumar, Singh et al. 2010) or can be result of TNF induction (Takeuchi, Jin et al. 2006). TNF is able to increase glutamate production by up-regulating glutaminase, which generates glutamate from glutamine and leads to glutamate release via Cx32 hemichannel. Here, we did not detect significant differences in glutamate release between Pfn1 knocked down and control microglia (fig.17). This result was consistent with our previous observations that Pfn1 knockdown in microglial cells (i) induces no differences in TNF mRNA relative expression comparing to control and (ii) have decreased ROS levels, having no increased demands for glutathione biosynthesis and, consequently, the activity of xc- transporter might be unaltered.

Increased ROS production is a hallmark of microglia activation (reviewed in (Rojo, McBean et al. 2014). Autocrine effect of ROS can be crucial for microglial pro-inflammatory signature. Acting as a second messenger, ROS are capable of modifying gene expression by activating kinase cascades and transcription factors, for instance NF-κB and NRF2, while extracellular ROS attack pathogens or damaged cells (reviewed in (Block, Zecca et al. 2007). We observed that Pfn1 knockdown dramatically decreased ROS production in microglia (fig.18) and, Pfn1 knockdown was also capable of preventing hypoxia-mediated ROS increase (fig.19).

Altogether, (i) the reduction of NF-κB levels in nucleus of Pfn1 knocked down cells, (ii) the decreased levels of pro-inflammatory cytokines and iNOS and (iii) the dramatic decrease in ROS production, indicated that Pfn1 is crucial for the expression of pro-inflammatory markers, suggesting that Pfn1 could be important for the acquisition of a microglial pro-inflammatory signature. Since Pfn1 was also important for the expression of anti-inflammatory markers, we conclude that Pfn1 is essential for microglial activation, regardless a pro or an anti-inflammatory polarization.

Given that ROS regulation appears highly dependent on Pfn1 in microglia cells, we aimed at investigating the molecular mechanisms by which Pfn1 would affect ROS generation. Firstly, we evaluated the effect of Pfn1 knockdown in Rac1 activation, since Rac1 is important for NOX assembly and activation (Block and Hong 2005). Our results showed that Pfn1 knockdown decreased Rac1 activity (fig. 20B), suggesting that Pfn1 impacts on ROS generation via NOX. Previously, Syriani and colleagues (2008), questioned whether Pfn1 overexpression might regulate Rac1 activity (Syriani, Gomez-Cabrero et al. 2008). They could not find an increase in Rac1 activity, probably because they used an affinity-precipitation assay to measure active Rac-GTP, which is less sensitive than the FRET approach we used. We also observed Rac1 activity upon hypoxia. Pfn1 knockdown kept Rac1 activity at low levels even upon hypoxia, however Rac1 activity did not increased in control cells (fig.20C), as expected, given the increase in ROS production in those conditions. These results do not refute our hypothesis but highlight the contribution of other ROS sources during hypoxia, such as xanthine oxidase activity (Widmer, Engels et al. 2007). Given so, we intend to repeat this experiment with other pro-inflammatory stimulus, which classically increased ROS production by NOX activity, for instance, LPS.

In order to understand better the role of Pfn1 in ROS production, we overexpressed different Pfn1 mutants in microglia to clarify the importance of different Pfn1 domains in modulating ROS production. As described above, Pfn1 actin- and PLP-binding domains are independent, however PIP2 binding site overlaps with both (fig.7). For that reason, we used Pfn1 mutants with point mutations already described in literature, which specifically impaired a single binding domain. $Pfn1^{R74E}$ was used as an actin binding domain defective, $Pfn1^{H133S}$ as a PLP binding domain defective (Ding, Gau et al. 2009). Also, $Pfn1^{S137D}$ is a phosphomimetic mutation that inhibit actin-binding ability (Sathish, Padma et al. 2004, Shao, Welch et al. 2008, Shao and Diamond 2012).

We observed decreased ROS content in microglia overexpressing Pfn1 with mutations in the actin ($Pfn1^{R74E}$) and PLP ($Pfn1^{H133S}$) binding domains in comparison to microglia overexpressing Pfn1 WT. However, the phospho-mimetic Pfn1 construct ($Pfn1^{S137D}$) was much less effective in decreasing ROS production (fig.21). As mention above, phosphorylation on Ser137 leads to impairment of actin binding by Pfn1 (Shao, Welch et al. 2008). So, we expected the same result for phospho-mimetic Pfn1 and Pfn1 with the mutation in the actin-binding domain. This could be just a consequence of the inability of such mutant to fully mimic phosphorylation or could reflect a biological difference that should be explored. We think that performing the same experiment

with a phospho-resistant Pfn1 mutant could be clarifying. Besides, the effect of Pfn1 interaction with phosphatidylinositol in ROS production should also be considered. In fact, it might be possible that the inability of Pfn1 to interact with actin and PLP ligands could target Pfn1 to the plasma membrane, increasing its binding with PIP2. Pfn1-PIP2 interaction might prevent the hydrolysis of PIP2 into DAG and IP3. Reducing DAG and IP3 content might lead to decreased activation of protein kinase C and abrogation of protein kinase C-dependent ROS production by NOX activation (Welch, Coadwell et al. 2003).

In light of our results and the existing literature, we believe that Pfn1 affects microglial cells, at least in part, via Rac1. We demonstrated that Pfn1 knockdown decreased Rac1 activity, both in basal and hypoxic conditions (fig.20), suggesting that Pfn1 might regulate Rac1 activity in microglial cells. Rac1 is an important Rho GTPase that regulates NOX and Fcγ receptor-mediated phagocytosis (Castellano, Montcourrier et al. 2000), Cheng, Diebold et al. 2006, McCann and Roulston 2013). Furthermore, there are evidences indicating that Rac1 activation triggers NRF2 translocation to nucleus and increases the expression of HO-1 via PI3K/AKT (a KEAP-independent regulation of NRF2) (Cuadrado, Martin-Moldes et al. 2014). Moreover, Cuadrado and colleagues (2014) demonstrated that Rac1 activates NF-κB through IκBα. In turn, NF-κB modulates NRF2 activity, which inhibits NF-κB, thus generating a feedback loop (Cuadrado, Martin-Moldes et al. 2014).

In conclusion, we hypothesise that Pfn1 reduction leads to a decrease in Rac1 activity, which could explain the decrease in phagocytic efficiency and in ROS production. Also, decreased Rac1 activity together with decreased ROS production can explain the decrease in pro- and anti-inflammatory mediators (see fig. 22). The putative regulation of Rac1 by Pfn1 must be explored. However, considering that (i) there are several pathways linking PI3K activation to the activation of guanine-nucleotide exchange factors (GEFs), which activate Rac1 (Welch, Coadwell et al. 2003, Hawkins, Davidson et al. 2007) and (ii) there are several evidences showing that PI3K/AKT pathway is sensitive to perturbations in Pfn1 expression (Das, Bae et al. 2009, Jin, Song et al. 2012), we hypothesised that, in our model, Pfn1 might modulate Rac1 activity via PI3K and downstream GEF activation.

In the future, the role Pfn1 in microglia activation should be addressed using pro- and anti-inflammatory stimuli. Also, the putative role of Pfn1 in modulating Rac1 activity and ROS production should be addressed. Moreover, in order to confirm and observe the relevance of the knockdown of Pfn1 in microglia, we ought to study microglia with targeted deletion of Pfn1 *in vivo*

using Cre-lox conditional knockout mice. Also, considering that Pfn1 knockdown decreases microglia activation and ROS production, it would be interesting to study whether Pfn1 knockdown would be protective in the context of neurodegeneration.

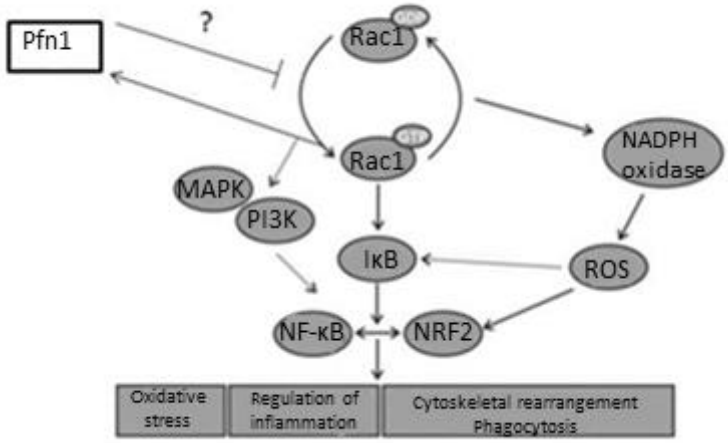

Figure 22 - Pfn1 might regulate Rac1 mediated inflammation. Rac1 activations induce NF-κB and NRF2 activation; is implicated in PI3K and MAPK signalling pathway and regulates NAPDH oxidase activation. Rac1 activation results in increase oxidative stress, regulation of inflammation and rearrangements of cytoskeleton involved in phagocytosis. Pfn1 reduction leads to decreased Rac1 activity which might explain decrease in oxidative stress, inflammation and phagocytosis. Adapted from Cuadrado, Martin-Moldes et al. 2014. Rac1-GDP: inactive Rac1; Rac1-GTP:active Rac1; MAPK: Mitogen-activated protein kinase; PI3K: phosphatidylinositide 3-kinases; IκB: Inhibitor of NF-κB; ROS: reactive oxygen species; NRF2: Nuclear factor erythroid 2–related factor 2; NF-κB: Factor nuclear kappa B.

5. Conclusions

In this work we investigated the role of Pfn1 in microglial cell function. We observed that Pfn1 is more active in hypoxia-challenged microglia and demonstrated that Pfn1 knockdown leads to a decrease in microglia-related activation markers. These observations suggest that Pfn1 modulates pro- and anti-inflammatory signatures in microglial cells. Moreover, we also showed that Pfn1 plays a critical role in ROS generation by microglia and it might be involved in Rac1 regulation.

6. References

Barger, S. W. and A. S. Basile (2001). "Activation of microglia by secreted amyloid precursor protein evokes release of glutamate by cystine exchange and attenuates synaptic function." J Neurochem **76**(3): 846-854.

Birbach, A. (2008). "Profilin, a multi-modal regulator of neuronal plasticity." Bioessays **30**(10): 994-1002.

Blasi, E., R. Barluzzi, V. Bocchini, R. Mazzolla and F. Bistoni (1990). "Immortalization of murine microglial cells by a v-raf/v-myc carrying retrovirus." J Neuroimmunol **27**(2-3): 229-237.

Block, M. L. and J. S. Hong (2005). "Microglia and inflammation-mediated neurodegeneration: multiple triggers with a common mechanism." Prog Neurobiol **76**(2): 77-98.

Block, M. L., L. Zecca and J. S. Hong (2007). "Microglia-mediated neurotoxicity: uncovering the molecular mechanisms." Nat Rev Neurosci **8**(1): 57-69.

Bocchini, V., R. Mazzolla, R. Barluzzi, E. Blasi, P. Sick and H. Kettenmann (1992). "An immortalized cell line expresses properties of activated microglial cells." J Neurosci Res **31**(4): 616-621.

Boillee, S., C. Vande Velde and D. W. Cleveland (2006). "ALS: a disease of motor neurons and their nonneuronal neighbors." Neuron **52**(1): 39-59.

Bonefeld, B. E., B. Elfving and G. Wegener (2008). "Reference genes for normalization: a study of rat brain tissue." Synapse **62**(4): 302-309.

Brown, G. C. (2010). "Nitric oxide and neuronal death." Nitric Oxide **23**(3): 153-165.

Brown, G. C. and C. E. Cooper (1994). "Nanomolar concentrations of nitric oxide reversibly inhibit synaptosomal respiration by competing with oxygen at cytochrome oxidase." FEBS Lett **356**(2-3): 295-298.

Bryan, H. K., A. Olayanju, C. E. Goldring and B. K. Park (2013). "The Nrf2 cell defence pathway: Keap1-dependent and -independent mechanisms of regulation." Biochem Pharmacol **85**(6): 705-717.

C.C. Portugal, R. S., T.G. Encarnção, I.C.L. Domith, M. Cossenza, R. Paes-de-carvalho (2014). Ascorbate Transport in Retinal Cells and Its Relationship with the Nitric Oxide System. Handbook of Nutrition, Diet and the Eye. V. Preedy, Academic Press.

Calabrese, V., C. Mancuso, M. Calvani, E. Rizzarelli, D. A. Butterfield and A. M. Stella (2007). "Nitric oxide in the central nervous system: neuroprotection versus neurotoxicity." Nat Rev Neurosci **8**(10): 766-775.

Carlsson, L., L. E. Nystrom, I. Sundkvist, F. Markey and U. Lindberg (1977). "Actin polymerizability is influenced by profilin, a low molecular weight protein in non-muscle cells." J Mol Biol **115**(3): 465-483.

Castellano, F., P. Montcourrier and P. Chavrier (2000). "Membrane recruitment of Rac1 triggers phagocytosis." J Cell Sci **113 (Pt 17)**: 2955-2961.

Chang, C. I., J. C. Liao and L. Kuo (1998). "Arginase modulates nitric oxide production in activated macrophages." Am J Physiol **274**(1 Pt 2): H342-348.

Cheng, G., B. A. Diebold, Y. Hughes and J. D. Lambeth (2006). "Nox1-dependent reactive oxygen generation is regulated by Rac1." J Biol Chem **281**(26): 17718-17726.

Cho, H. Y., S. P. Reddy, M. Yamamoto and S. R. Kleeberger (2004). "The transcription factor NRF2 protects against pulmonary fibrosis." Faseb j **18**(11): 1258-1260.

Coppolino, M. G., M. Krause, P. Hagendorff, D. A. Monner, W. Trimble, S. Grinstein, J. Wehland and A. S. Sechi (2001). "Evidence for a molecular complex consisting of Fyb/SLAP, SLP-76, Nck, VASP and WASP that links the actin cytoskeleton to Fcgamma receptor signalling during phagocytosis." J Cell Sci **114**(Pt 23): 4307-4318.

Cuadrado, A., Z. Martin-Moldes, J. Ye and I. Lastres-Becker (2014). "Transcription factors NRF2 and NF-kappaB are coordinated effectors of the Rho family, GTP-binding protein RAC1 during inflammation." J Biol Chem **289**(22): 15244-15258.

Das, T., Y. H. Bae, A. Wells and P. Roy (2009). "Profilin-1 overexpression upregulates PTEN and suppresses AKT activation in breast cancer cells." J Cell Physiol **218**(2): 436-443.

Dickhout, J. G., S. Basseri and R. C. Austin (2008). "Macrophage function and its impact on atherosclerotic lesion composition, progression, and stability: the good, the bad, and the ugly." Arterioscler Thromb Vasc Biol **28**(8): 1413-1415.

Ding, Z., Y. H. Bae and P. Roy (2012). "Molecular insights on context-specific role of profilin-1 in cell migration." Cell Adh Migr **6**(5): 442-449.

Ding, Z., D. Gau, B. Deasy, A. Wells and P. Roy (2009). "Both actin and polyproline interactions of profilin-1 are required for migration, invasion and capillary morphogenesis of vascular endothelial cells." Exp Cell Res **315**(17): 2963-2973.

Domke, T., T. Federau, K. Schluter, K. Giehl, R. Valenta, D. Schomburg and B. M. Jockusch (1997). "Birch pollen profilin: structural organization and interaction with poly-(L-proline) peptides as revealed by NMR." FEBS Lett **411**(2-3): 291-295.

Dong, J., B. Radau, A. Otto, E. Muller, C. Lindschau and P. Westermann (2000). "Profilin I attached to the Golgi is required for the formation of constitutive transport vesicles at the trans-Golgi network." Biochim Biophys Acta **1497**(2): 253-260.

Dong, J. H., G. X. Ying and C. F. Zhou (2004). "Entorhinal deafferentation induces the expression of profilin mRNA in the reactive microglial cells in the hippocampus." Glia **47**(1): 102-108.

Fedorov, A. A., K. A. Magnus, M. H. Graupe, E. E. Lattman, T. D. Pollard and S. C. Almo (1994). "X-ray structures of isoforms of the actin-binding protein profilin that differ in their affinity for phosphatidylinositol phosphates." Proc Natl Acad Sci U S A **91**(18): 8636-8640.

Gan, P., L. Zhang, Y. Chen, Y. Zhang, F. Zhang, X. Zhou, X. Zhang, B. Gao, X. Zhen, J. Zhang and L. T. Zheng (2015). "Anti-inflammatory effects of glaucocalyxin B in microglia cells." J Pharmacol Sci.

Garden, G. A. and A. R. La Spada (2012). "Intercellular (mis)communication in neurodegenerative disease." Neuron **73**(5): 886-901.

Gareus, R., A. Di Nardo, V. Rybin and W. Witke (2006). "Mouse profilin 2 regulates endocytosis and competes with SH3 ligand binding to dynamin 1." J Biol Chem **281**(5): 2803-2811.

Giudice, A., C. Arra and M. C. Turco (2010). "Review of molecular mechanisms involved in the activation of the Nrf2-ARE signaling pathway by chemopreventive agents." Methods Mol Biol **647**: 37-74.

Goldschmidt-Clermont, P. J., J. W. Kim, L. M. Machesky, S. G. Rhee and T. D. Pollard (1991). "Regulation of phospholipase C-gamma 1 by profilin and tyrosine phosphorylation." Science **251**(4998): 1231-1233.

Goldschmidt-Clermont, P. J., L. M. Machesky, J. J. Baldassare and T. D. Pollard (1990). "The actin-binding protein profilin binds to PIP2 and inhibits its hydrolysis by phospholipase C." Science **247**(4950): 1575-1578.

Green, J. A., P. T. Elkington, C. J. Pennington, F. Roncaroli, S. Dholakia, R. C. Moores, A. Bullen, J. C. Porter, D. Agranoff, D. R. Edwards and J. S. Friedland (2010). "Mycobacterium tuberculosis upregulates microglial matrix metalloproteinase-1 and -3 expression and secretion via NF-kappaB- and Activator Protein-1-dependent monocyte networks." J Immunol **184**(11): 6492-6503.

Guzy, R. D., B. Hoyos, E. Robin, H. Chen, L. Liu, K. D. Mansfield, M. C. Simon, U. Hammerling and P. T. Schumacker (2005). "Mitochondrial complex III is required for hypoxia-induced ROS production and cellular oxygen sensing." Cell Metab **1**(6): 401-408.

Hanisch, U. K. (2002). "Microglia as a source and target of cytokines." Glia **40**(2): 140-155.

Hausler, K. G., M. Prinz, C. Nolte, J. R. Weber, R. R. Schumann, H. Kettenmann and U. K. Hanisch (2002). "Interferon-gamma differentially modulates the release of cytokines and chemokines in lipopolysaccharide- and pneumococcal cell wall-stimulated mouse microglia and macrophages." Eur J Neurosci **16**(11): 2113-2122.

Hawkins, P. T., K. Davidson and L. R. Stephens (2007). "The role of PI3Ks in the regulation of the neutrophil NADPH oxidase." Biochem Soc Symp(74): 59-67.

Henn, A., S. Lund, M. Hedtjarn, A. Schrattenholz, P. Porzgen and M. Leist (2009). "The suitability of BV2 cells as alternative model system for primary microglia cultures or for animal experiments examining brain inflammation." Altex **26**(2): 83-94.

Heyworth, P. G., U. G. Knaus, J. Settleman, J. T. Curnutte and G. M. Bokoch (1993). "Regulation of NADPH oxidase activity by Rac GTPase activating protein(s)." Mol Biol Cell **4**(11): 1217-1223.

Hjorth, E., D. Frenkel, H. Weiner and M. Schultzberg (2010). "Effects of immunomodulatory substances on phagocytosis of abeta(1-42) by human microglia." Int J Alzheimers Dis **2010**.

Imai, Y. and S. Kohsaka (2002). "Intracellular signaling in M-CSF-induced microglia activation: role of Iba1." Glia **40**(2): 164-174.

Innamorato, N. G., A. I. Rojo, A. J. Garcia-Yague, M. Yamamoto, M. L. de Ceballos and A. Cuadrado (2008). "The transcription factor Nrf2 is a therapeutic target against brain inflammation." J Immunol **181**(1): 680-689.

Ito, D., K. Tanaka, S. Suzuki, T. Dembo and Y. Fukuuchi (2001). "Enhanced expression of Iba1, ionized calcium-binding adapter molecule 1, after transient focal cerebral ischemia in rat brain." Stroke **32**(5): 1208-1215.

Itoh, R. E., K. Kurokawa, Y. Ohba, H. Yoshizaki, N. Mochizuki and M. Matsuda (2002). "Activation of rac and cdc42 video imaged by fluorescent resonance energy transfer-based single-molecule probes in the membrane of living cells." Mol Cell Biol **22**(18): 6582-6591.

Janabi, N., S. Peudenier, B. Heron, K. H. Ng and M. Tardieu (1995). "Establishment of human microglial cell lines after transfection of primary cultures of embryonic microglial cells with the SV40 large T antigen." Neurosci Lett **195**(2): 105-108.

Janke, J., K. Schluter, B. Jandrig, M. Theile, K. Kolble, W. Arnold, E. Grinstein, A. Schwartz, L. Estevez-Schwarz, P. M. Schlag, B. M. Jockusch and S. Scherneck (2000). "Suppression of tumorigenicity in breast cancer cells by the microfilament protein profilin 1." J Exp Med **191**(10): 1675-1686.

Jin, H. Y., B. Song, G. Y. Oudit, S. T. Davidge, H. M. Yu, Y. Y. Jiang, P. J. Gao, D. L. Zhu, G. Ning, Z. Kassiri, J. M. Penninger and J. C. Zhong (2012). "ACE2 deficiency enhances angiotensin II-mediated aortic profilin-1 expression, inflammation and peroxynitrite production." PLoS One **7**(6): e38502.

Jockusch, B. M., K. Murk and M. Rothkegel (2007). "The profile of profilins." Rev Physiol Biochem Pharmacol **159**: 131-149.

Jung, K. A. and M. K. Kwak (2010). "The Nrf2 system as a potential target for the development of indirect antioxidants." Molecules **15**(10): 7266-7291.

Kadiu, I., M. Ricardo-Dukelow, P. Ciborowski and H. E. Gendelman (2007). "Cytoskeletal protein transformation in HIV-1-infected macrophage giant cells." J Immunol **178**(10): 6404-6415.

Kawai, T. and S. Akira (2010). "The role of pattern-recognition receptors in innate immunity: update on Toll-like receptors." Nat Immunol **11**(5): 373-384.

Kensler, T. W., N. Wakabayashi and S. Biswal (2007). "Cell survival responses to environmental stresses via the Keap1-Nrf2-ARE pathway." Annu Rev Pharmacol Toxicol **47**: 89-116.

Kettenmann, H., U.-K. Hanisch, M. Noda and A. Verkhratsky (2011). "Physiology of microglia." Physiological reviews **91**(2): 461-553.

Kim, J. G., M. Y. Moon, H. J. Kim, Y. Li, D. K. Song, J. S. Kim, J. Y. Lee, J. Kim, S. C. Kim and J. B. Park (2012). "Ras-related GTPases Rap1 and RhoA collectively induce the phagocytosis of serum-opsonized zymosan particles in macrophages." J Biol Chem **287**(7): 5145-5155.

Koenigsknecht, J. and G. Landreth (2004). "Microglial phagocytosis of fibrillar beta-amyloid through a beta1 integrin-dependent mechanism." J Neurosci **24**(44): 9838-9846.

Kumar, A., R. L. Singh and G. N. Babu (2010). "Cell death mechanisms in the early stages of acute glutamate neurotoxicity." Neurosci Res **66**(3): 271-278.

Lanone, S., S. Bloc, R. Foresti, A. Almolki, C. Taille, J. Callebert, M. Conti, D. Goven, M. Aubier, B. Dureuil, J. El-Benna, R. Motterlini and J. Boczkowski (2005). "Bilirubin decreases nos2 expression via inhibition of NAD(P)H oxidase: implications for protection against endotoxic shock in rats." Faseb j **19**(13): 1890-1892.

Lassing, I. and U. Lindberg (1985). "Specific interaction between phosphatidylinositol 4,5-bisphosphate and profilactin." Nature **314**(6010): 472-474.

Lawson, L. J., V. H. Perry, P. Dri and S. Gordon (1990). "Heterogeneity in the distribution and morphology of microglia in the normal adult mouse brain." Neuroscience **39**(1): 151-170.

Le Clainche, C. and M. F. Carlier (2008). "Regulation of actin assembly associated with protrusion and adhesion in cell migration." Physiol Rev **88**(2): 489-513.

Lederer, M., B. M. Jockusch and M. Rothkegel (2005). "Profilin regulates the activity of p42POP, a novel Myb-related transcription factor." J Cell Sci **118**(Pt 2): 331-341.

Lee, D. S., W. Ko, C. S. Yoon, D. C. Kim, J. Yun, J. K. Lee, K. Y. Jun, I. Son, D. W. Kim, B. K. Song, S. Choi, J. H. Jang, H. Oh, S. Kim and Y. C. Kim (2014). "KCHO-1, a Novel Antineuroinflammatory Agent, Inhibits Lipopolysaccharide-Induced Neuroinflammatory Responses through Nrf2-Mediated Heme Oxygenase-1 Expression in Mouse BV2 Microglia Cells." Evid Based Complement Alternat Med **2014**: 357154.

Lee, S. H. and R. Dominguez (2010). "Regulation of actin cytoskeleton dynamics in cells." Mol Cells **29**(4): 311-325.

Livak, K. J. and T. D. Schmittgen (2001). "Analysis of relative gene expression data using real-time quantitative PCR and the 2(-Delta Delta C(T)) Method." Methods **25**(4): 402-408.

Lund, S., K. V. Christensen, M. Hedtjarn, A. L. Mortensen, H. Hagberg, J. Falsig, H. Hasseldam, A. Schrattenholz, P. Porzgen and M. Leist (2006). "The dynamics of the LPS triggered inflammatory response of murine microglia under different culture and in vivo conditions." J Neuroimmunol **180**(1-2): 71-87.

McCann, S. K. and C. L. Roulston (2013). "NADPH Oxidase as a Therapeutic Target for Neuroprotection against Ischaemic Stroke: Future Perspectives." Brain Sci **3**(2): 561-598.

Mitsuishi, Y., H. Motohashi and M. Yamamoto (2012). "The Keap1-Nrf2 system in cancers: stress response and anabolic metabolism." Front Oncol **2**: 200.

Mori, I., Y. Imai, S. Kohsaka and Y. Kimura (2000). "Upregulated expression of Iba1 molecules in the central nervous system of mice in response to neurovirulent influenza A virus infection." Microbiol Immunol **44**(8): 729-735.

Murk, K., N. Wittenmayer, K. Michaelsen-Preusse, T. Dresbach, C. A. Schoenenberger, M. Korte, B. M. Jockusch and M. Rothkegel (2012). "Neuronal profilin isoforms are addressed by different signalling pathways." PLoS One **7**(3): e34167.

Murphy, S. (2000). "Production of nitric oxide by glial cells: regulation and potential roles in the CNS." Glia **29**(1): 1-13.

Nakahira, K., H. P. Kim, X. H. Geng, A. Nakao, X. Wang, N. Murase, P. F. Drain, X. Wang, M. Sasidhar, E. G. Nabel, T. Takahashi, N. W. Lukacs, S. W. Ryter, K. Morita and A. M. Choi (2006). "Carbon monoxide differentially inhibits TLR signaling pathways by regulating ROS-induced trafficking of TLRs to lipid rafts." J Exp Med **203**(10): 2377-2389.

Neumann, H., M. R. Kotter and R. J. Franklin (2009). "Debris clearance by microglia: an essential link between degeneration and regeneration." Brain **132**(Pt 2): 288-295.

Oeckinghaus, A. and S. Ghosh (2009). "The NF-kappaB family of transcription factors and its regulation." Cold Spring Harb Perspect Biol **1**(4): a000034.

Ohsawa, K., Y. Imai, H. Kanazawa, Y. Sasaki and S. Kohsaka (2000). "Involvement of Iba1 in membrane ruffling and phagocytosis of macrophages/microglia." J Cell Sci **113 (Pt 17)**: 3073-3084.

Okumoto, S., L. L. Looger, K. D. Micheva, R. J. Reimer, S. J. Smith and W. B. Frommer (2005). "Detection of glutamate release from neurons by genetically encoded surface-displayed FRET nanosensors." Proc Natl Acad Sci U S A **102**(24): 8740-8745.

Park, K. W., H. G. Lee, B. K. Jin and Y. B. Lee (2007). "Interleukin-10 endogenously expressed in microglia prevents lipopolysaccharide-induced neurodegeneration in the rat cerebral cortex in vivo." Exp Mol Med **39**(6): 812-819.

Park, S. Y., H. Lee, J. Hur, S. Y. Kim, H. Kim, J. H. Park, S. Cha, S. S. Kang, G. J. Cho, W. S. Choi and K. Suk (2002). "Hypoxia induces nitric oxide production in mouse microglia via p38 mitogen-activated protein kinase pathway." Brain Res Mol Brain Res **107**(1): 9-16.

Parkhurst, C. N., G. Yang, I. Ninan, J. N. Savas, J. R. Yates, 3rd, J. J. Lafaille, B. L. Hempstead, D. R. Littman and W. B. Gan (2013). "Microglia promote learning-dependent synapse formation through brain-derived neurotrophic factor." Cell **155**(7): 1596-1609.

Peri, F. and C. Nusslein-Volhard (2008). "Live imaging of neuronal degradation by microglia reveals a role for v0-ATPase a1 in phagosomal fusion in vivo." Cell **133**(5): 916-927.

Piani, D., M. Spranger, K. Frei, A. Schaffner and A. Fontana (1992). "Macrophage-induced cytotoxicity of N-methyl-D-aspartate receptor positive neurons involves excitatory amino acids rather than reactive oxygen intermediates and cytokines." Eur J Immunol **22**(9): 2429-2436.

Pilo Boyl, P., A. Di Nardo, C. Mulle, M. Sassoe-Pognetto, P. Panzanelli, A. Mele, M. Kneussel, V. Costantini, E. Perlas, M. Massimi, H. Vara, M. Giustetto and W. Witke (2007). "Profilin2 contributes to synaptic vesicle exocytosis, neuronal excitability, and novelty-seeking behavior." Embo j **26**(12): 2991-3002.

Ransohoff, R. M. and V. H. Perry (2009). "Microglial physiology: unique stimuli, specialized responses." Annu Rev Immunol **27**: 119-145.

Reinhard, M., K. Giehl, K. Abel, C. Haffner, T. Jarchau, V. Hoppe, B. M. Jockusch and U. Walter (1995). "The proline-rich focal adhesion and microfilament protein VASP is a ligand for profilins." Embo j **14**(8): 1583-1589.

Rojo, A. I., N. G. Innamorato, A. M. Martin-Moreno, M. L. De Ceballos, M. Yamamoto and A. Cuadrado (2010). "Nrf2 regulates microglial dynamics and neuroinflammation in experimental Parkinson's disease." Glia **58**(5): 588-598.

Rojo, A. I., G. McBean, M. Cindric, J. Egea, M. G. Lopez, P. Rada, N. Zarkovic and A. Cuadrado (2014). "Redox control of microglial function: molecular mechanisms and functional significance." Antioxid Redox Signal **21**(12): 1766-1801.

Romeo, G., J. V. Frangioni and A. Kazlauskas (2004). "Profilin acts downstream of LDL to mediate diabetic endothelial cell dysfunction." Faseb j **18**(6): 725-727.

Romeo, G. R., K. S. Moulton and A. Kazlauskas (2007). "Attenuated expression of profilin-1 confers protection from atherosclerosis in the LDL receptor null mouse." Circ Res **101**(4): 357-367.

Saijo, K. and C. K. Glass (2011). "Microglial cell origin and phenotypes in health and disease." Nature Reviews Immunology **11**(11): 775-787.

Salter, M. W. and S. Beggs (2014). "Sublime microglia: expanding roles for the guardians of the CNS." Cell **158**(1): 15-24.

Sathish, K., B. Padma, V. Munugalavadla, V. Bhargavi, K. V. Radhika, R. Wasia, M. Sairam and S. S. Singh (2004). "Phosphorylation of profilin regulates its interaction with actin and poly (L-proline)." Cell Signal **16**(5): 589-596.

Schilling, T., R. Nitsch, U. Heinemann, D. Haas and C. Eder (2001). "Astrocyte-released cytokines induce ramification and outward K+ channel expression in microglia via distinct signalling pathways." Eur J Neurosci **14**(3): 463-473.

Schmidt, A. and M. N. Hall (1998). "Signaling to the actin cytoskeleton." Annu Rev Cell Dev Biol **14**: 305-338.

Schutt, C. E., J. C. Myslik, M. D. Rozycki, N. C. Goonesekere and U. Lindberg (1993). "The structure of crystalline profilin-beta-actin." Nature **365**(6449): 810-816.

Shao, J. and M. I. Diamond (2012). "Protein phosphatase 1 dephosphorylates profilin-1 at Ser-137." PLoS One **7**(3): e32802.

Shao, J., W. J. Welch, N. A. Diprospero and M. I. Diamond (2008). "Phosphorylation of profilin by ROCK1 regulates polyglutamine aggregation." Mol Cell Biol **28**(17): 5196-5208.

Skare, P., J. P. Kreivi, A. Bergstrom and R. Karlsson (2003). "Profilin I colocalizes with speckles and Cajal bodies: a possible role in pre-mRNA splicing." Exp Cell Res **286**(1): 12-21.

Socodato, R., C. C. Portugal, T. Canedo, I. Domith, N. A. Oliveira, R. Paes-de-Carvalho, J. B. Relvas and M. Cossenza (2015). "c-Src deactivation by the polyphenol 3-O-caffeoylquinic acid abrogates reactive oxygen species-mediated glutamate release from microglia and neuronal excitotoxicity." Free Radic Biol Med **79**: 45-55.

Stankiewicz, T. R. and D. A. Linseman (2014). "Rho family GTPases: key players in neuronal development, neuronal survival, and neurodegeneration." Front Cell Neurosci **8**: 314.

Stuven, T., E. Hartmann and D. Gorlich (2003). "Exportin 6: a novel nuclear export receptor that is specific for profilin.actin complexes." Embo j **22**(21): 5928-5940.

Syriani, E., A. Gomez-Cabrero, M. Bosch, A. Moya, E. Abad, A. Gual, X. Gasull and M. Morales (2008). "Profilin induces lamellipodia by growth factor-independent mechanism." Faseb j **22**(5): 1581-1596.

Taille, C., J. El-Benna, S. Lanone, J. Boczkowski and R. Motterlini (2005). "Mitochondrial respiratory chain and NAD(P)H oxidase are targets for the antiproliferative effect of carbon monoxide in human airway smooth muscle." J Biol Chem **280**(27): 25350-25360.

Takeuchi, H., S. Jin, J. Wang, G. Zhang, J. Kawanokuchi, R. Kuno, Y. Sonobe, T. Mizuno and A. Suzumura (2006). "Tumor necrosis factor-alpha induces neurotoxicity via glutamate release from hemichannels of activated microglia in an autocrine manner." J Biol Chem **281**(30): 21362-21368.

Wang, Y., J. Zhang, H. Gao, S. Zhao, X. Ji, X. Liu, B. You, X. Li and J. Qiu (2014). "Profilin-1 promotes the development of hypertension-induced artery remodeling." J Histochem Cytochem **62**(4): 298-310.

Welch, H. C., W. J. Coadwell, L. R. Stephens and P. T. Hawkins (2003). "Phosphoinositide 3-kinase-dependent activation of Rac." FEBS Lett **546**(1): 93-97.

Widmer, R., M. Engels, P. Voss and T. Grune (2007). "Postanoxic damage of microglial cells is mediated by xanthine oxidase and cyclooxygenase." Free Radic Res **41**(2): 145-152.

Wilms, H., P. Rosenstiel, J. Sievers, G. Deuschl, L. Zecca and R. Lucius (2003). "Activation of microglia by human neuromelanin is NF-kappaB dependent and involves p38 mitogen-activated protein kinase: implications for Parkinson's disease." Faseb j **17**(3): 500-502.

Witke, W. (2004). "The role of profilin complexes in cell motility and other cellular processes." Trends Cell Biol **14**(8): 461-469.

Witke, W., J. D. Sutherland, A. Sharpe, M. Arai and D. J. Kwiatkowski (2001). "Profilin I is essential for cell survival and cell division in early mouse development." Proc Natl Acad Sci U S A **98**(7): 3832-3836.

Wong, C. H. and P. J. Crack (2008). "Modulation of neuro-inflammation and vascular response by oxidative stress following cerebral ischemia-reperfusion injury." Curr Med Chem **15**(1): 1-14.

Wu, C. H., C. Fallini, N. Ticozzi, P. J. Keagle, P. C. Sapp, K. Piotrowska, P. Lowe, M. Koppers, D. McKenna-Yasek, D. M. Baron, J. E. Kost, P. Gonzalez-Perez, A. D. Fox, J. Adams, F. Taroni, C. Tiloca, A. L. Leclerc, S. C. Chafe, D. Mangroo, M. J. Moore, J. A. Zitzewitz, Z. S. Xu, L. H. van den Berg, J. D. Glass, G. Siciliano, E. T. Cirulli, D. B. Goldstein, F. Salachas, V. Meininger, W. Rossoll, A. Ratti, C. Gellera, D. A. Bosco, G. J. Bassell, V. Silani, V. E. Drory, R. H. Brown, Jr. and J. E. Landers (2012). "Mutations in the profilin 1 gene cause familial amyotrophic lateral sclerosis." Nature **488**(7412): 499-503.

Yang, C., K. Patel, P. Harding, A. Sorokin and W. F. Glass, 2nd (2007). "Regulation of TGF-beta1/MAPK-mediated PAI-1 gene expression by the actin cytoskeleton in human mesangial cells." Exp Cell Res **313**(6): 1240-1250.

Yao, L., E. M. Kan, J. Lu, A. Hao, S. T. Dheen, C. Kaur and E. A. Ling (2013). "Toll-like receptor 4 mediates microglial activation and production of inflammatory mediators in neonatal rat brain following hypoxia: role of TLR4 in hypoxic microglia." J Neuroinflammation **10**: 23.

Zou, L., M. Jaramillo, D. Whaley, A. Wells, V. Panchapakesa, T. Das and P. Roy (2007). "Profilin-1 is a negative regulator of mammary carcinoma aggressiveness." Br J Cancer **97**(10): 1361-1371.

Appendix

Appendix I - qRT-PCR cycles

Pro-inflammatory cytokines; profilin 1 and Ywhaz					IL-10					NRF2 target genes				
Cycle	Repeats	Steps	Duration (min)	Temperature (ºC)	Cycle	Repeats	Steps	Duration (min)	Temperature (ºC)	Cycle	Repeats	Steps	Duration (min)	Temperature (ºC)
1	1	1	03:00	94	**1**	1	1	03:30	95	**1**	1	1	03:30	95
2	40	1	00:15	94ºC	**2**	40	1	00:15	94ºC	**2**	40	1	00:30	94ºC
		2	00:20	58ºC			2	00:20	62ºC			2	00:30	59ºC
		3	00:15	70ºC								3	00:30	72ºC
3	81	1	00:30	55-95	**3**	81	1	00:10	55-95	**3**	81	1	00:10	55-95

Appendix II –Publications

Cátia M Silva; Renato Socodato; João B Relvas and Camila C Portugal. **Profilin-1 is a regulator of microglia pro-inflammatory signature and ROS generation.** Zoom in microglia, Coimbra, Portugal, December 17th 2014. (see next page)

Renato Socodato, Camila C. Portugal, Tânia Martins, Teresa Canedo, Cátia M. Silva, Ana Keating, Ivan Domith, Nadia A. Oliveira, Vívian S.M Coreixas, Erick C. Loiola, Ana R. Santiago, Roberto Paes-de-Carvalho, António F. Ambrósio, João B. Relvas. **RhoA downregulation in microglia is sufficient to trigger a pro-inflammatory signature.** Zoom in microglia, Coimbra, Portugal, December 17th 2014.

Camila C. Portugal, Renato Socodato, Tânia Martins, Teresa Canedo, Cátia M. Silva, Vívian S.M Coreixas, Erick C. Loiola, Burkhard Gess, Dominik Röhr, Ana R. Santiago, Peter Young, Roberto Paes-de-Carvalho, António F. Ambrósio, João B. Relvas**. Downregulation of sodium vitamin C co-transporter-2 (SVCT-2) is a key step in the pro- inflammatory signature of microglial cells**. Zoom in microglia, Coimbra, Portugal, December 17th 2014.

Camila C. Portugal, Renato Socodato, Teresa Canedo, Cátia M. Silva, Tânia Martins, Vívian S.M Coreixas, Erick C. Loiola, Burkhard Gess, Dominik Röhr, Ana R. Santiago, Peter Young, Richard D. Minshall, Roberto Paes-de-Carvalho, António F. Ambrósio, João B. Relvas. **Sodium Vitamin C co-Transporter 2 (SVCT2) downregulation is necessary and sufficient to induce a pro-inflammatory polarization of microglia.** 4th Venusberg Meeting on Neuroinflammation, Bonn, Germany, May 7-9, 2015.

Renato Socodato, Camila C. Portugal, Tânia Martins, Teresa Canedo, Cátia M. Silva, Ivan Domith, Nadia A. Oliveira, Ana R. Santiago, Roberto Paes-de-Carvalho, António F. Ambrósio, João B. Relvas. **Specific downregulation of RhoA triggers a pro-inflammatory signature in microglia via a Rock2/Csk/c-Src signaling axis.** 4th Venusberg Meeting on Neuroinflammation, Bonn, Germany, May 7-9, 2015.

Camila C. Portugal, Renato Socodato, Teresa Canedo, Cátia M. Silva, Tânia Martins, Vívian S.M Coreixas, Erick C. Loiola, Burkhard Gess, Dominik Röhr, Ana R. Santiago, Peter Young, Richard D. Minshall, Roberto Paes-de-Carvalho, António F. Ambrósio, João B. Relvas. **The Sodium Vitamin C co-Transporter 2 (SVCT2) downregulation is necessary and sufficient to induce microglia pro-inflammatory activation.** XIV meeting of the portuguese society for neuroscience, Póvoa de Varzim, Portugal, 4-5 June 2015.

Renato Socodato, Camila C. Portugal, Teresa Canedo, Cátia M. Silva, Teresa Summavielle, João B. Relvas. **Ethanol triggers fast glutamate release from cortical microglia via c-Src/TNF signalling.** XIV meeting of the portuguese society for neuroscience, Póvoa de Varzim, Portugal, 4-5 June 2015.

Camila C. Portugal, Renato Socodato, Teresa Canedo, Cátia M. Silva, Tânia Martins, Vívian S.M Coreixas, Erick C. Loiola, Burkhard Gess, Dominik Röhr, Ana R. Santiago, Peter Young, Richard D. Minshall, Roberto Paes-de-Carvalho, António F. Ambrósio, João B. Relvas. **Sodium Vitamin C co-Transporter 2 (SVCT2) downregulation is necessary and sufficient for the pro-inflammatory microglia activation.** Manuscript in preparation

IBMC
INSTITUTO DE BIOLOGIA MOLECULAR E CELULAR
INSTITUTE FOR MOLECULAR AND CELL BIOLOGY

Profilin-1 is a regulator of microglia pro-inflammatory signature and ROS generation

Cátia M Silva[1,2]; Renato Socodato[1]; João B Relvas[1] and Camila C Portugal[1]

[1] Glial Cell Biology Group, IBMC - Institute for Molecular and Cell Biology, Portugal; [2]Departament of Biology, Aveiro University, Portugal

Introduction

Activated microglia status is associated with proliferation, migration to injury foci, increased phagocytic capacity, production and release of reactive oxygen species (ROS), cytokines, and reactive nitrogen species.

Dong et al. (2004) observed an increase in Pfn1 mRNA on activated microglial cells in murine hippocampus after unilateral destruction of its principally extrinsic, the entorhinal cortex. Profilin-1 (Pfn1) controls assembly of actin cytoskeleton and is important for several cellular processes, including motility, cell proliferation and cell survival. These results suggest that Pfn1 might be involved in microglial activation. The aim of our work was to study the role of Pfn1 in microglial cell function.

Methods

- Pfn1 Knockdown in primary cortical microglial cell cultures from Wistar rats by lentivirus-mediated shRNA delivery.
- Fluorescence microscopy, qRT-PCR and FRET-based live cell imaging.

Results

1. Pfn1 shRNA decreases Pfn1 mRNA and protein levels.

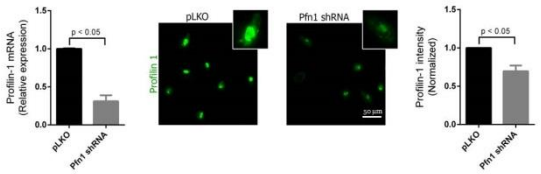

2. Reduction of Pfn1 tends to diminish phagocytosis efficiency but does not alter IBA1 fluorescence intensity significantly.

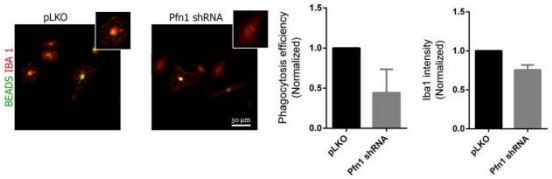

3. Pfn1 knockdown leads to a dramatic decrease in ROS production and prevents hypoxia-mediated ROS increase.

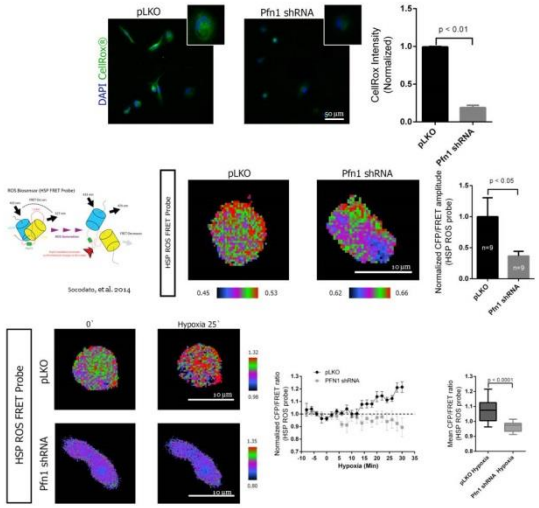

4. Pfn1 knockdown decreases mRNA levels of pro-inflammatory cytokines: interleukin-1 beta and interleukin-6

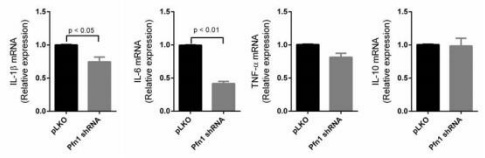

5. Pfn1 knockdown has no significant effect on glutamate release by microglia.

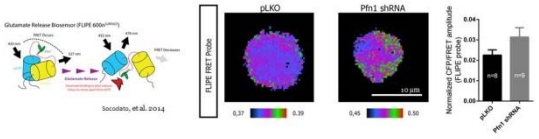

Conclusion

Pfn1 plays a key role on pro-inflammatory activation of microglial cells and is involved in ROS production by microglia.

References:
Dong JH, et al. Entorhinal deafferentation induces the expression of profilin mRNA in the reactive microglial cells in the hippocampus. Glia. 2004.
Socodato R, et al. c-Src deactivation by the polyphenol 3-O-caffeoylquinic acid abrogates reactive oxygen species-mediated glutamate release from microglia and neuronal excitotoxicity. Free Radic Biol Med. 2014 Dec 5.

Funding:
Post-doc fellowships: SFRH/BPD/91833/2012 (RS) and SFRH/BPD/91962/2012 (CC)
PTDC/SAU-NMC/119937/ 2010 FCOMP-01-0124-FEDER-021333